Braneworld black holes and black strings

Mistry, Bina

Braneworld Black Holes and Black Strings

Bina Mistry

A Thesis presented for the degree of
Doctor of Philosophy

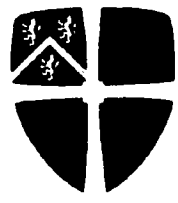

Centre for Particle Theory
Department of Mathematical Sciences
University of Durham
England

October 2008

Braneworld Black Holes and Black Strings

Bina Mistry

Submitted for the degree of Doctor of Philosophy
October 2008

Abstract

This thesis involves the study of strong and weak gravity phenomenology within the braneworld paradigm. We begin with a general overview of the hypothesised concept of extra spatial dimensions and explain why they are so interesting. Turning next to the topic of classical four-dimensional black holes, we discuss their formation via gravitational collapse and indicate some of the strong observational evidence of their existence. We then merge the two independent theories of extra dimensions and black holes together to form braneworld black holes. Focusing our attention on two distinct braneworld scenarios, we examine the effects produced from either strong or weak gravity. The prospect of obtaining experimental verification of the existence of additional spacelike dimensions in the upcoming ground-based accelerators, makes the theoretical research of braneworld gravity within this thesis even more enticing.

We start with a non-perturbative approach to look for exact, spherically symmetric star or black hole solutions on a Randall–Sundrum brane from the perspective of the five-dimensional spacetime. By fixing the background, we explore the permissible braneworld trajectories within it that correspond to a braneworld observer, the solutions of the brane Tolmann–Oppenheimer–Volkoff equations. A variety of static gravitating matter sources on the brane are obtained in a range of different backgrounds. Our final aim is a consistent brane embedding in a Schwarzschild–Anti de Sitter spacetime as these solutions are potential candidates for brane stars or black holes. The weak and dominant energy conditions determine the physically sensible solutions which have the interpretation of braneworld stars. We then study time-dependent trajectories as a possible description of time-dependent braneworld

black holes. This work is then generalised by relaxing the simplifying assumption of Z_2-symmetry, previously imposed around the brane. Non-Z_2 symmetric spacetimes are applicable in processes which concern only one side of the brane, for example black hole recoil or the emission of Hawking radiation. We determine that a subset of the allowed brane trajectories in an asymmetric background are exactly the same as the Z_2-symmetric case.

Next, we explore perturbative gravity in the Hořava–Witten model of heterotic M-theory. The study of scalar and gravitational fluctuations determines that the radion mode is coupled to the bulk scalar field, indicating only one single degree of freedom. Our analysis also determines the instability of a black string. We then compute the complete mass spectrum of the graviton mode. Using the five-dimensional gravitational physics, we determine what the gravitational interaction an observer on the braneworld would perceive. This analysis involves the computation of the Newtonian potential between two test masses on the visible brane, together with the four-dimensional tensor structure of the massless graviton propagator. Finally, as an application to the earlier work, we comment on work which is in progress: the study of possible brane black hole solutions in low energy heterotic M-theory.

Declaration

The work in this thesis is based on research carried out at the Centre of Particle Theory, Department of Mathematical Sciences, University of Durham, England. No part of this thesis has been submitted elsewhere for any other degree or qualification and is all my own work unless referenced to the contrary in the text.

Chapter 1 contains a general introduction to motivate the subject of this thesis. Chapter 2 is a review of the relevant background material required for the subsequent research chapters. Chapter 3 contains original work [1] done in collaboration with Prof. Ruth Gregory, Prof. Panagiota Kanti and Simon Creek. My contribution to the work in this chapter was primarily in section 3.5 for the time-dependent black hole background, although I also contributed to the work for the static black hole background of section 3.3. Chapter 4 contains original (unpublished) work done jointly in collaboration with Simon Creek. Chapter 5 is based on original work [2] (in preparation) done in collaboration with Prof. Ruth Gregory and Armalivia Leksono.

Acknowledgements

I would like to thank my supervisor Prof. Ruth Gregory for her guidance in the research during my PhD. I would also like to thank my collaborators Prof. Panagiota Kanti, Simon Creek and Armalivia Leksono for useful discussions, and the Engineering and Physical Sciences Research Council (EPSRC) for providing me with three and a half years of funding. Finally, I am grateful of being given the opportunity of attending an interesting Summer School on Black Holes in Mytilene, Island of Lesvos, Greece.

Contents

List of Figures

Chapter 1

Introduction

1.1 Extra dimensions

Gunnar Nordström (1914) first proposed the idea that extra spatial dimensions could exist in nature [3]. In his classical theory of gravitation, he discovered that a five-dimensional spacetime could be split into four-dimensional theories which describe gravity and electromagnetism. Unfortunately, Nordström's ideas were not taken seriously at the time and were therefore disregarded for the next several years.

During the early twentieth century, within a decade of Einstein having published his theory of gravity, Theodor Kaluza had formed a gravitational model which extended the general theory of relativity to five dimensions [4]. A few years later, Oskar Klein proposed that this extra spatial dimension, which cannot be detected by current experiments, is curled up in a very small circle of finite size [5]. These classes of theories, which feature an extra spatial dimension and unify the two fundamental forces of gravitation and electromagnetism, are referred to as the Kaluza–Klein theories.

Unfortunately, the fourth spatial dimension in Kaluza–Klein theories is extremely small, therefore cannot be seen in nature except in very extreme circumstances. This can be understood in a simple example provided by the hosepipe analogy [6]. If we view a three-dimensional object such as a pipe from afar, it will appear as a two-dimensional line. However, when viewed from close proximity, a point on the line corresponds to a point on the surface area of the pipe which is a circle.

This circle corresponds to the circumference of the pipe and represents the third dimension of space. This comparison can be extended one dimension further to describe the dimensions which make up our universe. What we naturally perceive as a point on a three-dimensional object may actually correspond to a small circle going round a fourth hidden spacelike dimension (when viewed from extremely close distances, *i.e.* Planck distances $l_{Pl} \sim 10^{-33}$cm). These ideas can also be applied to spacetimes consisting of more than one additional dimension. In this case, the extra dimensions are compactified on non-trivial topologies as opposed to a circle. This leaves us to explore the possibility that we may be living in a universe with extra hidden dimensions.

Klein revisited his hypothesis and was able to validate it by explicitly calculating the circumference of the curled up dimension [6]. He determined the size of the extra dimension by comparing the gravitational field strengths between particles, with the unit of electric charge carried by electrons and other particles. His calculation required the size of the extra dimension to be unobservably small, *i.e.* of order of the Planck scale. It is therefore not surprising that these results are consistent with the fact that we haven't been able to see the fourth dimension of space.

Ground based accelerators which accelerate particles close to the speed of light may give an insight into extra dimensions. The energies required to probe the additional dimensions in Kaluza–Klein theories are exceedingly high. If we set the size of the compactification radius of the extra dimension to be a finite value [7], say $R \lesssim 10^{-17}$cm, then the energy or mass scale corresponding to the massive Kaluza–Klein modes in the higher-dimensional spacetime is given by the relation $E \sim R^{-1}$. Since the compact space is microscopic, the resulting energy or mass value will be of order of the Planck mass $M_{Pl} \sim 10^{19}$GeV. The unlikely prospect of attaining these extreme energy scales, required to directly probe these compact extra dimensions, makes them impossible to detect[1].

At present, colliders can only reach energies that are less than R^{-1}. At distances greater than the compactification radius *i.e.* $\lambda > R$, the resulting energy scale

[1]We have used different units for the compactification scale of the extra dimension R and the corresponding energy scale $E \sim R^{-1}$ (*i.e.* cm and GeV scales respectively).

$E_\lambda \sim \lambda^{-1} < R^{-1}$ is within the scale which colliders can reach. However, at distances less than the compactification radius *i.e.* $\lambda < R$, the energy scale $E_\lambda \sim \lambda^{-1} > R^{-1}$ corresponds to very high energies which are beyond the reach of any current or foreseeable accelerators. These enormous energy values ensure that the low energy physics relating to our universe is effectively four-dimensional. This means that we can only produce massless particles in the collider experiments [7]. It therefore remains unlikely that progress in detecting additional dimensions in Kaluza–Klein models will be made.

Over the subsequent fifty years, interest in the Kaluza–Klein theories diminished. Instead, physicists became interested in the study of the weak and strong forces [6]. In order to construct a successful unified theory, it was realised that the strong and weak interactions must also be combined with the gravitational and electromagnetic forces. Physicists became very ambitious in these unification theories. It was hoped that all four forces of nature (*i.e.* the weak, strong, electromagnetic and gravitational forces) could be amalgamated into one simple underlying theory. This field of research still remains active today.

By the 1950's, electromagnetism was the only well understood force [6, 8] and one which belonged to a theory known as quantum electrodynamics (QED). The two other independent theories were: Einstein's classical theory of general relativity which applies to massive objects at very large distances (*e.g.* stars, planets), and quantum mechanics which applies to tiny objects on extremely small length scales (*i.e.* the atomic scale) [9]. In the mid-1960's, theoretical physicists became interested in combining these two distinct theories in order to find a unique theory which would explain how gravity would work at the Planck scale. Unfortunately, any attempts to unify quantum mechanics with general relativity at Planck distances had ultimately failed. To fix the problem, an entire new theory was introduced; string theory, a quantum theory of gravity.

In 1968, early string theorists modified the particle physics description of a fundamental particle. It was believed that the smallest constituent of matter is not a point-like particle, but in fact a one-dimensional string. These strings are analogous to instrumental strings such as those on a violin which can produce different sets of

harmonics. Similarly, the different modes of vibrations of a string in string theory yield a different set of particle excitations at various energies. These then contribute to the different types of string theories.

The bosonic string was the first string theory to be constructed in 1968, consisting of twenty-six dimensions. It was initially developed to describe the strong force in quantum chromodynamics (QCD) which held hadrons together [6]. The hadrons are made up of smaller entities called quarks. Since quarks exist in pairs, it was believed that a string-like object was responsible for holding the pair of quarks together. Unfortunately, during the 1970's, this string theory description failed to describe the strong force. Further calculations showed other problems associated with the bosonic string. The presence of a tachyon (a negative mass squared particle) rendered the theory unstable. Also, the prediction of a spin-2 particle in the theory raised some questions as it has not previously been observed in any experiments. Although the bosonic string was unsuccessful in describing the strong force, it did however provide a useful framework in which to develop the later string theories. Due to its 'failure', there was a sudden loss of interest in string theory for the next few years.

During the same decade (1970's), progress had been made in unification of the strong, electromagnetic and weak forces. The combination of the electrodynamics force of QED with the weak interaction led to electroweak theory. The subsequent union of the electroweak force with the strong interaction of QCD gave rise to the Standard Model of particle physics. This then left gravity as the sole force existing on its own. After the success of the Standard Model, physicists became fascinated again in string theory in the hope of finding a fundamental theory which would now combine the Standard Model forces with gravity.

Fortunately, the problems encountered in the bosonic string were resolved by introducing supersymmetry (symmetry between integer and half integer spin particles, namely bosons and fermions, respectively) into the theory. This led to the 1980's formulation of superstring theory; a theory which accommodates all Standard Model particles, in particular the spin half fermions which were not present in the bosonic string. Adding supersymmetry (and hence fermions) to the original bosonic

string removed the unwanted tachyon, giving a stable string configuration [6]. Also, the spin-2 particle predicted in earlier calculations revealed itself to have the same behaviour as the graviton (an elementary particle of spin-2 which mediates the force of gravity). Therefore the spin-2 particle wasn't a problem after all. In fact it served as evidence that string theory could be a possible theory in which to quantise gravity.

Superstring theory had superseded the bosonic string. The restriction on superstrings was its dimensionality; it is consistent in only ten dimensions [6]. Calculations in this particular number of dimensions allowed all the unwanted modes of vibration to drop out [9]. The miraculous cancellations of all unwanted anomalies (symmetry violation in a quantum mechanical process which are absent in the corresponding classical theory) provided a second confirmation that superstrings are only consistent in ten spacetime dimensions. During the mid 1970's, it was realised that supersymmetry could also be incorporated into gravity. This resulted in a supergravity theory which was found to be consistent in eleven dimensions.

The superstring theories became extremely popular and remain renowned today. These theories which are consistent in ten-dimensions allow the possibility of having six additional dimensions of space. These six extra microscopic dimensions are compactified on non-trivial manifolds, enabling us to obtain the relevant effective four-dimensional physics for the study of our universe. Therefore, superstring theories are higher-dimensional extensions of the five-dimensional Kaluza–Klein theories.

In the late 1990's, there was a revival of interest in a new type of extra-dimensional model known as braneworlds [10,11]. (For earlier proposals of braneworlds, see [12]–[17]). These models consist of infinite slices of spacetime (a brane) which exist in a higher-dimensional space (bulk). Braneworlds are interesting toy models in which to study the possibility that our universe can be described as a four-dimensional subspace (three-brane), living in a fundamentally multi-dimensional spacetime. The properties of braneworlds constrain all ordinary particles and forces (*i.e.* the Standard Model) to live on the three-brane. However, gravity and other exotic particles (which are weak and do not interact strongly with matter) are allowed to leak out of the hypersurface and travel into the dimension which extends beyond the brane.

The extra dimensions proposed in braneworlds can either be large [10] or infinite [11], unlike the Kaluza–Klein theories where the additional dimensions are unobservably small. Therefore, if the braneworld paradigm offers a construction of a model which can be realised in nature, then the theoretical prospect of detecting these large extra dimensions at reasonable energy scales makes the study of them highly exciting.

In general, when zero mode particles on the brane interact at high energies, they get excited. The large compact extra dimensions open up to become a continuum of Kaluza–Klein modes [7]. The particles are then able to escape the brane to large (or infinite) distances of the higher-dimensional world. Therefore, extra dimensions are experienced by particles which are able to leave the brane. To our knowledge, the particles which are allowed to enter into the additional dimensions in braneworld models correspond to the messenger particles of gravity and are more commonly referred to as Kaluza–Klein gravitons. Thus, the detection of a Kaluza–Klein graviton is evidence for the existence of extra spatial dimensions.

One possible process of producing these spin-2 gravitons is given in a high energy process, such as the collision of an electron with its antiparticle *i.e.* the positron. The collision causes the particle and antiparticle to annihilate to form a graviton and a virtual particle *i.e.* the gamma ray photon. The graviton produced in the high energy collision is likely to miss the detector (due to the weakness of the coupling) and escape into the higher dimensions. We therefore observe the experimental signatures as evidence of gravitons leaving our visible universe. This confirmation is provided by the continuum spectrum produced by gravitons, which can be detected indirectly by the missing energy signals [7] of the high energy collisions.

So far, there has been no direct or indirect evidence of large extra dimensions. We cannot perceive them directly simply because we don't live in these additional dimensions. However, the possibility of detecting the large extra dimensions indirectly in future colliders is what makes the topic highly exciting.

1.2 Stars and black holes

The vast amount of stars in our universe (*e.g.* each galaxy contains around 10^{10} stars [18]) are formed from clouds of dense gas called Nebulae, which are drawn together by the force of gravity. The accretion of Nebulae into a body with ample mass allows for high central temperatures to be attained. Thermonuclear reactions (namely fusion) are now able to take place leading to the formation of a star. Since hydrogen is the most abundant element in the universe, it provides the preliminary source of energy production in stars. One possible process that can occur at the core of the star involves the fusion of four hydrogen nuclei to produce a helium nucleus. Since the mass of helium is smaller than the total mass of the four constituent hydrogen nuclei, then some of the mass is converted to energy (according to the equivalence relation $E = mc^2$). This difference in mass is a measure of the binding energy which holds the nucleons of the atoms together. The greater the binding energy, the harder it is to free the electrons from their atomic orbits. The fusion reactions taking place within the core of the star occur constantly and are sustained for a long time. The energy produced here during the formation of the helium nucleus is released at the surface as heat and light, leading to the creation of a burning star.

A stars' lifetime lasts over a billion years, however they do not live forever. Eventually all the hydrogen and helium at the core of the star is exhausted, allowing no further energy to be produced (this process is applicable to less massive stars). The insufficient temperature at the center of the star leads to a carbon-oxygen inert core; a point at which nuclear reactions cease to occur. Stars which have greater masses allow for a more complicated chain of nuclear reactions beyond the helium stage [18]. This is because higher central pressures are now attainable for stars with a large mass, giving rise to greater temperatures at the core of the star which were not previously possible for lower mass stars. In this way, the synthesis of heavier nuclei (carbon, neon, oxygen, silicon *etc.*) proceeds with temperatures rising as elements of increasing atomic number are produced. This process continues until the most stable nuclei is formed, namely iron. Once the stars' core is converted entirely to iron, the nuclear reactions stop regardless of the extreme temperatures inside the

core. This is because iron has the largest binding energy per nucleon of all nuclei, making it very difficult to ionise. Thus, the inert iron-rich core of a star marks the end of the chain of fusion reactions; the star is near the end of its life cycle.

At the end of the stars' life cycle, it typically cools down and reduces in size. In time, the star stops emitting light and becomes unstable against the influence of its own gravity, eventually leading to its collapse. Depending on the size of the original star, two different processes can occur. Stars which are less massive and have size comparable to the sun, first expand to form a red giant, then subsequently cool and collapse to form a white dwarf star. However, larger mass stars (at least four times greater than the sun) show a more spectacular behaviour. They expand enormously to form a red supergiant, then rapidly cool and collapse and finally explode. This violent explosion releases a vast amount of energy in the form of light. The brightness produced is a hundred times the intensity of the original star. This prominent glow in the sky lasts for weeks, outshining the entire galaxy of which it is in. This explosion is known as a supernova [19], the remnants of which lead to the formation of a neutron star. There are strong upper limits that restrict the amount of pressure that can be resisted by a white dwarf or neutron star; if the mass of the star exceeds the maximum mass that can be supported by a compact star, then it will continue to collapse to form a stellar black hole (BH).

In the 1920's, an Indian astrophysicist, Subrahmanyan Chandrasekhar calculated that if the mass of a star was less than 1.4 solar masses (where a solar mass is defined as $M_{\odot} = 2 \times 10^{33} g$), then it would form a white dwarf. This upper limit on the mass of a star is known as the Chandrasekhar limit [20]. The formation of a white dwarf involves electrons being torn away from the nuclei, which get compressed inside the star. The electrons become extremely crowded within a dense region, resulting in very high pressures. Any further contraction of the star would violate the Pauli Exclusion Principle amongst electrons; two electrons cannot occupy the same place. Therefore, this degenerate electron pressure halts the stars collapse to form a white dwarf [19], the size of which is comparable to the earth.

Lev Davidovich Landau, a Russian scientist, later suggested another possible final state of a star [19]. If the mass of the star exceeds the Chandrasekhar limit,

then the force of gravity takes over and overcomes the degenerate electron pressure. The electrons are squashed and are now combined with the protons in the nucleus, forming additional neutrons. Eventually, all the protons get converted into neutrons. Neutrons also obey an analogous principle as the electrons; this time, two neutrons cannot occupy the same place (Pauli Exclusion Principle amongst neutrons). The degenerate neutron pressure stops the stars collapse, resulting in the formation of a neutron star (typical radius of a neutron star is 10km).

Before we discuss the ultimate collapse of a star, we state the general formulae that characterise its internal structure [20]. A star is a spherically symmetric compact object, with distinct exterior and interior gravitational fields. The field outside a star consists of empty space and is described by the Schwarzschild geometry (by Birkhoff's theorem). Thus, the vacuum Einstein equations are valid only outside the region of a star. However, the interior of the star is composed of matter. Thus, in order to describe a matter source within a star, we introduce an additional term in the empty-space field equations. The non-vacuum Einstein equation, describing a static spherically symmetric gravitating object, is given by

$$G_{\mu\nu} = R_{\mu\nu} - \frac{1}{2}Rg_{\mu\nu} = 8\pi G T_{\mu\nu} \tag{1.1}$$

where $G_{\mu\nu}$ is the Einstein tensor, $g_{\mu\nu}$ the metric tensor, $R_{\mu\nu}$ the Ricci tensor and R the Ricci scalar. We assume that the star is made up of a perfect fluid, with matter distribution given by the non-zero energy-momentum tensor

$$T_{\mu\nu} = [\rho(r) + P(r)]\, u_\mu u_\nu + P(r) g_{\mu\nu} \tag{1.2}$$

where $\rho(r)$ and $P(r)$ represent the energy density and isotropic pressure of the fluid, respectively. Furthermore, the vector $u_\mu = (\sqrt{-g_{tt}}, 0, 0, 0)$ represents the fluids 4-velocity, with g_{tt} corresponding to the time-component of the general, spherically symmetric metric

$$ds^2 = g_{tt}(r)dt^2 + g_{rr}(r)dr^2 + r^2(d\theta^2 + \sin^2\theta d\phi^2)\,. \tag{1.3}$$

Solving the non-vacuum Einstein equations determines the explicit form for the metric coefficients: g_{tt} and g_{rr}. This enables us to deduce two relativistic equations

governing the structure of stars:

$$\frac{dm(r)}{dr} = 4\pi r^2 \rho(r) \tag{1.4}$$

and

$$\frac{dP(r)}{dr} = -\frac{[\rho(r) + P(r)]\,[Gm(r) + 4\pi G r^3 P(r)]}{r(r - 2Gm)} \tag{1.5}$$

where $m(r)$ denotes the mass function. The last equation is known as the Tolman–Oppenheimer–Volkoff equation which gives an upper limit to the pressure that can be supported by a neutron star.

Neutron stars are smaller and dimmer than the white dwarf stars [19]. They also have a theoretical upper bound on their mass that is analogous to the Chandrasekhar limit for white dwarf stars. The degenerate neutron pressure is unable to support masses greater than 2.5 $M_{\odot}$. However, our galaxy contains stars with masses much bigger than this. Therefore, the neutron stars that exceed the upper limit that can be supported have sufficient matter to overcome the internal pressure, and continue to collapse entirely under the influence of their own gravity. All the light rays bend toward the star via the strong gravitational fields near the stars' surface. The star ultimately collapses to a single point, forming a very dense object where all the mass is highly concentrated. This gravitational collapse leads to the fabrication of a void in the cosmos.

John Michell, a British natural philosopher (1783) had first claimed the idea that 'dark stars' (a possible final state of a star) could exist in our galaxy [22]. As the name suggests, we will never be able to see them even with the most powerful telescopes because they don't emit any light. In 1916, the Schwarzschild solution had been obtained from Einstein's equations [21]. It was not until the mid 1960's that physicists had gained a better understanding of the Schwarzschild solution. The theory suggested the existence of dark stars. These dark objects are better known as stellar BHs.

BHs are massive objects with extremely strong gravitational fields around them. We will never be able to see a BH since they are the 'prisons of light' [22]. All forms of matter and electromagnetic radiation which pass beyond the event horizon (an imaginary surface which nothing can escape) is immediately drawn toward the exact

center of the BH. This central region is known as the singularity; a point at which the density, pressure and the curvature of spacetime are infinite. Unfortunately, the laws of general relativity fail to work at this highly dense region. Only a quantum theory of gravity will be able to explain what is happening at the BH singularity.

There has been no direct experimental or observational evidence for the existence of BHs. In fact there will never be direct evidence since light cannot escape out of a BH. The best way to search for the existence of a BH is indirectly, for example, by observing the gravitational deflection of light around the spacetime of a BH [19]. Since gravity is extremely strong near the region of the BH, the paths of light rays are expected to warp significantly near its vicinity. This warping will be much more significant compared to the warping produced when light rays pass close to the sun. This is because the spacetime around a sun is only slightly curved in contrast to that of a BH. Therefore, the strong deflection of light suggests the presence of a massive gravitational object.

The binary star system [19,23] indirectly provides observational evidence of either a compact star or a stellar BH. In the double star system, two stars appear as one star when viewed from a telescope. One of the stars is an ordinary star, whereas the second companion star (which cannot be viewed by a telescope) corresponds to a compact star or a stellar BH. The ordinary and companion star rotate in stable orbits relative to their common center of mass points. By studying the binary orbits of the two stars, it is possible to determine the mass of the companion star. If the mass of the companion star is well above the upper bound that can be supported by a neutron star, then it is a good indication that the companion star could be a stellar BH.

Cygnus X-1 is a strong candidate of a double star system which contains an ordinary star (HDE 226868 of mass $20M_{\odot}$) and a stellar BH [19,27,29]. The intense gravitational field of the BH causes the transfer of matter from the ordinary visible star to the stellar BH. This subsequently forms an accretion disc around the BH. The temperature of the matter increases considerably. As a result, energy is released from the accretion disc toward the visible star in the form of high energy compact X-ray sources. The X-rays produced on the ordinary star can be detected by satel-

lite observatories and are exceptionally bright (much brighter and distinguishable from the X-rays produced by binary stars consisting of either a white dwarf or a neutron star). Analysis of these bright and powerful X-rays reveals that Cygnus X-1 must be very compact, *i.e.* less than 300km in diameter. Furthermore, the invisible companion star of HDE 226868 is calculated to have mass $10M_{\odot}$. Therefore, calculations reveal that an object of $10M_{\odot}$ condensed in a volume of 300km can be nothing other than a stellar BH. Compact binary systems are therefore strong BH candidates.

There has also been strong observational evidence for the existence of BHs which weigh a million or a billion times more than the sun. These gigantic objects are known as supermassive black holes (SBHs) and are known to exist at the center of most galaxies [24, 25]. Advances in technology have provided powerful and robust evidence of these vastly large objects in several nearby galaxies including our own: the Milky Way [26]. Detailed observations (*e.g.* in the galaxy M87) measuring the brightness across the galaxy via astronomical telescopes revealed the presence of a prominent bright source [19]. Astronomers suggested that this luminous source corresponds to a high concentration of stars which are congested together within a small radius. The crowd of stars arise due to the existence of a SBH at the galactic center. Calculations showed that the strong compact source of gravity must weigh 5 billion $M_{\odot}$, and therefore must be a SBH. Astronomers also used spectroscopic observations to analyse the spectral lines across the galaxy. The lines were found to be broader toward the center of the galactic nuclei. This suggested that the stars closer to the galaxy move at much greater speeds, enabling them to survive. Calculations again revealed that the gravitational source must be around 5 billion $M_{\odot}$. Thus, the evidence of the existence of SBHs at the galactic core of M87 provides us with compelling evidence of solar system sized BHs.

Classically, we know that nothing, not even light can escape out of a BH (once it has gone past the event horizon). In 1971, two Soviet scientists Ya B. Zel'dovich and I. D. Novikov [19] (prior to Hawking 1974 [28]) discovered that tiny static BHs which are produced in the early universe can emit radiation. Stephen Hawking later calculated this by applying quantum mechanics to the electromagnetic fields near

the region of a BH. The results showed that BHs radiate continuously. Quantum field theory calculations show that the radiation that is emitted takes the form of a blackbody energy spectrum, with temperature inversely proportional to the BH mass. Thus, solar mass BHs produce negligible or small amounts of radiation compared to small sized BHs. The emission of radiation by BHs is only possible quantum mechanically through the Heisenberg uncertainty principle. The principle states that it is impossible to precisely know a particle's exact position and momentum at the same time. If a particle is at location x with uncertainty $\triangle x$ and has momentum p with uncertainty $\triangle p$, then both the uncertainty in position and momentum are not independent and are related by the formula $\triangle x \triangle p \approx h$. Furthermore, there is also an uncertainty relation in the particles energy and time $\triangle E \triangle t \approx \hbar$, suggesting that a particle-antiparticle pair can appear and disappear unexpectedly in a short time, 10^{-21} seconds. The many pairs of virtual particles that exist around a BH are continually being created and destroyed. If the pair annihilate in time less than $\triangle t \approx \hbar / \triangle E$, then no laws have been violated[2].

In the above process, the strong gravitational field around a BH provides the energy to create the particle-antiparticle pairs. After the particles have exchanged energy, the negative energy (virtual) particle falls below the event horizon and into the BH singularity and the positive energy particle manages to escape away (as Hawking radiation) from the event horizon to large distances (to infinity) [20]. The escaped particle becomes a real positive energy particle. This continuous process ultimately decreases the size and energy of the BH since particles are constantly being emitted and energy is continually being lost. The negative energy of the antiparticle is responsible for decreasing the mass of the BH. Eventually, at the end of its life, the BH will evaporate entirely and release a burst of radiation in the form of gamma rays. Unfortunately, this type of phenomena has not yet been observed. This process in which BHs radiate particles is known as the Hawking effect and is a consequence of the Heisenberg uncertainty principle.

There are also other types of BHs we have not discussed; they were created a few

[2]The Planck constant is $h = 6.65 \times 10^{-34}$ Js and $\hbar = h/2\pi$

seconds after the big bang and do not originate from the gravitational collapse of an ordinary star. They were created by the ideal conditions at the start of the universe; the enormous temperatures, pressures and densities allow clouds of dense gas to be compressed to tiny BHs, also known as primordial black holes (PBHs). They are extremely dense objects (have masses of mountains [19]) and are of subatomic size. Small PBHs (mass less than 4 billion tonnes) have higher temperatures, hence higher emission rates. They evaporate very quickly and therefore do not survive. The PBHs that have survived have masses greater than 4 billion tonnes and they are larger and have lower temperatures. They therefore radiate at a slower rate and a small proportion are still present in the universe today. These microscopic PBHs (of masses greater than 4 billion tonnes) are possible to detect through Hawking radiation. Eventually the emission of radiation will decrease the size of the PBH, resulting in an explosion of gamma rays which can be detected by the flashes of light in the night sky. Detection of surplus gamma ray bursts in the night sky will suggest the presence of a strongly evaporating PBH in our universe. PBHs are possible dark matter candidates as they are still yet to be observed.

We therefore have very strong observational evidence of the existence of astrophysical BHs [29]; from stellar sized BHs in binary systems to the larger scale of SBHs which exist in the center of most galaxies. As the observational techniques continue to develop, we will acquire a better understanding of these mysterious and fascinating objects that exist in nature. The possibility of detecting mini BHs via Hawking radiation in the upcoming accelerators makes the study of them even more challenging.

1.3 Braneworld gravity

So far, we have discussed four-dimensional astrophysical BHs. We extend the analysis further to consider these massive gravitational objects in higher-dimensional theories, involving extra spatial dimensions. The properties and physics of BHs in theories consisting of more than four dimensions are expected to be significantly different compared to the known physics of the four-dimensional world [31]. Thus, by taking into account the extra-dimensional effects, *i.e.* the new physics corresponding to the higher-dimensional world, we can modify the description of the classical four-dimensional BHs.

This thesis deals with two types of extra-dimensional models which are widely used in model building: the Randall–Sundrum (RS) model (of which there are two types, RSI [10] and RSII [11]) and the Hořava–Witten model of heterotic M-theory [32]. The latter model derived by Lukas, Ovrut, Stelle and Waldram is based on the eleven-dimensional Hořava–Witten construction [34] and will be identified as the LOSW model (named after the initials of the above authors) in this thesis. A detailed description of the two independent braneworld scenarios is given in the following chapter.

The RSI scenario consists of two four-dimensional manifolds bounded at the end of a five-dimensional Anti-de Sitter spacetime. All Standard Model particles are constrained to live on the hypersurface. However, the characteristic nature of gravity allows it to permeate into the direction orthogonal to the brane (*i.e.* the extra dimension). The Hořava–Witten construction features two ten-dimensional branes, bounding the ends of an eleven-dimensional spacetime. Each hyperplane contains a different set of particles and forces which are equivalent to the forces of the heterotic string [9]. In contrast to the RSI model, the ten-dimensional branes of the Hořava–Witten setup includes the full Grand Unification Theories [9] as well as the Standard Model. Moreover, the Hořava–Witten construction is supersymmetric [30], unlike the RSI model [9]. For the Hořava–Witten theory to be realistic and correspond to our visible universe, six of the spatial dimensions are wrapped up on a tiny manifold giving rise to the LOSW model; a possible representation of our domain wall universe. Hence, the pictorial setup of the LOSW and RSI models are analogous.

A finite interval of the fifth dimension is separated by two three-branes. Although the setup between the two distinct braneworlds is similar, the physics is quite different. The fifth spatial dimension between the heterotic branes now contains a bulk scalar particle (which is a consequence of the compactification). Thus the presence of the additional bulk matter field makes the model distinct to its descendant (*i.e.* the RSI braneworld). Since the properties of the braneworlds are distinct, we expect the physics in each braneworld model to be different.

The detection of the hidden extra spatial dimension in the braneworld is achieved through studying the behaviour of gravity. Thus, the best physical objects to study within the braneworld are objects with enormous gravitational fields such as black holes or their higher-dimensional analogues, black strings.

Black holes are objects that possess massive gravitational fields. The study of these enormous objects within the braneworld allows us to explore the two independent theories in one single framework. We are particularly interested in investigating the impact of BHs within the context of the RSII model (featuring a single three-brane embedded in a fifth dimension). So far, there has been no successful attempts in describing strong gravity phenomenology (*i.e.* braneworld black holes) within the RS models. To this end, we continue to explore this fascinating topic using a non-perturbative approach in the hope of finding a four-dimensional metric which corresponds to a braneworld black hole. We then focus our attention on another higher-dimensional object known as the black string. We explore these gravitating objects in the LOSW model. Using perturbation theory this time, we investigate weak gravity in this model and determine the instability of a Schwarzschild black string [37].

Whether the above braneworlds are realistic or not depends on whether we can theoretically reproduce the correct known four-dimensional gravitational physics corresponding to our universe. Collider experiments may soon be able to determine whether the braneworlds are a true representation of our universe. Unfortunately, the Hořava–Witten model is hard to test experimentally as the six additional space-like dimensions are extremely small [9]. This would require colliders to probe to extremely high energies, comparable to the string scale. Only after reaching such

high energies, we would be able to detect these extremely small additional dimensions, and then perceive the world in eleven dimensions [30]. It is therefore virtually impossible to test the Hořava–Witten construction, since any current and future accelerators cannot attain these gigantic energy scales. However, the theoretical study involving the Hořava–Witten model still remains exciting.

Fortunately, the RS model can be tested since the energies are attainable in the upcoming accelerators. The extra dimensions will reveal themselves through Kaluza–Klein particles, which are detected in the four-dimensional world [9]. They will provide revolutionary information regarding the physics corresponding to the unseen five-dimensional universe. The study of black holes within the RS braneworld is particularly exciting as it may soon provide experimental signatures for the existence of an extra hidden spacelike dimension. If experimental data produced in the upcoming ground-based accelerators is in strong agreement with the predicted results of the tested RS braneworld model, then we certainly have a toy model which provides a true description of our four-dimensional universe.

The BHs in the RS braneworld involves a highly curved background geometry. However, the properties of BHs are remarkably different if we consider them on small scale theories featuring large and flat extra dimensions [31]. High energy particle collisions can produce four-dimensional astrophysical and higher-dimensional BHs. In general, when matter trapped on a visible four-dimensional brane undergoes gravitational collapse, it forms a BH which extends into the extra dimension forming a higher dimensional object. The radius of the horizon of the massive object determines whether or not the BH corresponds to a higher-dimensional object. If the size of the BH horizon exceeds the size of the extra dimension, then we essentially recover an effective four-dimensional massive object. However, if the BH has a radius less than the size of the extra dimension, then a small BH is formed which appears to be a higher-dimensional gravitating object. These higher-dimensional objects correspond to mini BHs.

Attainable energies allow the possibility of probing these mini BHs via high energy particle collisions. Although the small BHs evaporate quickly, they can still be identified in accelerators. Their presence is detected by the emission of

thermal black body radiation. This process releases elementary particles onto the brane and also into the extra dimensions. As the BH emits radiation, it loses energy and simultaneously decays. The energy released will form a spectrum of thermal radiation also known as visible Hawking radiation [31]. The particles that are emitted onto the brane correspond to the brane-bound particles (*i.e.* the Higgs particle, gauge bosons and fermions). These particles can easily be detected in accelerators.

Small BHs also emit radiation into the bulk. In this case, the radiation is invisible and corresponds to particles that propagate into the extra dimension such as gravitons and scalar fields. These particles cannot be detected as they propagate in the higher-dimensional space. However, their presence can be determined by the missing energy signals produced in the collision process. The amount of missing energy will also tell us how much energy remains on the brane [31].

So far, there has been no evidence of Hawking radiation emitted by large four-dimensional astrophysical BHs. This is because the wavelengths emitted are large and undetectable. The only four-dimensional BHs that emit Hawking radiation at a reasonable wavelength and can be detected correspond to PBHs [19]. Unfortunately, to date, there is no evidence linking Hawking radiation from PBHs; they are dark matter candidates. However, the possible detection of Hawking radiation arising from small evaporated BHs (in theories involving large, flat additional dimensions) looks promising. The upcoming accelerators may provide ground-breaking signatures regarding our hypothesised extra-dimensional world.

The two distinct braneworld models which are the subject of this thesis can be recovered from the general action

$$S_5 = \frac{1}{2}\int_{5d} d^5x\sqrt{-g}\left[R - \frac{1}{2}(\partial\phi)^2 - V(\phi)\right] \pm \int_{4d} d^4x\sqrt{-g^{\pm}}\sigma^{\pm}U(\phi)$$

by taking the following two limiting cases:

- $\phi \to 0$: $V(\phi) = V_0 = \Lambda_{RS}$, $U(\phi) = U_0 = 1$ Randall–Sundrum model.
- $V \to \frac{1}{3}\alpha^2 e^{-2\phi}$, $U \to e^{-\phi}$: $\sigma = \sqrt{2}\alpha$ LOSW model.

Chapter 2

Gravity in the Braneworld

In this chapter we give a compelling alternative to the old traditional method of Kaluza–Klein compactification where the radius of the extra dimension is taken to be the order of the Planck scale. We concentrate on braneworld scenarios which feature additional dimensions that are now large and compact. There are two distinct types of braneworld models which are of interest to us. First, we consider the Randall–Sundrum (RS) models of which there are two types: RSI and RSII. They correspond to one of the simplest types of phenomenological braneworld models involving either a large or infinite sized extra dimension. The motivation behind the RSI scenario is to construct a framework in which the Hierarchy problem of the Standard Model is resolved in the most elegant way (the Hierarchy problem being the difference of sixteen orders of magnitude between the scales of particle physics and that of gravity, *i.e.* the electroweak $m_{EW} \sim 10^3$GeV and Planck scales $m_{Pl} \sim 10^{19}$GeV respectively). The RSII model is appealing from the perspective of the different nature of gravity. Even with an infinite sized extra dimension the model reproduces brane-localised gravity. We then focus our attention on a second type of braneworld scenario which are ancestors of the RSI model. This type of model corresponds to the Hořava–Witten model of heterotic M-theory and are initially constructed from string theory duality.

2.1 The Randall–Sundrum scenarios

Two basic models of braneworld gravity [10, 11] were proposed by Randall and Sundrum. Both models depict our universe as a four-dimensional manifold living on the edge of a five-dimensional Anti-de Sitter (AdS_5) spacetime. Since there are conflicts with observational data, Standard Model particles are forbidden to travel to large distances in the extra dimension and are therefore trapped on the hypersurface, consisting of the usual three macroscopic spatial dimensions. However, this solution does not work for gravity since it is the only force that is directly linked to the structure of spacetime. Therefore, gravity has the freedom to enter into the higher dimension.

2.1.1 Randall–Sundrum I model

The RSI model [10] consists of two parallel three-branes bounding an AdS_5 spacetime. The branes are located at orbifold fixed points of the fifth dimension: $y = 0$ and $y = y_c$. The extra dimension lies in the direction orthogonal to each boundary brane. The RSI scenario can also be represented on the S^1/Z_2 orbifold. This particular setup involves the compactification of the additional dimension on a circle, with opposite ends of the circle being identified in a Z_2-identification $(x^\mu, y_c) \leftrightarrow (x^\mu, -y_c)$ where x^μ represents the coordinates of the four-dimensional spacetime. Thus, by taking periodicity in the extra dimension and making the above identification, we are ensuring that the spacetime on each side of the hypersurface is indistinguishable. The brane-bound particles of our visible universe are assumed to reside on the negative energy brane.

We begin by solving the five-dimensional Einstein equations. Our starting point is the five-dimensional classical action; a sum of the Einstein–Hilbert action and the actions of each brane, respectively,

$$\begin{aligned} S = \int d^4x \int_{-y_c}^{+y_c} dy \sqrt{-g^{(5)}} \left(2M_{Pl}^3 R - \Lambda_5\right) \\ - \sigma_{vis} \int_{y=0} d^4x \sqrt{-g_{vis}} - \sigma_{hid} \int_{y=y_c} d^4x \sqrt{-g_{hid}} \end{aligned} \tag{2.1}$$

where M_{Pl} denotes the five-dimensional Planck mass, R is the five-dimensional scalar

curvature, Λ_5 is the bulk cosmological constant, $g^{(5)}$ is the determinant of the bulk metric, g_{vis} (g_{hid}) and σ_{vis} (σ_{hid}) represent the determinant of the four-dimensional induced metric and the brane cosmological constant on the visible (hidden) brane, respectively. Hence, the setup corresponds to five-dimensional gravity with a negative bulk cosmological constant, coupled to the brane cosmological constants.

The five-dimensional Einstein equation derived from the above action is given by

$$G_{ab} = -\frac{1}{4M_{Pl}^3}\left[\Lambda_5 g_{ab} + g_{\mu\nu}^{vis}\delta_a^\mu\delta_b^\nu\delta(y-y_c)\frac{\sigma_{vis}}{\sqrt{g_{yy}}} + g_{\mu\nu}^{hid}\delta_a^\mu\delta_b^\nu\delta(y)\frac{\sigma_{hid}}{\sqrt{g_{yy}}}\right] \tag{2.2}$$

where G_{ab} is the five-dimensional Einstein tensor. The Greek indices run in the direction parallel to the brane $\mu, \nu = 0, 1, 2, 3$ whereas the Latin indices run over all five dimensions $a, b = 0, 1, 2, 3, 4$.

The following five-dimensional metric ansatz

$$ds^2 = a^2(y)\eta_{\mu\nu}dx^\mu dx^\nu + r_c^2 dy^2\,, \qquad a(y) = e^{-kr_c|y|} \tag{2.3}$$

is a solution to Einstein equations (2.2). The symbols r_c and k correspondingly represent the compactification radius of the extra dimension and a constant yet to be determined. We will take the signature of the flat four-dimensional Minkowski metric to be $\eta_{\mu\nu} = \mathrm{diag}(-,+,+,+)$. The metric is evidently non-factorisable since the exponential function, also known as the warp factor, is a rapidly decaying and implicit function of the fifth dimension.

Setting $w(y) = kr_c|y|$ and inserting (2.3) into (2.2) gives two sets of differential equations

$$w'^2 = -\frac{r_c^2\Lambda_5}{24M_{Pl}^3} \tag{2.4}$$

$$w'' = \frac{r_c}{12M_{Pl}^3}\left[\sigma_{hid}\delta(y) + \sigma_{vis}\delta(y-y_c)\right] \tag{2.5}$$

where prime denotes differentiation with respect to y. The first order differential equation (2.4) can be solved easily to give

$$w(y) = r_c|y|\sqrt{\frac{-\Lambda_5}{24M_{Pl}^3}} \tag{2.6}$$

where we have taken into account the orbifold symmetry $y \leftrightarrow -y$. The constant k can be identified as

$$k = \sqrt{\frac{-\Lambda_5}{24M_{Pl}^3}} \tag{2.7}$$

which suggests that the bulk cosmological constant must be negative $\Lambda_5 < 0$, indicating that we must have an AdS_5 spacetime in between the two branes. Thus, k corresponds to the inverse Anti-de Sitter radius.

Furthermore, if we double differentiate (2.6) and use (2.7), we obtain

$$w''(y) = 2kr_c[\delta(y) - \delta(y - y_c)] \tag{2.8}$$

where the delta function arises from the double differentiation of $|y|$. To ensure that (2.8) is consistent with the Einstein equations, we equate it with the second order differential equation (2.5). This shows that a fine tuning is required between the brane cosmological constants (often called the brane tensions) and the bulk cosmological constant:

$$\sigma_{hid} = -\sigma_{vis} = 24M_{Pl}^3 k\,, \qquad \Lambda_5 = -24M_{Pl}^3 k^2\,. \tag{2.9}$$

Thus, the brane tensions have been carefully attuned so that they are equal but opposite in sign and depend on the single scale factor k. Hence, the visible and hidden branes have negative and positive tensions, respectively. The careful adjustment of the tensions of each brane with the negative bulk cosmological constant ensures that we have zero effective four-dimensional cosmological constant on each brane. In other words, the intrinsic geometry that is consequently induced on both branes takes the form of a four-dimensional flat Minkowski spacetime. The branes in this configuration are also referred to as critical Randall–Sundrum branes.

Relation between the four and five-dimensional Planck masses and gravitational constants

We can compute a relation between the fundamental five-dimensional mass scale M_{Pl} and the four-dimensional mass scale m_{Pl} using the gravitational part of the action (2.1):

$$S_{grav} = 2M_{Pl}^3 \int d^4x \int_{-y_c}^{y_c} dy \sqrt{-g^{(5)}}\, R. \tag{2.10}$$

Substituting the metric (2.3) into the last equation and integrating over the extra dimension yields the corresponding expression for the effective length scale on the visible brane

$$\begin{aligned} m_{Pl}^2 &= M_{Pl}^3 r_c \int_{-y_c}^{y_c} dy\, a^2(y) = 2M_{Pl}^3 r_c \int_0^{y_c} dy\, e^{-2kr_c|y|} \\ &= \frac{M_{Pl}^3}{k}\left[1 - e^{-2kr_c y_c}\right] \end{aligned} \tag{2.11}$$

where we have taken into account the orbifold symmetry in the extra dimension. The formula tells us that the four-dimensional Planck mass depends weakly on y_c in the limit of large ky_c. This suppression has been provided by the negative bulk curvature.

The following definitions

$$m_{Pl}^2 = \frac{1}{16\pi G_4}, \qquad M_{Pl}^3 = \frac{1}{16\pi G_5} \tag{2.12}$$

can be substituted into (2.11) to yield an analogous relation between the four and five-dimensional gravitational constants

$$G_4 = G_5 k \left[1 - e^{-2kr_c y_c}\right]^{-1}. \tag{2.13}$$

This expression shows that the gravitational interactions are weaker for the negative tension brane at large y_c compared to the positive tension brane at $y = 0$. Thus, in the large y_c limit, relations (2.11) and (2.13) approximate to

$$m_{Pl}^2 = k^{-1} M_{Pl}^3, \qquad G_4 = G_5 k. \tag{2.14}$$

2.1.2 Randall–Sundrum II model

The RSI model which features two parallel three-branes is now modified by alternating the roles of the branes. We now assume that the Standard Model lives on the positive tension brane at $y = 0$. Thus, the problem associated with the RSI model (*i.e.* living on a negative tension brane with matter made up of negative energy density, making gravity repulsive [38]) is now removed. Our visible universe now

lives on a brane with matter composed of positive energy density making gravity attractive. Moreover, the hidden brane of negative tension at $y = y_c$ is sent to infinity $r_c \to \infty$ and is therefore removed entirely from the setup. As a result, the circle parameterising the fifth dimension becomes non-compact, suggesting that it is possible to live in $4+n$ dimensions (where n is the number of extra spatial dimensions). We now have a single, positive tension three-brane embedded in an AdS_5 bulk of infinite dimension. This setup gives an 'alternative to compactification' and is known as the RSII model [11].

Localisation of gravity

We discuss the different nature of gravity in the RSII braneworld using a perturbative approach. There are two distinct calculations that determine that five-dimensional braneworld gravity is in fact consistent with four-dimensional general relativity. The two computations we perform next will show:

- The Newtonian gravitational potential is the property of both the four and five-dimensional gravity.

- The tensor structure of the four-dimensional massless graviton propagator can be reproduced from the five-dimensional massless graviton propagator.

Gravitational fluctuations

The study of gravitational fluctuations in the RSII scenario enables us to investigate the behaviour of gravity around a point mass source on the RSII brane. Our starting point is the derivation of the graviton wavefunction, corresponding to Kaluza–Klein excitations which are generated on the brane by the massive modes of the five-dimensional background. These four-dimensional Kaluza–Klein modes are merely imprints of the higher-dimensional gravitons and may provide vital information regarding the extra dimensions [9]. Once we have obtained the graviton wavefunction, we can compute the effective potential induced on the brane and then comment on the localisation of gravity. Our results determine that the massive Kaluza–Klein modes contribute to Newton's inverse square law of the static gravi-

tational potential between two Standard Model particles on the visible brane in the form of a power law potential. However, at large distances away from the brane (*i.e.* distances much greater than the AdS radius $r \gg k^{-1}$), we essentially recover the results of four-dimensional Einstein gravity.

For calculational purposes, the negative tension brane is reintroduced at a finite distance $y = y_c$ from the physical, positive tension brane at $y = 0$. Therefore, the negative energy brane merely acts as a 'regulator brane' and is only present for calculational purposes; it enables us to obtain a correct integration over the mass and a correct normalisation for the graviton wavefunction [39]. At the end of the calculation, we take the limit $y_c \to \infty$ which removes the regulator brane from the setup.

For simplicity, we will set the compactification radius to unity $r_c = 1$ in the analysis which follows. Taking into account the orbifold symmetry, the flat metric of (2.3) now takes the form

$$ds^2 = e^{-2k|y|}\eta_{\mu\nu}dx^\mu dx^\nu + dy^2\,, \qquad -y_c \leq y \leq y_c \tag{2.15}$$

with the branes at their respective orbifold fixed points. We assume that the warp factor is normalised at the position of the visible brane such that it is equal to unity: $a(0) = 1$. To study the spectrum of linearised gravity fluctuations around the background metric (2.15), we consider the following metric perturbation

$$g_{\mu\nu} \to g_{\mu\nu} + h_{\mu\nu} \tag{2.16}$$

where the original metric is defined as $g_{\mu\nu} = e^{-2k|y|}\eta_{\mu\nu}$ and the tensor $h_{\mu\nu}(x^\mu, y)$ corresponds to the small variations of the metric tensor. The perturbed line element then reads

$$ds^2 = \left[e^{-2k|y|}\eta_{\mu\nu} + h_{\mu\nu}(x, y)\right] dx^\mu dx^\nu + dy^2\,. \tag{2.17}$$

Gravity can be described by the transverse and traceless components of the metric perturbation $h_{\mu\nu}(x^\mu, y)$ [39]. We therefore fix the gauge such that the metric perturbation is transverse-tracefree in the bulk

$$h = h^\mu_\mu = 0\,, \qquad \partial_\nu h_\mu{}^\nu = 0\,. \tag{2.18}$$

In addition to the above gauge choice, we can also impose the Gaussian Normal coordinate system:

$$g_{yy} = 1\,, \quad g_{\mu y} = 0 \tag{2.19}$$

which immediately implies that the y-components of the metric perturbation are zero: $h_{yy} = 0$ and $h_{\mu y} = 0$. The combination of the transverse-tracefree gauge together with the Gaussian Normal coordinate system is known as the Randall–Sundrum gauge and is consistent only in vacuum. Condition (2.19) ensures that the branes remain fixed at their original positions. Later, we will see that the inclusion of a matter source on the brane renders the Randall–Sundrum gauge inconsistent. In this situation, it is necessary to define a new coordinate system in which the branes are once again Gaussian Normal. However, for the analysis which follows, we will use the Randall–Sundrum gauge.

We can rewrite the five-dimensional Einstein equations (2.2) entirely in terms of the Ricci tensor

$$R_{ab} = \frac{\Lambda}{6M^3} g_{ab} + \frac{\sigma}{3M^3} g_{ab}[\delta] - \frac{\sigma}{4M^3} g_{\mu\nu}\delta^{\mu}_{a}\delta^{\nu}_{b}[\delta] \tag{2.20}$$

where $[\delta] = [\delta(y) - \delta(y - y_c)]$ represents the boundary of the spacetime. We use the definition for the perturbation of the Ricci tensor, also known as the Lichnerowicz operator

$$\Delta_L h_{ab} \equiv -2\delta R_{ab} = \Box^{(5)} h_{ab} + 2R_a{}^c{}_b{}^d h_{cd} - 2\nabla_{(a}\nabla_{|c|}\bar{h}^{c}_{b)} - 2R_{c(a}h_{b)}{}^{c} \tag{2.21}$$

to compute the non-zero gauge quantities[1]

$$\begin{aligned} \Box^{(5)} h_{\mu\nu} &= a^{-2}\Box^{(4)} h_{\mu\nu} + h''_{\mu\nu} - 2h_{\mu\nu}\left[a^{-1}a'' + 2\left(a^{-1}a'\right)^2\right] \\ &= a^{-2}\Box^{(4)} h_{\mu\nu} + h''_{\mu\nu} - 6k^2 h_{\mu\nu} \end{aligned} \tag{2.22}$$

$$R_{\mu}{}^{c}{}_{\nu}{}^{d} h_{cd} = \left(a^{-1}a'\right)^2 h_{\mu\nu} = k^2 h_{\mu\nu} \tag{2.23}$$

$$R_{c(\mu}h_{\nu)}{}^{c} = \frac{\Lambda}{6M^3} h_{\mu\nu} + \frac{\sigma}{12M^3} h_{\mu\nu}[\delta]\,. \tag{2.24}$$

[1]The components of the Lichnerowicz operator are given in terms of the warp factor in Appendix B.2.

The operator $\Box^{(5)} = g^{\alpha\beta}\nabla_\alpha\nabla_\beta$ denotes the five-dimensional covariant Laplacian operator for curved spacetime. Its corresponding four-dimensional analogue is given by the operator $\Box^{(4)} = \eta^{\mu\nu}\partial_\mu\partial_\nu$. We note that the Randall–Sundrum gauge has simplified the gauge quantities significantly. Furthermore, once we take the regulator brane to infinity, there is no vector or scalar components of the linearised field equations. If we look at the tensor perturbation of the field equations

$$\Box^{(4)}h_{\mu\nu} + \left[a^4\left(a^{-2}h_{\mu\nu}\right)'\right]' = 0 \tag{2.25}$$

this can be solved using the boundary condition imposed by the three-brane. Equation (2.25) and its corresponding boundary condition at the location of the visible brane can be expressed as

$$\left[\partial_y^2 + a^{-2}\Box^{(4)} - 4k^2\right]h_{\mu\nu} = 0 \tag{2.26}$$

$$\left(\partial_y + 2k\right)h_{\mu\nu}\Big|_{y=0} = 0\,. \tag{2.27}$$

The following separation of variables ansatz

$$h_{\mu\nu}(x^\mu, y) = \psi_m(y)e^{ip_\mu x^\mu} \tag{2.28}$$

determines the solution of (2.26) in terms of four-dimensional plane waves. Here, we note that the higher-dimensional particle carries extra-dimensional momentum and projects it onto the four-dimensional brane [9]. Thus, the effective four-dimensional momentum p_μ of the higher-dimensional graviton is related to the effective mass m of the higher-dimensional gravitational field by the relation $p_\mu p^\mu = -m^2$. Equation (2.28) enables us to rewrite (2.26) and (2.27) as

$$\psi'' + \frac{m^2}{a^2(y)}\psi - 4k^2\psi = 0 \tag{2.29}$$

$$\left(\psi' + 2k\psi\right)\Big|_{y=0} = 0 \tag{2.30}$$

where $\psi \equiv \psi_m$ (we have dropped the subscripts) represents the physical graviton of the four-dimensional effective theory.

Since we have obtained the tensor equation of motion and its corresponding boundary condition, we now proceed to determine the full mass spectrum of the gravitons.

We show that there are two types of solutions which can be extracted from the above set of equations [40]:

• The zero mode solution is given by $m = 0$. This mode (ψ_0) describes the massless graviton which is highly likely to be concentrated in the region near the brane. This solution reproduces the behaviour of four-dimensional Einstein gravity.

• The massive modes have solutions given by $m > 0$. These modes (ψ_m) represent the Kaluza–Klein excitations and are weakly coupled to the brane. These solutions lead to the modification of standard four-dimensional gravity.

The zero mode eigenstate

We proceed to solve equations (2.29) and (2.30) for the massless graviton mode. Setting $m = 0$ in (2.29) and applying the boundary condition (2.30) yields the zero mode solution

$$\psi_0(y) = \mathcal{N}_0 e^{-2k|y|} \tag{2.31}$$

where $\mathcal{N}_0$ is the normalisation constant. The wavefunction of the Kaluza–Klein gravitons is normalised according to the integral

$$\int_{-y_c}^{y_c} \frac{1}{a^2(y)} |\psi_0|^2 dy = 2 \int_0^{y_c} \frac{1}{a^2(y)} |\psi_0|^2 dy = 1 \tag{2.32}$$

which determines the normalisation constant

$$\mathcal{N}_0^2 = k(1 - e^{-2ky_c})^{-1} . \tag{2.33}$$

The massless eigenstate is therefore

$$\psi_0 = \frac{\sqrt{k} e^{-2k|y|}}{\sqrt{1 - e^{-2ky_c}}} \tag{2.34}$$

and is clearly normalisable with a sharp peak at $y = 0$. The warping behaviour indicates that the coupling of gravity to the particles on the negative tension brane at large distances is weaker than at the positive tension brane. We have therefore obtained a massless bound graviton state which is localised on the brane, corresponding to four-dimensional gravity.

The massive eigenstates

In addition to the massless four-dimensional graviton mode (2.34), there also exists massive graviton modes which are sensed on the brane. They correspond to the five-dimensional gravitons which have escaped from the four-dimensional hypersurface and into the extra dimension. In order to determine the massive eigenfunction, we solve equations (2.29) and (2.30) for the case where $m > 0$.

It is convenient to change from the physical coordinate to the conformal coordinate $y \longrightarrow z(y)$ by the following change of variables

$$z = \frac{1}{k} e^{k|y|} . \tag{2.35}$$

Hence, the line element (2.15) can be re-expressed as

$$ds^2 = a(z)^2 \left(\eta_{\mu\nu} dx^\mu dx^\nu + dz^2\right) \tag{2.36}$$

and equations (2.29) and (2.30) become

$$\ddot{\psi} + \frac{1}{z}\dot{\psi} + \left[m^2 - \frac{4}{z^2}\right]\psi = 0 \tag{2.37}$$

$$\dot{\psi} + \frac{2}{z}\psi\Big|_{z=k^{-1}} = 0 \tag{2.38}$$

where the overdot denotes differentiation with respect to the conformal variable z. Thus, the above change of variables makes the linearised tensor field equation and its corresponding boundary condition much easier to implement. Equation (2.37) is a Bessel differential equation of order two, with solution given by

$$\psi(z) = \mathcal{A}_m J_2(mz) + \mathcal{B}_m N_2(mz) \tag{2.39}$$

where $\mathcal{A}_m$ and $\mathcal{B}_m$ are arbitrary constants (independent of z) and $J_2(mz)$ and $N_2(mz)$ represent second order Bessel functions of the first and second kind, respectively. Here, m denotes the mass of the excitation. We can determine the constant $\mathcal{A}_m$ from the boundary condition (2.38) at $z = k^{-1}$ together with the following recurrence relation for Bessel functions [41]

$$\partial_x J_n(x) + \frac{n}{x} J_n(x) = J_{n-1}(x) . \tag{2.40}$$

This yields the linear combination

$$\psi(z) = \mathcal{B}_m \left[-\frac{N_1(\frac{m}{k})}{J_1(\frac{m}{k})} J_2(mz) + N_2(mz) \right] \tag{2.41}$$

where $\mathcal{B}_m$ represents a normalisation constant. Thus, for $m > 0$, we have a continuous mass spectrum on the brane. To determine the normalisation constant, we use the following integral for the normalisation of the massive graviton wavefunction:

$$\int_{-z_c}^{z_c} \frac{1}{a(z)} \psi_m^{(\alpha)} \psi_m^{(\beta)} \, dz = 2 \int_0^{z_c} \frac{1}{a(z)} \psi_m^{(\alpha)} \psi_m^{(\beta)} \, dz = \delta(\alpha - \beta) \, . \tag{2.42}$$

We also make use of the continuum integral (Bessel function orthonormality relation)

$$\int_0^\infty x J(\alpha x) J(\beta x) \, dx = \frac{1}{\alpha} \delta(\alpha - \beta) \, . \tag{2.43}$$

The last two integrals vanish for $\alpha \neq \beta$. However, for $\alpha = \beta$ we determine the normalisation constant

$$\mathcal{B}_m^2 = \frac{m}{2k} \left[\frac{J_1^2(\frac{m}{k})}{N_1^2(\frac{m}{k}) + J_1^2(\frac{m}{k})} \right] \tag{2.44}$$

which can be inserted back into the eigenstate (2.41) to produce the normalised Kaluza–Klein graviton wavefunction in the physical coordinate system

$$\psi_m(y) = \sqrt{\frac{m}{2k}} \frac{\left[J_1(\frac{m}{k}) N_2(\frac{m}{k} e^{k|y|}) - N_1(\frac{m}{k}) J_2(\frac{m}{k} e^{k|y|}) \right]}{\sqrt{N_1^2(\frac{m}{k}) + J_1^2(\frac{m}{k})}} \, . \tag{2.45}$$

Asymptotics of the Bessel function

We now study the asymptotics of Bessel functions in order to determine the behaviour of the eigenstate (2.45) for large and small arguments. Generally, for large values of parameter x say, the Bessel functions behave according to [41,43]:

$$J_p(x) \sim \sqrt{\frac{2}{\pi x}} \cos\left(x - \frac{\pi}{4} - \frac{p\pi}{2} \right) , \qquad N_p(x) \sim \sqrt{\frac{2}{\pi x}} \sin\left(x - \frac{\pi}{4} - \frac{p\pi}{2} \right) . \tag{2.46}$$

If we apply this rule to the Bessel functions of (2.45) for large values of y, we obtain the following approximations

$$\sqrt{\frac{m}{2k}}J_2\left(\frac{m}{k}e^{ky}\right) \sim \frac{1}{\sqrt{\pi e^{ky}}}\cos\left(\frac{m}{k}e^{ky}-\frac{5\pi}{4}\right)$$

$$\sqrt{\frac{m}{2k}}N_2\left(\frac{m}{k}e^{ky}\right) \sim \frac{1}{\sqrt{\pi e^{ky}}}\sin\left(\frac{m}{k}e^{ky}-\frac{5\pi}{4}\right). \tag{2.47}$$

Substituting (2.47) into (2.45) yields a wavefunction with a sinusoidal effect:

$$\psi_m(y) = \frac{\left[J_1\left(\frac{m}{k}\right)\sin\left(\frac{m}{k}e^{ky}-\frac{5\pi}{4}\right) - N_1\left(\frac{m}{k}\right)\cos\left(\frac{m}{k}e^{ky}-\frac{5\pi}{4}\right)\right]}{\sqrt{\pi e^{ky}}\sqrt{N_1^2(\frac{m}{k})+J_1^2(\frac{m}{k})}}. \tag{2.48}$$

Conversely, for small values of y such as $y = 0$, the wavefunctions become suppressed at the brane:

$$\psi_m(0) = \sqrt{\frac{m}{2k}}\frac{\left[J_1(\frac{m}{k})N_2(\frac{m}{k}) - N_1(\frac{m}{k})J_2(\frac{m}{k})\right]}{\sqrt{N_1^2(\frac{m}{k})+J_1^2(\frac{m}{k})}} \sim -\sqrt{\frac{m}{2k}} \qquad (m \ll k) \tag{2.49}$$

where in the last line we have used the following identity [39,41,44] in the numerator:

$$J_n(x)N_{n+1}(x) - N_n(x)J_{n+1}(x) = -\frac{2}{\pi x} \tag{2.50}$$

and the following first order approximations for Bessel functions [41] in the denominator:

$$J_n(x) \sim \frac{1}{n!}\left(\frac{x}{2}\right)^n, \qquad N_n(x) \sim -\frac{(n-1)!}{\pi}\left(\frac{x}{2}\right)^{-n}. \tag{2.51}$$

To sum up, we have obtained a full mass spectrum of graviton states; the massless graviton zero mode ($m = 0$) together with the tower of massive Kaluza–Klein modes ($m > 0$). The approximate value of the massive eigenstate at the region of the brane (2.49) will be used next to compute the Newtonian potential on the brane and the four-dimensional graviton propagator.

2.1.3 The Newtonian potential on the brane

The graviton wavefunction enables us to compute the static gravitational potential between two unit point masses which are placed a distance r apart on the visible brane. Physically, when the two particles on the brane interact, they communicate

by the emission of a virtual graviton in a scattering process [39]. Consequently, a gravitational potential is generated. The total potential is then given by the sum of the potentials of the massless zero mode and the massive Kaluza–Klein modes

$$V(r) = V_N(r) + V_{KK}(r) \tag{2.52}$$

where the gravitational potential for a massless graviton is simply

$$V_N(r) = -\frac{G_4}{r} \tag{2.53}$$

and G_4 is the four-dimensional Newton constant. In order to deduce the overall potential (2.52), we need to compute the contribution to the gravitational potential $V_{KK}(r)$ generated by the massive modes. Calculations from field theory reveal that the scattering process between two particles actually corresponds to a Yukawa-type interaction [7,46]. Thus, the general form of the potential corresponding to a Yukawa interaction is given by

$$V_{KK}(r) = -G_5 \int_0^\infty dm \frac{e^{-mr}}{r} |\psi_m(y=0)|^2 . \tag{2.54}$$

Using the standard definite integral

$$\int_0^\infty x^n e^{-ax} dx = \frac{n!}{a^{n+1}} \quad \text{for} \quad n = 0, 1, 2 \ldots \text{and} \quad a > 0 \tag{2.55}$$

where $x = m$, $n = 1$ and $a = r$ in our case, and inserting (2.49) into (2.54) gives

$$V_{KK}(r) \sim -\frac{G_4}{2k^2 r^3} \tag{2.56}$$

where we have used (2.14) to set $G_4 = G_5 k$. Inserting the last line into (2.52) yields the total gravitational potential

$$V(r) \sim -\frac{G_4}{r}\left(1 + \frac{1}{2k^2 r^2}\right) . \tag{2.57}$$

The first term of the above expression represents the dominant four-dimensional gravity term and corresponds to the massless graviton, which is highly likely to be found in the region of the visible brane. The second term takes the form of a power law potential and gives the modifications to the Newtonian potential, arising

from the massive modes due to the fifth dimension. The probability of the massive Kaluza–Klein modes being found on the brane is highly suppressed because at distances much greater than the AdS_5 radius: $r \gg k^{-1}$, the corrections of the Newtonian potential become negligible. This implies that gravity experienced by matter on the positive tension brane is effectively four-dimensional. The model is therefore theoretically consistent with experimental tests of Newton's inverse square law at large distances. Thus, the RSII braneworld has succeeded in exhibiting brane-localised gravity and is a viable model to represent our universe.

2.1.4 The brane graviton propagator

A second confirmation to show that the RSII model does reproduce the results of four-dimensional Einstein gravity is provided by the computation of the brane graviton propagator. Generally, the tensor structure for an n-dimensional massless propagator is given by

$$G_n(x-\tilde{x})_{\mu\nu\rho\sigma} = \int \frac{d^n p}{(2\pi)^n} \frac{e^{ip.(x-\tilde{x})}}{p^2-(\omega+i\epsilon)^2} \left(\frac{1}{2}(g_{\mu\rho}g_{\nu\sigma}+g_{\mu\sigma}g_{\nu\rho}) - \frac{1}{n-2} g_{\mu\nu}g_{\rho\sigma} \right) . \tag{2.58}$$

Since we are interested in the five and four-dimensional spacetimes, we will set $n = 5$ and $n = 4$ in the above equation. This determines the explicit form of the massless bulk and brane propagators [47]:

$$G_5(x-\tilde{x})_{\mu\nu\rho\sigma} = \int \frac{d^5 p}{(2\pi)^5} \frac{e^{ip.(x-\tilde{x})}}{p^2-(\omega+i\epsilon)^2} \left(\frac{1}{2}(g_{\mu\rho}g_{\nu\sigma}+g_{\mu\sigma}g_{\nu\rho}) - \frac{1}{3} g_{\mu\nu}g_{\rho\sigma} \right) \tag{2.59}$$

$$G_4(x-\tilde{x})_{\mu\nu\rho\sigma} = \int \frac{d^4 p}{(2\pi)^4} \frac{e^{ip.(x-\tilde{x})}}{p^2-(\omega+i\epsilon)^2} \left(\frac{1}{2}(g_{\mu\rho}g_{\nu\sigma}+g_{\mu\sigma}g_{\nu\rho}) - \frac{1}{2} g_{\mu\nu}g_{\rho\sigma} \right) \tag{2.60}$$

The last term of each of the above expressions contains a different numerical factor, implying that the tensor structure in five and four dimensions is clearly distinct. This discrepancy originates from the three additional polarisation states which are present in the five-dimensional theory [48, 49]. Thus, when we compute the brane propagator, we must remove these unwanted states. The explicit calculation of the brane graviton propagator in the RSII braneworld has been given in the original papers by Garriga and Tanaka [50] and by Giddings, Katz and Randall [51].

Calculation of the Graviton propagator

We concentrate on the derivation of the graviton propagator. As we will shortly see, it is useful to introduce an additional matter source on the brane as this will elucidate the cancellation of the unwanted polarisation states. We employ the methods of [50]. In the original coordinate system (x^μ, y), the unperturbed brane without matter is located at the coordinate origin $y = 0$. However, the inclusion of an arbitrary matter source on the brane causes the brane to bend, altering the brane position to $y = -\xi^y$. Thus, in order to explore the effects of the brane 'flutter', it is convenient to introduce a new coordinate system $(\bar{x^\mu}, \bar{y})$ in which the brane will once again lie at the coordinate origin $\bar{y} = 0$. In this new system, the brane respects the Gaussian Normal condition: $\bar{g}_{yy} = 1$, $\bar{g}_{\mu y} = 0$ and is once again flat. We will use the overbar notation to denote quantities in the new coordinate system. The two distinct systems are related by the following parameterisation

$$y \rightarrow y + \xi^y(x^\mu, y) \tag{2.61}$$

$$x^\mu \rightarrow x^\mu + \xi^\mu(x^\mu, y) \tag{2.62}$$

where ξ^y and ξ^μ correspond to infinitesimal fluctuations in the coordinates (x^μ, y). These arbitrary functions parameterise the brane by encoding both the brane-bending effect and the transformation between the two distinct coordinate systems [42]. Moreover, (2.61) and (2.62) ensure that the new coordinate system also satisfies the metric (2.17). Using the gauge invariance property

$$h_{ab} \rightarrow h_{ab} + \nabla_a \xi_b + \nabla_b \xi_a \tag{2.63}$$

we can readily obtain the two gauge parameters

$$\xi^y = f(x^\mu), \qquad \xi^\mu = -\int \frac{1}{a^2} f_{,\nu} \eta^{\mu\nu} dy + \eta^{\mu\nu} \epsilon_\nu(x^\mu) \tag{2.64}$$

where $f(x^\mu)$ is interpreted as the brane bending term. In the subsequent analysis, we will drop the $\epsilon_\nu(x^\mu)$ term which arises from an integration constant.[2] The metric

[2]The full details of the gauge transformations are covered in Appendix B.6.

perturbation relating the two distinct coordinate systems (*i.e.* the Randall–Sundrum gauge and the Gaussian Normal gauge)

$$h_{\mu\nu} = \bar{h}_{\mu\nu} - 2a^2 \int \frac{1}{a^2} f_{,\mu\nu} dy + 2aa' \eta_{\mu\nu} f \tag{2.65}$$

takes account of the brane fluctuation parameter. Here, $h_{\mu\nu}$ physically corresponds to the transverse-tracefree four-dimensional tensor (*i.e.* in the Randall–Sundrum gauge) and $\bar{h}_{\mu\nu}$ corresponds to the metric tensor in the Gaussian Normal gauge. The last equation can be expressed more explicitly as

$$h_{\mu\nu} = \bar{h}_{\mu\nu} - \frac{1}{k} f_{,\mu\nu} - 2kf\eta_{\mu\nu} e^{-2k|y|} \,. \tag{2.66}$$

To solve the (non-vacuum) equations of motion, we need to take into account of the brane by imposing the Israel junction conditions at the boundary of the spacetime at which the brane is located. The junction conditions correspond to five-dimensional generalisations of the usual four-dimensional boundary conditions. If we exclude the brane tension, then the jump in extrinsic curvature $\triangle K_{\mu\nu}$ across the two sides of the wall is related to the brane energy-momentum tensor $T_{\mu\nu}$ via

$$\triangle K_{\mu\nu} = K_{\mu\nu}(\bar{y} = 0^+) - K_{\mu\nu}(\bar{y} = 0^-) = -\kappa_5 (T_{\mu\nu} - \frac{1}{3} T \eta_{\mu\nu}) \tag{2.67}$$

where the trace of the energy-momentum is denoted as $T^{\lambda}_{\lambda} = T$ and $\kappa_5 = 8\pi G_5$. Since we are assuming the simplifying assumption of Z_2-symmetry across the wall, then the jump in extrinsic curvature is double the value of the extrinsic curvature on one side of the brane. The linearised tensor field equation (2.25) and the boundary condition (2.27) are now modified and take the form:

$$a^{-2} \Box^{(4)} \bar{h}_{\mu\nu} + a^{-2} \left[a^4 \left(a^{-2} \bar{h}_{\mu\nu} \right)' \right]' = -2\kappa_5 \delta(y) (T_{\mu\nu} - \frac{1}{3} T \eta_{\mu\nu}) \tag{2.68}$$

$$\bar{h}'_{\mu\nu} + 2k \bar{h}_{\mu\nu} \Big|_{\bar{y}=0^+} = -\kappa_5 (T_{\mu\nu} - \frac{1}{3} T \eta_{\mu\nu}) \,. \tag{2.69}$$

The latter equations therefore account for a general matter perturbation due to the presence of an arbitrary matter source on the brane. Equation (2.69) represents the boundary condition in the Gaussian Normal gauge. The corresponding boundary

condition in terms of the variables of the original coordinate system (*i.e.* in the RS gauge) is obtained by substituting $\bar{h}_{\mu\nu}$ from (2.66) into (2.69). This gives

$$h'_{\mu\nu} + 2kh_{\mu\nu}\Big|_{y=0^+} = -\kappa_5(T_{\mu\nu} - \frac{1}{3}T\eta_{\mu\nu}) - 2f_{,\mu\nu} \tag{2.70}$$

where we notice the extra 'flutter' term appearing in the last term of the above equation. The bulk equation of motion without a matter source (2.26) can now be conveniently combined with the modified bulk boundary condition (2.70) to give

$$\left[e^{2k|y|}\Box^{(4)} + \partial_y^2 - 4k^2 + 4k\delta(y)\right] h_{\mu\nu} = -2\delta(y)\left[\kappa_5(T_{\mu\nu} - \frac{1}{3}T\eta_{\mu\nu}) + 2f_{,\mu\nu}\right] \tag{2.71}$$

where the discontinuity at the wall has been considered through the delta function. We note that the additional factor of 2 arises from the Z_2-symmetry. As in Ref. [50], the five-dimensional retarded Green's function is defined as

$$\left[e^{2k|y|}\Box^{(4)} + \partial_y^2 - 4k^2 + 4k\delta(y)\right] G_R(x,y;\tilde{x},\tilde{y}) = \delta^{(4)}(x-\tilde{x})\delta(y-\tilde{y}) \tag{2.72}$$

with the formal solution of (2.71) given by

$$h_{\mu\nu}(x,y) = -2\kappa_5 \int d^4\tilde{x}\; G_R(x,y;\tilde{x},0)\left(T_{\mu\nu} - \frac{1}{3}T\eta_{\mu\nu} + \frac{2}{\kappa_5}f_{,\mu\nu}\right)(\tilde{x})\,. \tag{2.73}$$

Thus, in order to evaluate the metric induced on the brane, we need to first determine the brane bending parameter. Since the metric perturbation in the RS gauge is traceless $h^\mu_\mu = 0$, this implies that the RHS of (2.73) must also be traceless. This gives us an important implicit expression for the displacement of the brane

$$\Box^{(4)} f = \frac{\kappa_5 T}{6} \tag{2.74}$$

which shows the coupling between the brane bending parameter and the trace of the perturbation of the brane energy-momentum. Since we are interested in the perturbation on the brane, we return back to Gaussian Normal coordinates. At position $y = 0$, equation (2.66) becomes

$$\bar{h}_{\mu\nu} = h^{(m)}_{\mu\nu} + h^{(f)}_{\mu\nu} + \frac{1}{k}f_{,\mu\nu} + 2kf\eta_{\mu\nu} \tag{2.75}$$

where we have decomposed $h_{\mu\nu}$ into a matter field perturbation and a brane bending perturbation, respectively:

$$h_{\mu\nu} = h^{(m)}_{\mu\nu} + h^{(f)}_{\mu\nu} \tag{2.76}$$

where

$$h^{(m)}_{\mu\nu} = -2\kappa_5 \int d^4\tilde{x}\; G_R(x,y;\tilde{x},0)(T_{\mu\nu} - \frac{1}{3}T\eta_{\mu\nu})(\tilde{x}) \tag{2.77}$$

$$h^{(f)}_{\mu\nu} = -4 \int d^4\tilde{x}\; G_R(x,y;\tilde{x},0) f_{,\mu\nu}(\tilde{x})\,. \tag{2.78}$$

If we gauge away some of the terms appropriately in (2.75) and set $y = 0$ in (2.77), we can obtain a simple expression for the metric perturbation on the brane

$$\bar{h}_{\mu\nu}(x,0) = h^{(m)}_{\mu\nu} + 2kf\eta_{\mu\nu}\,. \tag{2.79}$$

In order to compute the induced metric on the brane $\bar{h}_{\mu\nu}(x,0)$, we first need to define the Green's function and give the explicit solution of (2.74) for the brane fluctuation parameter.

The Green's function and the brane displacement

The Green's function[3] which is required to solve for the metric perturbation in the RSII setup [11] is defined by

$$G_R(x,y;\tilde{x},\tilde{y}) = -\int \frac{d^4p}{(2\pi)^4} e^{ip.(x-\tilde{x})} \left[\frac{k\; a^2(y)a^2(\tilde{y})}{p^2 - (\omega + i\epsilon)^2} + \int_0^\infty dm \frac{\psi_m(y)\psi_m(\tilde{y})}{p^2 + m^2 - (\omega + i\epsilon)^2} \right] \tag{2.80}$$

where the first and second terms correspond to the bound state of the five-dimensional graviton (*i.e.* the zero mode) and the continuum tower of massive Kaluza–Klein states, respectively. The massive wavefunction $\psi_m(y)$ has been identified previously in (2.45). The above expression can be written in a more compact form

$$G_R(x,y;\tilde{x},\tilde{y}) = k\; a^2(y)a^2(\tilde{y})\; D_0(x-\tilde{x}) + \int_0^\infty dm\; D_m(x-\tilde{x})\psi_m(y)\psi_m(\tilde{y}) \tag{2.81}$$

[3] A detailed derivation of the Green's function is given in [52].

where the massless and massive graviton propagators (in the standard flat four dimensions) are given respectively as:

$$D_0(x-\tilde{x}) = -\int \frac{d^4p}{(2\pi)^4} \frac{e^{ip.(x-\tilde{x})}}{[p^2-(\omega+i\epsilon)^2]} \tag{2.82}$$

$$D_m(x-\tilde{x}) = -\int \frac{d^4p}{(2\pi)^4} \frac{e^{ip.(x-\tilde{x})}}{[p^2+m^2-(\omega+i\epsilon)^2]} . \tag{2.83}$$

Since we are interested in the interaction of two point masses on the four-dimensional hypersurface, we restrict the perturbation exclusively to the brane $y = \tilde{y} = 0$ (or $z = \tilde{z} = k^{-1}$). Then, the Green's function is simply

$$G_R(x,0;\tilde{x},0) = k\, D_0(x-\tilde{x}) + \int_0^\infty dm\; D_m(x-\tilde{x})|\psi_m(0)|^2 . \tag{2.84}$$

Here, we also give the formal solution of (2.74) in terms of the massless propagator

$$f(x) = \kappa_5 \int d^4\tilde{x}\; D_0(x-\tilde{x}) \frac{T(\tilde{x})}{6} . \tag{2.85}$$

The zero mode contribution

For the massless mode, we are only interested in the physics on the brane. We can therefore safely ignore the contributions which arise from the massive graviton modes in the bulk. Then, the behaviour of the induced metric at long distances would be dominated by the zero mode. The substitution of the first term of (2.84)

$$G_R^{zm}(x,0;\tilde{x},0) = k\, D_0(x-\tilde{x}) \tag{2.86}$$

together with the brane fluctuation parameter (2.85) into (2.79) gives

$$\begin{aligned} \bar{h}_{\mu\nu}^{zm} &= -2\kappa_5 k \int d^4\tilde{x}\; D_0(x-\tilde{x}) \left(T_{\mu\nu} - \frac{1}{3} T\eta_{\mu\nu}\right) + 2\kappa_5 \eta_{\mu\nu} k \int d^4\tilde{x}\; D_0(x-\tilde{x}) \frac{T}{6} \\ &= -2\kappa_5 k \int d^4\tilde{x}\; D_0(x-\tilde{x}) \left(T_{\mu\nu} - \frac{1}{3} T\eta_{\mu\nu} - \frac{1}{6} T\eta_{\mu\nu}\right) . \end{aligned} \tag{2.87}$$

If the last term was absent we would have obtained five-dimensional gravity, however this is not the case. Using the definition (2.14) of the four-dimensional Newton constant $G_4 = G_5 k$, we find

$$\bar{h}_{\mu\nu}^{zm} = -16\pi G_4 \int d^4\tilde{x}\; D_0(x-\tilde{x}) \left(T_{\mu\nu} - \frac{1}{2} T\eta_{\mu\nu}\right) \tag{2.88}$$

which is precisely the metric corresponding to four-dimensional perturbative Einstein gravity. Thus, the desired cancellation of the factor $\frac{1}{3} \rightarrow \frac{1}{2}$ in the metric perturbation has been obtained, giving us a second confirmation that the RSII braneworld does relate to our observable universe. Hence, all classical predictions of general relativity (*e.g.* the bending of light around the sun, the precession rate of orbit around the planet Mercury [47]) in the RSII model are consistently reproduced.

Corrections to Einstein gravity

We now determine the contribution arising from the massive continuum modes which we had previously ignored. Inserting the second term of (2.84)

$$G_R^{ctm}(x,0;\tilde{x},0) = \int_0^\infty dm\ D_m(x-\tilde{x})\ |\psi(0)|^2 \tag{2.89}$$

into (2.77) yields the contribution to (2.79) for the massive eigenstates. The metric perturbation for the massive modes is then given by

$$\bar{h}_{\mu\nu}^{ctm} = -2\kappa_5 \int d^4\tilde{x} \int_0^\infty dm\ \frac{m}{2k}\ D_m(x-\tilde{x})\ \left(T_{\mu\nu} - \frac{1}{3}T\eta_{\mu\nu}\right) \tag{2.90}$$

where we have used equation (2.49) in the last line. The total metric perturbation is obtained by adding (2.88) and (2.90):

$$\bar{h}_{\mu\nu} = \bar{h}_{\mu\nu}^{zm} + \bar{h}_{\mu\nu}^{ctm} \tag{2.91}$$

which gives the following expression

$$\begin{aligned}\bar{h}_{\mu\nu} = &-2\kappa_5 k \int d^4\tilde{x}\ D_0(x-\tilde{x})(T_{\mu\nu} - \frac{1}{2}T\eta_{\mu\nu}) \\ &- 2\kappa_5 k \int d^4\tilde{x} \int_0^\infty dm\ \frac{m}{2k^2} D_m(x-\tilde{x})(T_{\mu\nu} - \frac{1}{3}T\eta_{\mu\nu})\,.\end{aligned} \tag{2.92}$$

For the stationary (static) case, the Green's function $G_R(\mathbf{x}, y; \tilde{\mathbf{x}}, \tilde{y})$ for the Laplacian operator [50] is related to the previous Green's function $G_R(x, y; \tilde{x}, \tilde{y})$ by

$$G_R(\mathbf{x}, y; \tilde{\mathbf{x}}, \tilde{y}) = \int_{-\infty}^\infty d\tilde{t}\ G_R(x, y; \tilde{x}, \tilde{y}) \tag{2.93}$$

where $\mathbf{x}$ denotes the spatial coordinates on the brane. More explicitly, the last equation is given by [45]

$$G_R(\mathbf{x}, y; \tilde{\mathbf{x}}, \tilde{y}) = -\frac{1}{4\pi r}\left[ka^2(y)a^2(\tilde{y}) + \int_0^\infty dm\ \psi_m(y)\psi_m(\tilde{y})\ e^{-mr}\right] \tag{2.94}$$

where $\psi_m(y)$ is the mode function given in (2.45) and $r \equiv |\mathbf{x} - \tilde{\mathbf{x}}|$. On the brane, the Green's function (for the Laplace operator) takes the form

$$G_R(\mathbf{x}, 0; \tilde{\mathbf{x}}, 0) = -\frac{k}{4\pi r}\left[1 + \int_0^\infty dm\ \frac{m}{2k^2}\ e^{-mr}\right] \tag{2.95}$$

$$= -\frac{k}{4\pi r}\left[1 + \frac{1}{2k^2r^2}\right] \tag{2.96}$$

where, in the last two lines, we have used the definition of the mode function (2.49) evaluated at $y = 0$. We have also used the standard integral given in (2.55) together with the following relations

$$\int d^4\tilde{x}\ D_0(x - \tilde{x})\ \delta(\tilde{x}) = -\frac{1}{4\pi r}\,, \qquad \int d^4\tilde{x}\ D_m(x - \tilde{x})\ \delta(\tilde{x}) = -\frac{e^{-mr}}{4\pi r}\,. \tag{2.97}$$

Inserting (2.97) into (2.92) yields the metric perturbation outside a spherical source

$$\bar{h}_{\mu\nu}(x, 0) = \frac{2G_4}{r}\int d^3\tilde{x}\left[2\left(T_{\mu\nu} - \frac{1}{2}T\eta_{\mu\nu}\right) + \frac{1}{k^2r^2}\left(T_{\mu\nu} - \frac{1}{3}T\eta_{\mu\nu}\right)\right]\,. \tag{2.98}$$

In order to deduce the correction to Einstein gravity explicitly, we consider the effect of a point mass source [46] defined by

$$T_{ab} \sim m\delta^0_a\delta^0_b\delta(\mathbf{r})\delta(y)\,, \qquad T \sim m\delta(\mathbf{r})\,. \tag{2.99}$$

Inserting (2.99) into (2.98) yields the desired expression for the metric perturbation on the brane

$$\bar{h}_{\mu\nu}(x, 0) = \frac{2G_4m}{r}\left[\mathrm{diag}(1, 1, 1, 1) + \frac{1}{3k^2r^2}\mathrm{diag}(2, 1, 1, 1)\right] \tag{2.100}$$

with the corresponding linearised metric components

$$\bar{h}_{tt} = \frac{2G_4m}{r}\left(1 + \frac{2}{3k^2r^2}\right)\,, \qquad \bar{h}_{ij} = \frac{2G_4m}{r}\left(1 + \frac{1}{3k^2r^2}\right)\delta_{ij}\,. \tag{2.101}$$

We can then deduce the Newtonian potential describing the attraction between two particles a distance r apart on the brane:

$$\phi(r) \equiv \frac{1}{2}\bar{h}_{tt} = \frac{G_4 m}{r}\left(1 + \frac{2}{3k^2r^2}\right) . \tag{2.102}$$

Again, the first term of the Newtonian potential corresponds to the massless graviton mode whereas the second term denotes the contribution arising from the massive Kaluza–Klein modes. Clearly the corrections are suppressed at large distances away from the brane and the effects of standard non-brane gravity are restored for distances much greater than the Anti-de Sitter radius $r \gg k^{-1}$.

We note that the corrections in (2.102) differ by a factor of 4/3 from the corrections computed earlier for the Yukawa-type interaction (2.57). The modification in the tensor structure arises as matter sources were not included earlier when the Yukawa potential was formulated. Thus, the relative 4/3 factor originates from the massive modes and is a net result of the brane-bending effect [39]. However, the overall form of the Newtonian potential[4] in both cases stays the same:

$$V(r) \sim -\frac{G_4}{r}\left(1 + \triangle r\right) , \qquad \triangle(r) \sim \frac{1}{k^2r^2} . \tag{2.103}$$

We note that the Garriga–Tanaka computation of the Newtonian potential (2.102) is the correct (and accurate) calculation.

Summary

In this section we have given two detailed derivations that confirm the RSII model is a candidate model to represent our universe, *i.e.* both derivations show that gravity is localised on the brane. First, we computed the Newtonian potential on the brane. We found that the corrections to the potential are suppressed at large distances from the brane, indicating an effective four-dimensional Newtonian potential. A second confirmation of brane-localised gravity was provided through the computation of

[4]See the following references for the computation of the Newtonian potential: In [39, 44] the authors determine the Newtonian potential without using the brane-bending effect whereas in [53] the brane-bending effect is used.

the brane graviton propagator. The consideration of an addition matter source on the brane caused the brane to 'flutter'. This led to a brane fluctuation parameter which turned out to be a crucial ingredient in the analysis; it exactly compensates for the unwanted states which are present in the five-dimensional theory. Thus, the cancellation of the additional states in the bulk theory yields a formula for the brane graviton propagator with correct tensor structure corresponding to four-dimensional linearised gravity. Hence, both computations show that even with an extra dimension of infinite size, the bulk curvature provides an effective compactification, yielding the behaviour of four-dimensional Einstein gravity. Thus, the RSII braneworld is a theoretically viable model describing our universe.

2.2 Hořava–Witten model of heterotic M-theory

The Hořava–Witten model of heterotic M-theory [32] (also referred to as the LOSW model) is a predecessor of the RSI braneworld. Pictorially, the models are very similar as they both contain two four-dimensional domain walls, bounding the ends of a finite interval. However, the similarity is only notional. The physics of each model is remarkably different; exotic matter fields are contained in the bulk of low energy heterotic M-theory. We therefore expect a different gravitational spectrum of five-dimensional general relativity in the LOSW model in contrast to the RSI braneworld.

2.2.1 Heterotic M-theory

The eleven-dimensional Hořava–Witten construction [33,34] is motivated from string theory duality. The strong coupling limit of the $E_8 \times E_8$ heterotic string yields a theory which consists of an eleven-dimensional bulk spacetime, bounded by two ten-dimensional orbifold fixed planes. Each orbifold fixed plane represents two distinct universes; one representing the physical world in which we live in and the second brane representing the hidden universe. In order for a consistent theory to be constructed from this setup, a set of E_8 gauge fields (equivalent to the forces of the heterotic string [9]) are required to reside on each of the ten-dimensional hy-

perplanes. This forms a relation between the ten-dimensional Yang-Mills and the eleven-dimensional gravitational coupling constants, the details of which are given in [35]. The corresponding metric of the eleven-dimensional supergravity theory is given by

$$ds_{11}^2 = V^{-2/3} g_{\alpha\beta} dx^\alpha dx^\beta + V^{1/3} \Omega_{AB} dx^A dx^B \tag{2.104}$$

where $g_{\alpha\beta}$ denotes the metric of the five-dimensional spacetime, Ω_{AB} (also known as the Calabi-Yau space) represents the metric of the six additional spacelike dimensions and V (the modulus) measures the deformation of the internal Calabi-Yau space.

If the Hořava–Witten construction is to represent our universe, then six of the spatial dimensions must be hidden in order to yield an effective five-dimensional theory analogous to the RSI braneworld. The explicit calculation of the reduction from eleven dimensions down to five dimensions was performed in [32]. The derivation involves the compactification of the M-theory limit (eleven-dimensional supergravity) on six additional spacelike dimensions known as a Calabi-Yau three-fold [35]. This compactification is achieved through a generalised Kaluza–Klein reduction and it is due to this compactification that a five-dimensional effective scalar field (dilaton) arises in the bulk which is responsible for driving the deformation of the Calabi-Yau space. This yields the effective five-dimensional $E_8 \times E_8$ Heterotic M-theory which describes the low energy physics of the strongly coupled heterotic string. The resulting five-dimensional effective metric is then given by

$$ds_5^2 = a(y)^2 \eta_{\mu\nu} dx^\mu dx^\nu + b(y)^2 dy^2 \tag{2.105}$$

where $a(y)$ and $b(y)$ represent metric functions dependent on the extra dimension. A subsequent reduction of the five-dimensional effective theory down to four dimensions is achieved by compactifying the fifth dimension on a line element, corresponding to the S^1/Z_2 orbifold. This yields two $N = 1$ supersymmetric three-branes embedded in a five-dimensional spacetime [35], providing us with the appropriate background for the setup of our early universe. Moreover, if we match the theoretical values for the gravitational and grand-unified couplings, it suggests that the size of

the orbifold is one order of magnitude greater than the size of the Calabi-Yau manifold. This suggests an intermediate regime in which the early universe may have appeared effectively five-dimensional [35,36]. It is therefore important to study the five-dimensional effective Hořava–Witten theory.

To solve the background equations of low energy heterotic M-theory, we begin with the dimensionally reduced five-dimensional effective action [32] which consists of terms which describe gravity, the bulk scalar field and two boundary branes, respectively:

$$\begin{aligned} S^{(5)} =& \frac{1}{2\kappa_5}\int_{\mathcal{M}_5} d^5x\sqrt{-g}\left[R+\frac{1}{2}V^{-2}\partial_\alpha V\partial^\alpha V+\frac{1}{3}V^{-2}\alpha^2\right] \\ &+\frac{\sqrt{2}\alpha}{\kappa_5}\left[\int_{\mathcal{M}_4^{(1)}} d^4x\sqrt{-g^-}V^{-1}-\int_{\mathcal{M}_4^{(2)}} d^4x\sqrt{-g^+}V^{-1}\right] \end{aligned} \tag{2.106}$$

where $\phi = \ln V$ represents the bulk scalar field, R is the five-dimensional Ricci scalar, $\kappa_5 = 8\pi G_5$ is the five-dimensional Newton constant, $g^{\pm}_{\mu\nu}$ is the induced metric on each brane and α is an arbitrary coupling constant which parameterises the number of units of 4-form flux which threads the Calabi-Yau [105]. The boundary branes have equal and opposite tensions and are positioned parallel to each other at $y = \pm y_0$ where y represents the direction perpendicular to the brane. Here, we note that the exponential term $V(\phi) = \frac{1}{3}V^{-2}\alpha^2$ in the above action plays a similar role to the bulk cosmological constant in the RS model.

The resulting five-dimensional equations of motion derived from the above action are given by

$$\begin{aligned} G^{(5)}_{ab} =& \frac{1}{2}V_{,a}V_{,b}V^{-2}-\frac{1}{4}g_{ab}V_{,}{}^{c}V_{,c}V^{-2}-\frac{1}{6}g_{ab}\,\alpha^2V^{-2} \\ &+\sqrt{2}\alpha[\delta(y+y_0)-\delta(y-y_0)]\delta^\mu_a\delta^\nu_b g_{\mu\nu}\frac{V^{-1}}{\sqrt{g_{yy}}} \end{aligned} \tag{2.107}$$

$$\Box^{(5)}\phi = -\frac{2}{3}\alpha^2V^{-2}+2\sqrt{2}\alpha[\delta(y+y_0)-\delta(y-y_0)]\frac{V^{-1}}{\sqrt{g_{yy}}} \tag{2.108}$$

where $G^{(5)}_{ab}$ and $\Box^{(5)} = \eta^{\mu\nu}\partial_\mu\partial_\nu + \partial_y{}^2$ represent the five-dimensional Einstein tensor and curved space d'Alembertian operator, respectively. Again, the Greek indices

run over the four dimensions $\mu, \nu = 0, 1, 2, 3$ whereas the Latin indices run over all five dimensions $a, b = 0, 1, 2, 3, 4$.

The metric ansatz (2.105) is a solution to Einstein equations (2.107). The corresponding solutions for the static 3-brane in the background of heterotic M-theory are given by the following set of formulae

$$\begin{aligned} ds_5^2 &= a_0^2 H(y)\eta_{\mu\nu}dx^\mu dx^\nu + b_0^2 H^4(y)dy^2 \\ V(y) &= b_0 H^3(y) \\ H(y) &= \frac{\sqrt{2}}{3}\alpha|y \pm y_0| + c_0 \end{aligned} \tag{2.109}$$

where the symbols a_0, b_0 and c_0 represent arbitrary constants and $H(y)$ denotes a linear harmonic function. Finally, imposing an additional Z_2-symmetry at $y = +y_0$ enables us to produce a second domain wall.

Summary

In this section we have obtained the background solutions of low energy heterotic M-theory. The subject of perturbations around these solutions is the content of chapter 5.

Chapter 3

Braneworld Stars and Black Holes

In this chapter we study the possibility of describing strong gravitational phenomenology within the context of the Randall–Sundrum II model. The main objective is to consistently embed a three-brane in a five-dimensional, spherically symmetric spacetime. We fix the background and assume that the three-brane contains matter content in terms of a non-zero energy-momentum tensor. We analyse three types of background: Anti-de Sitter, Schwarzschild and Schwarzschild–Anti de Sitter. Concentrating our study on static braneworld slicing of the given spacetimes, we are able to derive expressions describing the shape of the brane. We also compute the energy density and pressure induced on the brane. In particular, we are interested in branes that are embedded in a Schwarzschild–Anti de Sitter background as these solutions will potentially correspond to either brane stars or black holes. Finally, we extend our analysis to include time dependence in the model. In particular, we explore time-dependent trajectories in a Schwarzschild–Anti de Sitter background as these solutions are possible descriptions of time-dependent braneworld black holes. We then give a qualitative discussion of the effects induced on the brane energy-momentum when matter is present on the brane. This involves an analysis of the energy and pressure profiles. The weak and dominant energy conditions then determines the physically sensible solutions.

3.1 Introduction

Black holes are a fascinating topic of research for the theoretical physics community. These massive objects are vital in our understanding of the gravitational force, the least understood force of nature. Over the past two decades, braneworlds have offered a revolutionary approach to the study of black holes. These paradigms allow extra dimensions to be concealed in the most elegant way. They also offer a resolution to the Hierarchy problem; explaining why the power of gravity is so much more diluted in contrast to the other forces of nature. The ability of the braneworld construction to hide the additional spacelike dimensions and to solve the Hierarchy problem provides us with a possible toy model for our universe and one in which to explore the effects of strong gravity phenomenology. Thus, the subject of this chapter is braneworld black holes. (See Ref. [54] for a review on braneworld black holes).

The nature of black holes within the framework of the Randall-Sundrum (RS) scenario has not been fully understood. There have been many different attempts in trying to comprehend the subject, but the unsolved problem in braneworlds remain; no one has yet been able to pin down an exact solution for a four-dimensional metric corresponding to a static localised brane black hole. Some (of the many) analytical attempts at resolving the problem are discussed next (although numerical techniques have also been explored in [55–57]).

The first attempts to find a static black hole solution on the RS brane was made by Chamblin, Hawking and Reall (CHR) [37]. Using the warped metric ansatz of the RS scenario

$$ds^2 = e^{-2ky}[-dt^2 + d\mathbf{x}^2] + dy^2 \tag{3.1}$$

the authors replaced the flat Minkowski metric with a Schwarzschild spacetime: $\eta_{\mu\nu} \rightarrow g^{Sch}_{\mu\nu}$. The above metric is then modified to:

$$ds^2 = e^{-2ky}\left[-\left(1-\frac{2M}{r}\right)dt^2 + \left(1-\frac{2M}{r}\right)^{-1}dr^2 + r^2 d\Omega_{II}^2\right] + dy^2 . \tag{3.2}$$

From the brane perspective, this substitution forms a Schwarzschild black hole solu-

tion on the brane. Extending this solution off the brane and into the fifth dimension by the addition of an extra flat spatial dimension yields an unstable singularity. The solution now appears to be a higher dimensional object in five-dimensional Anti-de Sitter space (AdS_5), *i.e.* the Schwarzschild black string $Sch_4 \times R$. Clearly, from the five-dimensional perspective, this solution fails to describe a localised four-dimensional brane black hole. If our world is indeed part of an exotic multi-dimensional universe, then for a truly localised brane black hole, we would expect gravitational collapse of matter on the brane to form a black hole on (or close to) the brane. This is certainly not the case for the CHR black string; the horizon of the black hole stretches all the way out to the AdS horizon and becomes singular at the end. Although the CHR black string suffers from the above problems (the extended bulk singularity and the classical instability [58]), it is to date, the closest (but unsuccessful) exact solution that looks like a black hole, at least from the four-dimensional perspective.

Chamblin *et al* later acknowledged that a true description of a static black hole would correspond to a five-dimensional slice of an accelerating black hole. This is because the RS brane trajectory does not follow a geodesic of the AdS bulk; in fact it experiences a constant acceleration [61]. Thus, a black hole residing on the wall must accelerate simultaneously with the wall in order to keep up with the motion of the domain wall. In four-dimensions, the metric describing an accelerating black hole is referred to as the C-metric, the basic properties of which are well known and were first considered by Kinnersley and Walker [62]. Unfortunately, a generalisation of the C-metric in five dimensions has not yet been found and remains a project worthwhile to explore.

Emparan, Horowitz and Myers explored black holes in a lower-dimensional setup of the RS scenario [63,64]. By 'subtracting' one dimension from the RS model, they were able to explore the possibility of intersecting a three-dimensional black hole using a two-brane. In the analysis, the authors realised that the black holes on the brane are in fact accelerating. Taking this into account by using the aforementioned C-metric, a class of exact solutions in four dimensions were discovered. Thus, the success of this lower dimensional model may provide a useful insight into generalising

this model to dimensions beyond the familiar four. Unfortunately, to date, there have been no extensions of this lower dimensional model to five dimensions or more.

More recently, Emparan, Fabbri and Kaloper [65] applied the AdS/CFT conjecture [66] to try and solve the problem. They state that a localised black hole solution on the brane can be obtained by solving the classical bulk equations of the AdS_5 space. The projection of the classical bulk solution would form a four-dimensional quantum corrected (not classical) black hole on the brane. Since there has been no success yet in quantising gravity, it is not surprising that nobody has yet resolved the mystery of the missing four-dimensional brane black hole.

Shiromizu, Maeda and Sasaki used a brane-based formalism to derive the effective four-dimensional Einstein equations on a three-brane world [67]. Using the Israel [70] and Gauss-Codazzi equations (a differential geometry approach to finding gravitational solutions which involves an n-dimensional infinitesimally thin membrane embedded in an $(n+1)$-dimensional spacetime [71–73]), they were able to project the five-dimensional gravitational equations onto the four-dimensional hypersurface, confining all the analysis exclusively to the brane. Unfortunately, this method involves an unspecified Weyl tensor term. This is an unknown quantity which encodes all the information regarding the geometry of the bulk. This is where the heart of the problem lies; we do not have a closed system of equations on the brane.

Seahra [68] and Galfard, Germani and Ishibashi [69] (the latter authors used an AdS/CFT inspired conjecture in their analysis) explored the subject using an entirely new approach. They used a bulk-based method which took into account both the four and five-dimensional spacetimes. The advantage of this method in comparison to the brane-based analysis of Shiromizu *et al* is that we have no undefined variables in the system, allowing us to obtain a full bulk plus brane solution. Using the perception that our visible world exists as a slice of a higher dimensional universe, planar slicing of five-dimensional metrics were taken. The aim was to obtain a spacetime slice that intersects exactly through a bulk black hole. In particular, non-vacuum branes were considered because it is not possible to obtain solutions using vacuum domain walls [37]. Unfortunately, the slicing produced in both papers

exhibited curvature singularities; these are not acceptable solutions for candidate black holes.

In this chapter, we employ the same methodology as the previous authors in a further attempt to obtain a brane slicing which cuts through a black hole. Our methods have the same restriction as that of the previous work; the branes must be non-vacuum. By deriving a full system of bulk and brane equations, using the Israel formalism, we explore the possible brane trajectories that are allowed. The layout of the chapter is as follows. We will restrict our analysis to the case of a fixed, five-dimensional spherically symmetric bulk. Since it is impossible to intersect a black hole with a vacuum domain wall, we study branes characterised by a non-vanishing energy-momentum tensor. A solution to the brane equations of motion can then be found. Assuming that the brane contains a general isotropic fluid source living on it, we derive the general formulae which are equivalent to the Tolman–Oppenheimer–Volkoff (TOV) equations; the characteristics equations of a gravitating star. Focusing on the general static system, we show that the static brane is completely integrable. We then explore the trajectories of the branes when they are embedded in a variety of backgrounds, exploring all possible black hole or stellar solutions. Our final goal is a consistent embedding of a three-brane in a Schwarzschild–Anti de Sitter bulk; a possible candidate solution for a brane black hole. Finally, we take a look at the time-dependent solutions, after which we conclude.

3.2 The general brane equations

We begin by adopting a spherically symmetric coordinate system. We write the 5-dimensional line-element in the form:

$$ds^2 = -U(r)\,d\tau^2 + \frac{1}{U(r)}\,dr^2 + r^2(d\chi^2 + \sin^2\chi\, d\Omega_{II}^2) \tag{3.3}$$

where $U(r)$ is a general function of the global radial coordinate. The function $\chi(\tau, r)$ denotes the location of the brane in the five-dimensional spacetime. The explicit form of the line-element on a unit 2-sphere is given by $d\Omega_{II}^2 = d\theta^2 + \sin^2\theta d\phi^2$. We are

considering configurations within the Randall–Sundrum II model, with a reflection symmetric spacetime around a single positive tension brane.

The position of the brane in the bulk is given by the following 5-vector $x^\mu = (\tau, r, \chi(\tau, r), \theta, \phi)$. We can form a new basis in terms of the (unnormalised) tangent vectors and the (normalised) unit normal:

$$\begin{aligned} T^\mu &= (1, 0, \dot{\chi}, 0, 0) \\ R^\mu &= (0, 1, \chi', 0, 0) \\ \Theta^\mu &= (0, 0, 0, 1, 0) \\ \Phi^\mu &= (0, 0, 0, 0, 1) \\ n_\mu &= n(-\dot{\chi}, -\chi', 1, 0, 0)\,. \end{aligned} \tag{3.4}$$

In the above, overdot and prime denote partial differentiation with respect to τ and r, respectively. The unit normal above has been deduced by using the orthogonality relations between the normal and tangent vectors: $T^\mu n_\mu = 0$ and $R^\mu n_\mu = 0$. We use the spacelike property of the normal vector $n_\mu n^\mu = 1$ to determine the normalisation constant

$$\frac{1}{n^2} = \left(-\frac{\dot{\chi}^2}{U} + U\chi'^2 + \frac{1}{r^2} \right) . \tag{3.5}$$

The tensor $h_{\mu\nu} = g_{\mu\nu} - n_\mu n_\nu$ projects vectors onto the wall whereas its tangential components define the induced metric on the brane. In the aforementioned basis, the induced metric can be simply evaluated as

$$h_{\mu\nu} = \begin{pmatrix} -U + r^2\dot{\chi}^2 & r^2\dot{\chi}\chi' & & & \\ r^2\dot{\chi}\chi' & \frac{1}{U} + r^2\chi'^2 & & & \\ & & r^2\sin^2\chi & & \\ & & & r^2\sin^2\chi\sin^2\theta & \\ & & & & 0 \end{pmatrix} .$$

The Israel junction conditions [70], triggered by the presence of the brane with a non-vanishing distributional energy-momentum tensor $T_{\mu\nu}$, take the form

$$[K_{\mu\nu} - K h_{\mu\nu}]^+_- = \kappa_5 T_{\mu\nu} \tag{3.6}$$

where $K_{\mu\nu} = h^{\rho}_{\mu} h^{\sigma}_{\nu} \nabla_{\rho} n_{\sigma}$ is the extrinsic curvature of the brane and $\kappa_5 = 8\pi G_5$ denotes the five-dimensional gravitational constant. We use the simplifying assumption of Z_2-reflection symmetry around the wall: $K_{\mu\nu}(0^+) = -K_{\mu\nu}(0^-)$ to obtain

$$[K_{\mu\nu}]^{+}_{-} = K_{\mu\nu}(0^+) - K_{\mu\nu}(0^-) = 2K_{\mu\nu}(0^+) \,. \tag{3.7}$$

The Israel conditions (3.6) then simplify to

$$K_{\mu\nu} = \frac{\kappa_5}{6} \left(3T_{\mu\nu} - h_{\mu\nu} T\right) \,. \tag{3.8}$$

We deviate from the simplified ansatz of CHR [37] in which the brane was characterised only by a constant self-energy. In this work we assume that the matter distribution on the brane, given in terms of the energy-momentum tensor, may take the general form of a perfect isotropic fluid source

$$T_{\mu\nu} = \left[\rho(\tau, r) + p(\tau, r)\right] h_{\mu\sigma} h_{\nu\rho} \, u^{\sigma} u^{\rho} + p(\tau, r) \, h_{\mu\nu} \,. \tag{3.9}$$

In the above ansatz, $\rho(\tau, r)$ and $p(\tau, r)$ represent the fluid's energy density and pressure, respectively. The vector u^{μ} is the fluid's 4-velocity which satisfies the normalisation condition $u^{\mu} u^{\nu} h_{\mu\nu} = -1$. It can be easily shown that working in the rest frame of the fluid on the brane

$$u^{\mu} = \frac{1}{\sqrt{-h_{TT}}} \left(1, 0, 0, 0, 0\right) \tag{3.10}$$

in the basis (T, R, Θ, Φ, n), is equivalent to taking the fluid's 4-velocity u^{μ} to be parallel to the time-like tangent vector T^{μ} in the original basis $(\tau, r, \chi, \theta, \phi)$. The ansatz (3.10) allows us to rewrite the brane energy-momentum tensor as:

$$T_{\mu\nu} = -(\rho + p) \frac{h_{\mu T} h_{\nu T}}{h_{TT}} + p \, h_{\mu\nu} \,. \tag{3.11}$$

Furthermore, the trace of the energy-momentum tensor yields the relation $T = T_{\mu\nu} h^{\mu\nu} = 3P - \rho$. For convenience, we will write the energy density and pressure of the perfect fluid on the brane in terms of an "equation of state" $p(\tau, r) = w(\tau, r)\rho(\tau, r)$ and define for later convenience the quantity

$$v(\tau, r) \equiv 2 + 3w(\tau, r) \,. \tag{3.12}$$

By using the form of the energy-momentum tensor given in (3.11) together with (3.12), we can rewrite the Israel conditions for a brane containing a perfect fluid in the form

$$K_{\mu\nu} = \frac{\kappa_5}{6}\rho\left[h_{\mu\nu} - (1+v)\frac{h_{\mu T}h_{\nu T}}{h_{TT}}\right]. \tag{3.13}$$

The Israel equations (3.13) are given explicitly as:

$$K_{TT} = -n\left[\ddot{\chi} + Ur\chi'\dot{\chi}^2 - \frac{1}{2}UU'\chi'\right] = -\frac{\kappa_5}{6}\rho v\left(-U + r^2\dot{\chi}^2\right) \tag{3.14}$$

$$K_{RR} = -n\left[\chi'' + \frac{2\chi'}{r} + \frac{U'\chi'}{2U} + Ur\chi'^3\right] = \frac{\kappa_5}{6}\rho\left[\frac{1}{U} + r^2\chi'^2 + \frac{(1+v)\,r^4\dot{\chi}^2\chi'^2}{U - r^2\dot{\chi}^2}\right] \tag{3.15}$$

$$K_{TR} = -n\left[\dot{\chi}' + \frac{\dot{\chi}}{r} + Ur\chi'^2\dot{\chi} - \frac{U'\dot{\chi}}{2U}\right] = -\frac{\kappa_5}{6}\rho v r^2\dot{\chi}\chi' \tag{3.16}$$

$$K_{\Theta\Theta} = -n\left[Ur\chi'\sin^2\chi - \sin\chi\cos\chi\right] = \frac{\kappa_5}{6}\rho r^2\sin^2\chi \tag{3.17}$$

where we have excluded $K_{\Phi\Phi} = K_{\Theta\Theta}\sin^2\theta$ as it is not an independent equation. The τ and r derivatives of the inverse of the normalisation constant n are given respectively:

$$\frac{\partial}{\partial\tau}(n^{-1}) = n\left[U\dot{\chi}'\chi' - \frac{\dot{\chi}\ddot{\chi}}{U}\right] \tag{3.18}$$

$$\frac{\partial}{\partial r}(n^{-1}) = n\left[-\frac{\dot{\chi}\dot{\chi}'}{U} + \frac{1}{2}\frac{\dot{\chi}^2U'}{U^2} + \frac{1}{2}U'\chi'^2 + U\chi'\chi'' - \frac{1}{r^3}\right]. \tag{3.19}$$

We differentiate (3.17) with respect to τ and r separately and use (3.18)–(3.19) together with (3.14)–(3.16) to eliminate any double derivatives. This yields two additional, but not independent equations for the conservation of energy-momentum:

$$\dot{\chi}\left[1 + \frac{1}{2}U'r - U + \frac{\kappa_5\rho}{6n}(1+v)r^2\cot\chi\right] = -\frac{\kappa_5\dot{\rho}}{6n}r^2 \tag{3.20}$$

$$\chi'\left[1 + \frac{1}{2}U'r - U + \frac{\kappa_5\rho}{6n}(1+v)\frac{r^4\dot{\chi}^2\cot\chi}{-U + r^2\dot{\chi}^2}\right] = -\frac{\kappa_5\rho'}{6n}r^2. \tag{3.21}$$

We may summarise the above results by saying that a four-dimensional brane containing a perfect fluid, described by its energy density $\rho(\tau, r)$ and equation of state $p(\tau, r) = w(\tau, r)\rho(\tau, r)$, can be successfully embedded in a five-dimensional spherically symmetric background defined by a single function $U(r)$ as long as we can find a consistent set of functions $\rho(\tau, r)$, $w(\tau, r)$ and $\chi(\tau, r)$ - satisfying (3.14)-(3.17) and (3.20)-(3.21).

The following definition $\alpha = r\cos\chi$ enables us to rewrite the Israel and conservation equations (3.14)-(3.17) and (3.20)-(3.21) as:

$$\frac{r^2\ddot{\alpha}}{U} - (\alpha' r - \alpha)\left[\frac{U'r}{2} - U\right] + \alpha + \frac{(1+v)}{U}\left[U(\alpha' r - \alpha) + \alpha\right]\left[-U + \frac{r^2\dot{\alpha}^2}{r^2 - \alpha^2}\right] = 0 \quad (3.22)$$

$$Ur^2\alpha'' + (\alpha' r - \alpha)\left[\frac{U'r}{2} - U\right] - \alpha + (1+v)\frac{\left[U(\alpha' r - \alpha) + \alpha\right]Ur^2\dot{\alpha}^2(\alpha' r - \alpha)^2}{(r^2 - \alpha^2)\left[r^2\dot{\alpha}^2 - U(r^2 - \alpha^2)\right]} = 0 \quad (3.23)$$

$$r\dot{\alpha}' - \frac{1}{2}\frac{U'r}{U}\dot{\alpha} + (1+v)[U(\alpha' r - \alpha) + \alpha]\frac{\dot{\alpha}(\alpha' r - \alpha)}{(r^2 - \alpha^2)} = 0 \quad (3.24)$$

$$U(\alpha' r - \alpha) + \alpha = \frac{\kappa_5}{6}\rho r\left[-\frac{r^2\dot{\alpha}^2}{U} + U(\alpha' r - \alpha)^2 + r^2 - \alpha^2\right]^{\frac{1}{2}} \quad (3.25)$$

$$\frac{\dot{\rho}r}{\rho} = r\dot{\alpha}\left[\frac{1 + \frac{1}{2}U'r - U}{U(\alpha' r - \alpha) + \alpha} + (1+v)\frac{\alpha}{r^2 - \alpha^2}\right] \quad (3.26)$$

$$\frac{\rho' r}{\rho} = (\alpha' r - \alpha)\left[\frac{1 + \frac{1}{2}U'r - U}{U(\alpha' r - \alpha) + \alpha} + \frac{(1+v)}{(r^2 - \alpha^2)}\frac{r^2\dot{\alpha}^2\alpha}{\left[r^2\dot{\alpha}^2 - U(r^2 - \alpha^2)\right]}\right] \quad (3.27)$$

where we have also used (3.17) in the above equations to eliminate the quantity

$$\frac{\kappa_5\rho}{6n} = \frac{\cot\chi}{r^2} - \frac{U\chi'^2}{r}. \quad (3.28)$$

In Appendix A.3, we have checked consistency of (3.22)–(3.27) for a brane evolving with time: $v = -1$. This gives the following two consistency relations:

$$\chi' \left[\frac{U'}{2} - \frac{U}{r} + \frac{1}{r} \right] = 0 \,, \qquad \dot{\chi} \left[\frac{U'}{2} - \frac{U}{r} + \frac{1}{r} \right] = 0 \tag{3.29}$$

with the trivial solution corresponding to an Anti-de Sitter bulk $U(r) = 1 + k^2 r^2$. Thus, a positive tension brane $v = -1$ (*i.e.* a cosmological constant brane) with energy density $\rho = 6k/\kappa_5$ and brane equation $kr \cos\chi = \sqrt{1 + k^2 r^2} \cos k\tau - 1$ consistently satisfies the Israel and conservation equations. In fact, this solution corresponds to the Randall–Sundrum model.

Equations (3.22)–(3.27) may lead to either static or time-dependent brane configurations, depending on whether time-dependence is permitted in the brane trajectory $\chi(\tau, r)$. By eliminating the time dependence $\chi(r)$, we are able to study the permissible static brane embeddings in a chosen background. We then attempt to solve the more complicated case of time-dependent trajectories.

3.2.1 The static brane: an exact solution

If we assume that the brane trajectory is time-independent, then considerable simplifications occur. Since $\dot{\chi} = \dot{\alpha} = 0$, then $\dot{\rho} = 0$ from (3.26). The remaining equations (apart from (3.24) which is trivially satisfied) become:

$$v = -(\alpha' r - \alpha) \left[\frac{\frac{1}{2} U' r}{U(\alpha' r - \alpha) + \alpha} \right] \tag{3.30}$$

$$U r^2 \alpha'' + (\alpha' r - \alpha) \left[\frac{1}{2} U' r - U \right] - \alpha = 0 \tag{3.31}$$

$$U(\alpha' r - \alpha) + \alpha = \frac{\kappa_5}{6} \rho r \left[U(\alpha' r - \alpha)^2 + r^2 - \alpha^2 \right]^{\frac{1}{2}} \tag{3.32}$$

$$\frac{\rho' r}{\rho} = (\alpha' r - \alpha) \left[\frac{1 + \frac{1}{2} U' r - U}{U(\alpha' r - \alpha) + \alpha} \right] . \tag{3.33}$$

Integrating (3.33) gives the energy density as

$$\rho(r) = \frac{\rho_0}{r^2} \left[U(\alpha' r - \alpha) + \alpha \right] \tag{3.34}$$

where ρ_0 is an integration constant. Substituting for $\rho(r)$ in (3.32) yields

$$U(\alpha' r - \alpha)^2 - \alpha^2 + \left[1 - \frac{36}{\kappa_5^2 \rho_0^2}\right] r^2 = 0\,. \tag{3.35}$$

In fact, equations (3.31) and (3.35) for $\alpha(r)$ can be completely integrated out. If we define a new variable $\alpha(r) \equiv r\cos\chi(r) = r\zeta(r)$ and substitute it into (3.35), we obtain the modified radial variable:

$$\tilde{r} \equiv \int \frac{dr}{r\sqrt{U}} = \int \frac{d\zeta}{\sqrt{\zeta^2 - 1 + \frac{36}{\kappa_5^2\rho_0^2}}}\,. \tag{3.36}$$

The integral can be evaluated to give

$$\tilde{r} = \log\left[\left(\zeta^2 - 1 + \frac{36}{\kappa_5^2\rho_0^2}\right)^{1/2} + \zeta\right] \tag{3.37}$$

where

$$\cos\chi = ae^{\tilde{r}} + be^{-\tilde{r}} \tag{3.38}$$

and

$$4ab = 1 - \frac{36}{\kappa_5^2\rho_0^2}\,. \tag{3.39}$$

Alternatively, (3.31) can be integrated out to yield the general solution (3.38). The energy density and pressure can then be straightforwardly obtained from (3.34) together with (3.30) and (3.12):

$$\rho = \frac{6}{\kappa_5 r\sqrt{1-4ab}}\left[\sqrt{U}\left(ae^{\tilde{r}} - be^{-\tilde{r}}\right) + ae^{\tilde{r}} + be^{-\tilde{r}}\right] \tag{3.40}$$

$$p(r) = -\frac{2}{3}\rho(r) - \frac{U'}{\kappa_5\sqrt{U(1-4ab)}}\left(ae^{\tilde{r}} - be^{-\tilde{r}}\right)\,. \tag{3.41}$$

Finally, the induced metric on the brane is

$$ds^2 = -Ud\tau^2 + \frac{(1-4ab)\,r^2dr^2}{U(r^2-\alpha^2)} + (r^2-\alpha^2)\,d\Omega_{II}^2\,. \tag{3.42}$$

Note that the constants a and b encode the same information as the integration constant ρ_0 and the arbitrary constant corresponding to the zero point of $\tilde{r}$ from the integration in (3.36).

3.3 Static braneworld "stars"

In the previous section, we showed that the static brane equations admitted an implicit exact solution in terms of the radial variable $\tilde{r}$, which depended on an integral of the bulk Newtonian potential $U(r)$. Although this is an exact solution, the actual properties of the brane depend on the specifics of the relation between $\tilde{r}$ and r. We therefore need to specify $U(r)$ explicitly for various backgrounds in order to determine the corresponding brane equations. Once this is determined, we have a solution describing a static, spherically symmetric distribution of an isotropic perfect fluid on the brane, *i.e.* a solution to the brane TOV system. Not all the trajectories we will find will have the interpretation of a braneworld star. Thus, a careful examination of the energy density and pressure profiles will be required to confirm the extent to which the solutions are physically sensible and hence correspond to braneworld stars.

3.3.1 A five-dimensional vacuum bulk

Let us first consider the simplest possible bulk—the vacuum: $U = 1$. In this case, the modified radial variable is simply $\tilde{r} = \ln r$ and the brane trajectory which is a solution to equations (3.31) and (3.35) is given by $\alpha(r) = ar^2 + b$. We introduce the polar coordinates

$$x^* = r\cos\chi\,, \quad y^* = r\sin\chi\,, \tag{3.43}$$

in order to write the brane trajectories in the form

$$\left(x^* - \frac{1}{2a}\right)^2 + y^{*2} = \frac{1}{4a^2} - \frac{b}{a} \tag{3.44}$$

with $x^* = b$ in the particular case $a = 0$. These solutions are of limited physical importance as they have constant energy and pressure: $\rho = 2a\rho_0$, $p = -2\rho/3$. They correspond to an Einstein static universe

$$ds^2 = -d\tau^2 + R_0^2 d\Omega_{\rm III}^2 \tag{3.45}$$

where $R_0^2 = (1 - 4ab)/4a^2$ and $d\Omega_{\rm III}^2 = dR^2 + \sin^2 R\; d\Omega_{\rm II}^2$ is the explicit form of the line-element on a unit 3-sphere.

3.3.2 A general family of bulk spacetimes

Now let us consider a more general family of bulk spacetimes. If we make the choice $U(r) = 1 + Cr^n$ for the bulk metric function, where C and n are arbitrary constants, then the radial coordinate

$$\tilde{r} = \int \frac{dU}{n(U-1)\sqrt{U}} \tag{3.46}$$

can be integrated straightforwardly to give an analytic solution

$$\tilde{r} = \frac{1}{n} \ln \left| \frac{\sqrt{U}-1}{\sqrt{U}+1} \right| . \tag{3.47}$$

This allows us to write the solution of (3.31) in the general form:

$$\begin{aligned} \alpha(r) &= r^{1-\frac{n}{|n|}} \left[A \left| \sqrt{U}-1 \right|^{\frac{2}{|n|}} + B \left(\sqrt{U}+1 \right)^{\frac{2}{|n|}} \right] \\ &= A\alpha_1 + B\alpha_2 \end{aligned} \tag{3.48}$$

where A and B are convenient redefinitions of the integration constants a and b appearing in the general solution (3.38). By using (3.35), we determine

$$\rho_0 = \frac{6}{\kappa_5 \sqrt{1 - 4ABC^{\frac{2}{|n|}}}} \tag{3.49}$$

which can be substituted back into (3.34) to yield the energy density

$$\rho = \frac{6\left[(1+Cr^n)(\alpha' r - \alpha) + \alpha\right]}{\kappa_5 r^2 \sqrt{1 - 4ABC^{\frac{2}{|n|}}}} . \tag{3.50}$$

For the matter density on the brane to be real, we require

$$1 - 4ABC^{\frac{2}{|n|}} > 0 . \tag{3.51}$$

Equations (3.30) and (3.12) determines the pressure on the brane

$$p(r) = -\frac{2}{3}\rho(r) - \frac{1}{6}\rho(r) \left[\frac{nCr^n(\alpha' r - \alpha)}{(1+Cr^n)(\alpha' r + \alpha) + \alpha} \right] . \tag{3.52}$$

The following formula

$$r d\chi = -\frac{n}{|n|}\frac{dr}{\sqrt{U} r \sin\chi}(A\alpha_1 - B\alpha_2) \tag{3.53}$$

enables us to compute the general form of the metric induced on the brane

$$ds^2 = -U(r)d\tau^2 + \frac{r^2 dr^2}{U(r)}\left[\frac{1 - 4ABC^{\frac{2}{|n|}}}{r^2 - \alpha^2}\right] + \left(r^2 - \alpha^2\right) d\Omega_{II}^2 . \tag{3.54}$$

These solutions (3.48), in conjunction with the choice for the bulk metric function $U(r) = 1 + Cr^n$, describe different brane configurations in a variety of spherically symmetric bulk backgrounds. Two five-dimensional backgrounds of immediate physical significance are:

- The pure AdS spacetime: $n = 2$ and $C = k^2$.
- The pure Schwarzschild solution: $n = -2$ and $C = -\mu$.

3.3.3 A five-dimensional Anti-de Sitter bulk

In the case of a five-dimensional bulk filled with a negative cosmological constant, the bulk metric function may be written as $U(r) = 1 + k^2 r^2$, where k is the inverse AdS radius. The shape of the brane, $\alpha(r)$, is then given by the expression:

$$\alpha(r) \equiv r\cos\chi(r) = A\left(\sqrt{U} - 1\right) + B\left(\sqrt{U} + 1\right) \tag{3.55}$$

where, in terms of (3.38), we have set $\tilde{r} = 0$ at infinity and $A = a/k$, and $B = b/k$. Using the polar coordinates (3.43), the above trajectory may be written as

$$(1 - \beta)\left(x^* + \frac{(A - B)}{1 - \beta}\right)^2 - \beta y^{*2} = \frac{(A + B)^2\,(1 - 4ABk^2)}{(1 - \beta)} \tag{3.56}$$

where $\beta = k^2(A + B)^2$. These brane trajectories can be seen to be conic sections classified by the parameter β:

- For $\beta = 1$, the brane is a paraboloid with a critical tension.
- For $\beta > 1$, the brane is an ellipsoid with super-critical tension.

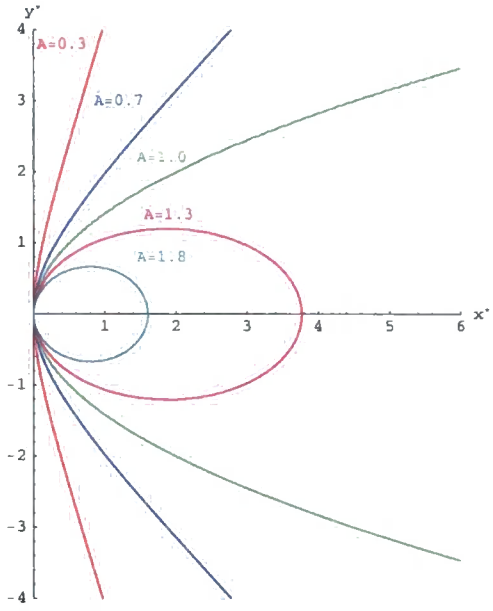

Figure 3.1: A selection of branes of varying coefficient A, for the case $B = 0, k = 1$ in a five-dimensional Anti-de Sitter bulk.

- For $\beta < 1$ the brane is a hyperboloid with sub-critical tension.

For the special case where $\beta = 0$, the brane corresponds to a straight line. In figure 3.1, we display the resulting brane configurations for some indicative values of the integration parameters A and B. For simplicity, we have set $k = 1$ and $B = 0$. Then, as A varies, the shape of the brane changes gradually covering all three cases outlined above.

The physical significance of β becomes apparent from the computation of the energy density from (3.34):

$$\rho = k^2\rho_0(A - B) = \frac{6k}{\kappa_5}\frac{k(A - B)}{\sqrt{1 - \beta + k^2(A - B)^2}} . \tag{3.57}$$

where

$$\rho_0 = \frac{6}{\kappa_5\sqrt{1 - 4ABk^2}} . \tag{3.58}$$

This reveals that the energy density is constant throughout the brane and, for $A > B$, it remains positive. Then, for the critical value $\beta = 1$, the energy density has precisely the Randall–Sundrum critical value $\rho_{RS} = 6k/\kappa_5$, while for β less (greater) than unity we have a sub- (super-) critical brane.

Turning to the equation of state on the brane by using equations (3.30) and (3.12), we find that

$$p(r) = -\rho + \frac{(A+B)k^2\rho_0}{3\sqrt{U}} = -\rho + \frac{2(A+B)k^2}{\kappa_5\sqrt{U}\sqrt{1-\beta+k^2\left(A-B\right)^2}}\,. \tag{3.59}$$

It is worth noting that we cannot get a static trajectory for a critical or super-critical brane with a pure tension energy-momentum ($w = -1$): such a solution follows only for $A + B = 0$, that corresponds to $\beta = 0$ and thus to a sub-critical ($\beta < 1$), or Karch–Randall brane [74]. For $\beta \neq 0$, we have a varying tension on our brane, equivalent to a surplus pressure in the braneworld.

Finally, using (3.54), we can evaluate the induced metric on the brane:

$$ds^2 = -U(r)\,d\tau^2 + \left(\frac{1-4ABk^2}{r^2-\alpha^2(r)}\right)\frac{r^2dr^2}{U(r)} + \left(r^2-\alpha^2(r)\right)d\Omega_{II}^2\,. \tag{3.60}$$

Using the substitution $\hat{r}^2 = r^2 - \alpha^2$, we are able to rewrite the last line as

$$ds^2 = -U(r(\hat{r}))d\tau^2 + \left(\frac{1-4ABk^2}{1-4ABk^2+(1-\beta)k^2\hat{r}^2}\right)d\hat{r}^2 + \hat{r}^2d\Omega_{II}^2 \tag{3.61}$$

where the Newtonian potential in the new variable $\hat{r}$ is given by the complex expression

$$U\left(r(\hat{r})\right) = \frac{k^2\left(A^2+B^2+\frac{1}{2}\hat{r}^2\right)^2}{(A-B)^2}\,. \tag{3.62}$$

The radial part of the metric can be simplified by making use of (3.57) and (3.58). This gives

$$ds^2 = -U\left(r(\hat{r})\right)\,d\tau^2 + \frac{d\hat{r}^2}{1-\frac{1}{3}\lambda\hat{r}^2} + \hat{r}^2d\Omega_{II}^2 \tag{3.63}$$

where

$$\frac{1}{3}\lambda = -k^2 + \frac{\rho^2\kappa_5^2}{36} \tag{3.64}$$

defines the effective cosmological constant on the brane. Clearly, the spatial part of the metric takes the form of a constant curvature space. Depending on the value of λ, the metric can be flat, Anti-de Sitter or de Sitter depending on whether the brane is critical ($\lambda = 0$), sub-critical ($\lambda < 0$) or super-critical ($\lambda > 0$), respectively. Notice

that the critical brane yields precisely the energy density of the Randall–Sundrum model $\rho = 6k/\kappa_5$. Furthermore, the subcritical branes correspond to Karch–Randall branes; AdS branes embedded in AdS bulk spacetime [74].

Since the relation between r and $\hat{r}$ is in general convoluted, the brane has a nontrivial Newtonian potential (3.62). This is because unless $A = -B$, there is a nonvanishing excess pressure on the brane (3.59) which acts as a source, resulting in a non-asymptotically flat (or (A)dS) spacetime. This can be seen explicitly by considering the critical brane where we set $\beta = k^2(A+B)^2 = 1$. Thus, the critical metric on the brane is

$$ds_c^2 = -\frac{k^2\left(A^2+B^2+\frac{1}{2}\hat{r}^2\right)^2}{(A-B)^2}\,d\tau^2 + d\hat{r}^2 + \hat{r}^2\,d\Omega_{II}^2\,. \tag{3.65}$$

Computation of the components of the energy-momentum tensor

$$T_0^0 = 0\,, \qquad T_r^r = T_\theta^\theta = T_\varphi^\varphi = \frac{4}{\kappa_5(2A^2+2B^2+\hat{r}^2)} \tag{3.66}$$

shows that the spacetime is clearly not asymptotically flat, and corresponds to a source. In fact, the source relates to the actual pressure discrepancy on the brane: $p + 6k/\kappa_5$. These results correspond to the critical branes, similar results also hold for sub- or super-critical branes, in which case $T_0^0 = \lambda \neq 0$.

To sum up, we have seen that these particular trajectories for the AdS background have excess pressure on the brane. This results in metrics which do not asymptote exact Randall–Sundrum or Karch–Randall branes. However, if the values of $|kA|$ and $|kB|$ are sufficiently large, then the metric can be flat (or asymptotically (A)dS) over many orders of magnitude before the effect of the pressure kicks in.

3.3.4 A five-dimensional Schwarzschild bulk

We now assume that the five-dimensional bulk contains a mass that creates a spherically symmetric Schwarzschild background with $U(r) = 1 - \mu/r^2$, where μ is related to the actual mass of the black hole by $M = 3\pi\mu/8G_5$. In this case, $n = -2$ and $C = -\mu$. The equation (3.48) which describes the shape of the brane takes the following form

$$\alpha(r) = r^2 \left[A\left(\sqrt{U} - 1\right) + B\left(\sqrt{U} + 1\right)\right] \tag{3.67}$$

where now $A = -b/\sqrt{\mu}$, $B = a/\sqrt{\mu}$ and $\tilde{r} = 0$ at the horizon.

Following the same analysis as before, the brane energy density and pressure are now given by

$$\rho(r) = \rho_0 \left[B(\sqrt{U} + 1)^2 - A(\sqrt{U} - 1)^2 \right] \tag{3.68}$$

$$p(r) = -\rho(r) + \frac{\rho_0}{3\sqrt{U}} \left[B(\sqrt{U} + 1)^2(2\sqrt{U} - 1) - A(\sqrt{U} - 1)^2(2\sqrt{U} + 1) \right] \tag{3.69}$$

where

$$\rho_0 = \frac{6}{\kappa_5 \sqrt{1 + 4AB\mu}} \,. \tag{3.70}$$

Clearly, the energy density is not constant for these branes, in contrast to the AdS background. We must therefore explore the energy and pressure profiles in order to determine which of our solutions are in fact physically sensible. For our solution to correspond to a braneworld star or black hole, we require the energy density ρ to be positive and to increase towards the center of the matter distribution on the brane. The latter condition gives a solution which has the interpretation of energy sources on the brane. The analysis is not quite as straightforward as expected; we cannot have ρ being a decreasing function of r. This is because the brane radial coordinate is actually $r \sin \chi$. Taking this point into account, we can carefully study each trajectory in turn.

To examine the shape of the brane, we square equation (3.67)

$$4AB\, r^2 + 2(B - A) r \cos\chi - \cos\chi^2 = \mu(A + B)^2 \tag{3.71}$$

and use (3.43) to convert to planar coordinates

$$4AB(x^{*2} + y^{*2}) + 2(B - A)x^* - \frac{x^{*2}}{x^{*2} + y^{*2}} = \mu(A + B)^2 \,. \tag{3.72}$$

The parametric solutions of (3.71) can be written in terms of polar coordinates:

$$r = \sqrt{\mu} \cosh\lambda \tag{3.73}$$

$$\cos\chi = \sqrt{\mu}(Be^{\lambda} - Ae^{-\lambda}) \,. \tag{3.74}$$

In fact, these solutions correspond to hyperbolae in the $(\cos\chi, r)$-plane. Clearly there are constraints on the range of the parameter λ, since we require

$$|\cos\chi| \leq 1\,, \qquad \rho \geq 0\,. \tag{3.75}$$

With these two constraints in mind, we can see qualitatively the different families of trajectories that are allowed. Combining the two restrictions yields an inequality for which the brane can touch the event horizon

$$0 < B - A \leq \frac{1}{\sqrt{\mu}}\,. \tag{3.76}$$

The following derivative

$$\frac{d\chi}{dr} = \frac{-(Be^{\lambda} + Ae^{-\lambda})}{\sinh\lambda\sqrt{1-\mu(Be^{\lambda} - Ae^{-\lambda})^2}} \tag{3.77}$$

shows that unless $B = -A$, $\frac{d\chi}{dr} \to \infty$ at the horizon, meaning that the brane touches the horizon at a tangent. As we will shortly see, for the special case $B = -A$, the brane passes through the horizon, eventually hitting the central singularity.

The general shape of the brane trajectories are determined from equation (3.72). Using different values for the quantity AB, we analyse the general brane shapes that are allowed. Whether the brane touches the horizon depends on the inequality (3.76). Setting the mass parameter equal to $\mu = 0.03$, we can write the critical value of the inequality as $1/\sqrt{\mu} \sim 5.77$. Furthermore, the radius of the event horizon is $r_h = \sqrt{\mu} \sim 0.17$ and is shown by the dashed circle in the following figures. In order to study the trajectories, we take a look at a range of values of the quantity $B - A$. If the value of $B - A$ lies within the range of the above inequality, then the brane will definitely touch the event horizon. Conversely, if the value of $B - A$ lies outside this range, the brane will not touch the horizon at all.

Analysis of figure 3.2 for the case $AB > 0$

• The branes can completely enclose the event horizon. This is shown in by the red circle for the values $A = 20$ and $B = 1$. Clearly, $B - A = -19$ lies outside the range of the inequality and violates positivity of ρ. This corresponds to a trajectory that misses the horizon.

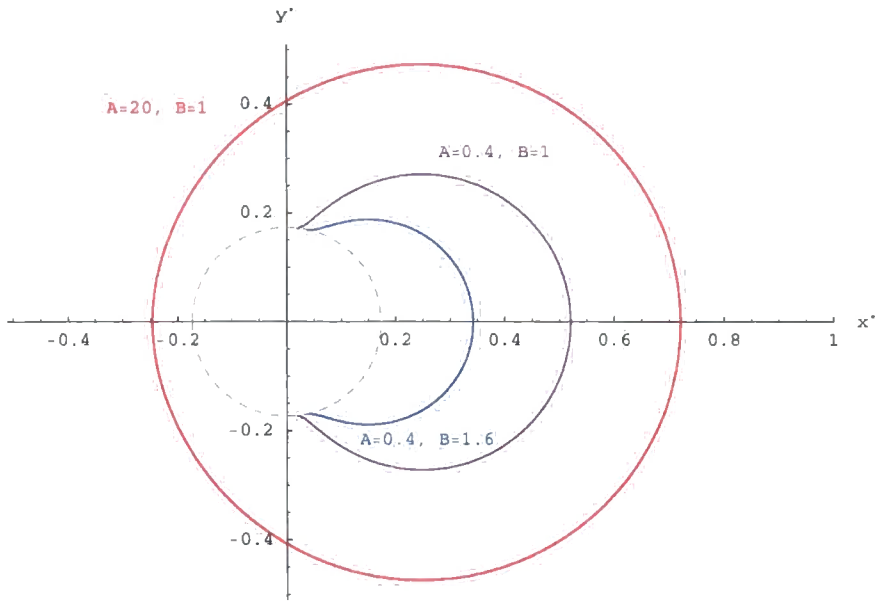

Figure 3.2: A selection of branes (solid lines) for the case $AB > 0$, in a five-dimensional Schwarzschild bulk of fixed mass parameter $\mu = 0.03$. The dashed line denotes the corresponding horizon radius.

• For $B > A$, the brane touches the event horizon and terminates there. The purple ($A = 0.4,\ B = 1$) and blue ($A = 0.4,\ B = 1.6$) trajectories highlight these two possible trajectories.

• Since $B > A > 0$, equation (3.68) shows that the energy density will always remain positive throughout the brane. However, (3.69) implies that the pressure acquires an infinite value at any point where the brane touches the event horizon.

Analysis of figure 3.3 for the case $AB < 0$

• Positivity of energy ($B > A$) requires A to be negative. In this case, the branes can be a single arc touching the horizon. This is shown by the blue lines ($A = -0.9$, $B = 0.6$ or $A = -0.6$, $B = 0.9$). Again, the pressure will diverge for these branes as they terminate on the event horizon.

• The branes can also form a closed loop ($A = -6,\ B = 1$) as shown by the red 'kidney bean' shape.

• For the special case where $A = -B$, the brane equation (3.67) is given by

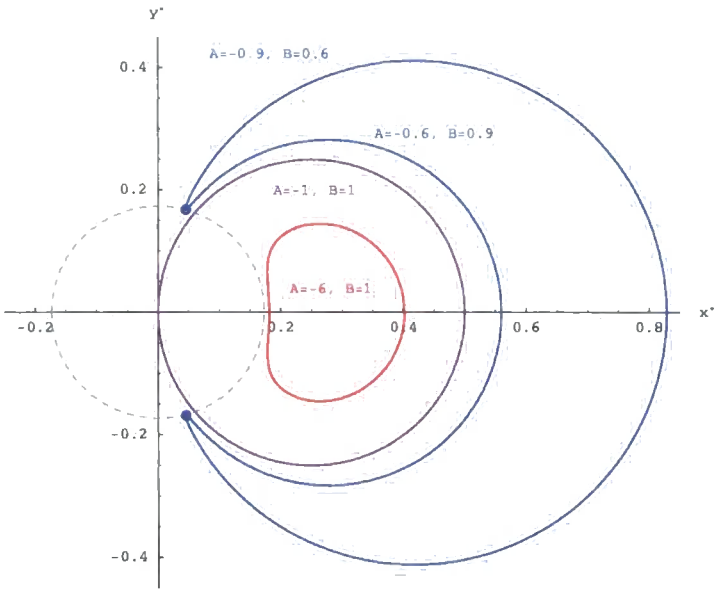

Figure 3.3: A selection of branes for the case $AB < 0$, in a five-dimensional Schwarzschild bulk of fixed mass parameter $\mu = 0.03$. The dashed line denotes again the corresponding horizon radius.

$$y^{*2} + \left(x^* - \frac{1}{4B}\right)^2 = \frac{1}{16B^2} \tag{3.78}$$

which corresponds to a circle translated to the right of the origin. This trajectory is shown by the purple line ($A = -1$, $B = 1$). The brane in this case extends beyond the event horizon and passes through the origin, *i.e.* the brane hits the central singularity.

Analysis of figure 3.4 for the case $AB = 0$

- For the case $A = 0$, the brane will touch the horizon if

$$0 < B \leq \frac{1}{\sqrt{\mu}}. \tag{3.79}$$

The brane equation (3.67) for $A = 0$ becomes

$$2x^*B - \frac{x^{*2}}{x^{*2} + y^{*2}} = \mu B^2 \tag{3.80}$$

and corresponds to a brane exterior to the horizon if $|\cos\chi| = rB\left(1 + \sqrt{U}\right) \leq 1$. These trajectories start tangent to the event horizon, curve out into the bulk, then

return to the event horizon. They are shown by the incomplete blue circle ($A = 0$, $B = 1$). Again, the pressure diverges when the brane touches the horizon.

• For the case $B = 0$, the brane will touch the horizon if

$$0 < -A \leq \frac{1}{\sqrt{\mu}}. \tag{3.81}$$

The brane equation (3.67) in this case is

$$-2x^*A - \frac{x^{*2}}{x^{*2} + y^{*2}} = \mu A^2. \tag{3.82}$$

If we use $x^* = r\cos\chi$ and $r^2 = x^{*2} + y^{*2}$ in the latter equation, we determine that the second term vanishes for large r. These trajectories asymptote according to

$$r\cos\chi = -\frac{\mu A}{2}. \tag{3.83}$$

The branes remain roughly straight at large r, until they approach near the vicinity of the horizon, at which point they bend away. These $B = 0$ trajectories are shown by the blue, purple and red 'vertical' lines corresponding to $A = -1$, $A = -10$ and $A = -30$, respectively.

Before we discuss the energy and pressure for the $B = 0$ trajectories, let us state which trajectories are the most physically useful. We are using the definition of the extrinsic curvature of the brane such that the normal, defined in (3.4), is pointing out of the spacetime being kept in this Z_2-symmetric identification. This means that, typically, for a trajectory which escapes to infinity, it is the *right* hand side of the bulk spacetime which is retained. For closed branes, it is the *interior* of the bubble that is kept. In other words, for the brane trajectories with $B = 0$, the spacetime without the black hole corresponds to the bulk appropriate to the brane trajectory. Similarly, with the small red bubble ('kidney bean' shape) in figure 3.3, it is the interior of the bubble which is kept, which has no segment of the event horizon in it.

• The energy density (3.68) and pressure (3.69) for the asymptotically flat ($B = 0$) trajectories have a particularly simple form:

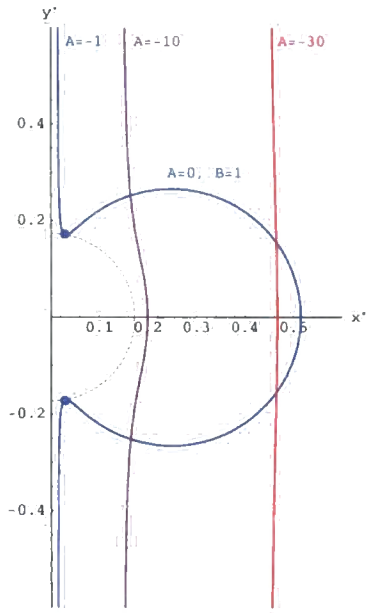

Figure 3.4: A selection of branes for the case $AB = 0$, in a five-dimensional Schwarzschild bulk of fixed mass parameter $\mu = 0.03$. The case $A = 0, B = 1$ is shown together with a set of branes with $B = 0$ and variable A. The dashed line denotes again the event horizon.

$$\rho = \frac{-6A}{\kappa_5}\left(\sqrt{U}-1\right)^2, \qquad p = -\frac{\rho}{3}\frac{(\sqrt{U}-1)}{\sqrt{U}}. \tag{3.84}$$

For $A < 0$, these branes have ρ positive and uniformly decreasing as r increases, *i.e.* the energy density is greatest at the center of the matter distribution on the brane. If $|A| \leq 1/\sqrt{\mu}$, the brane touches the horizon at a tangent and the pressure is divergent there. However, if $|A| > 1/\sqrt{\mu}$, the brane never touches the horizon and avoids it all together by bending away. In this case, the pressure remains finite everywhere. Let us Taylor expand the energy density and pressure expressions above. Substituting the following expansions

$$(\sqrt{U}-1)^2 = \frac{1}{4}\frac{\mu^2}{r^4} + \mathcal{O}\left(\frac{1}{r^4}\right), \qquad \frac{(\sqrt{U}-1)^3}{\sqrt{U}} = -\frac{1}{8}\frac{\mu^3}{r^6} + \mathcal{O}\left(\frac{1}{r^6}\right) \tag{3.85}$$

into (3.84) gives the energy density and pressure on the brane

$$\rho = -\frac{3A\mu^2}{2\kappa_5 r^4}, \qquad P = -\frac{1}{4}\frac{\mu^3 A}{\kappa_5 r^6}. \tag{3.86}$$

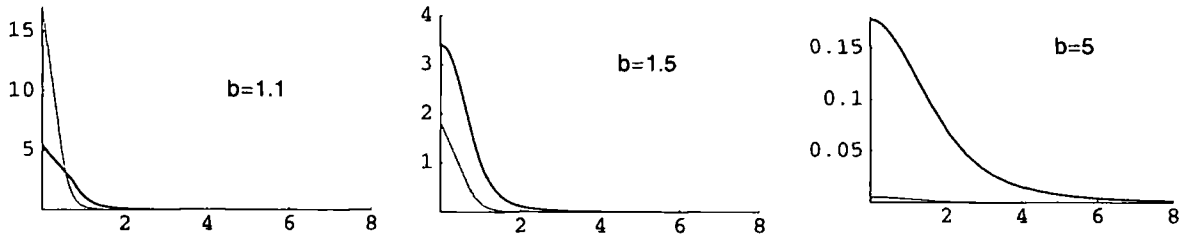

Figure 3.5: The energy (dark line) and pressure (grey line) of brane stars with a pure Schwarzschild bulk as a function of the brane radial coordinate $\hat{r}$. The black hole mass is fixed at $\mu = 1$, and the distance of closest approach to the horizon increases across the plots.

Equation (3.86) shows that the energy and pressure behave like $1/r^4$ and $1/r^6$, respectively. The energy density is peaked around $\hat{r} = r\sin\chi = 0$, as is the pressure; these branes correspond to asymptotically empty branes with positive mass sources. The energy and pressure profiles clearly shows that this solution does indeed correspond to a localised matter source, with the peak energy density dependent on the minimal radius from the horizon. These solution therefore correspond to a TOV star.

Setting $x^* = r\cos\chi = -r$ for the minimum value (using $\cos\chi = -1$), together with the substitution $r^2 = x^{*2} + y^{*2}$, we can compute the minimal radius of the $B = 0$ brane trajectory:

$$r_m = \frac{\mu|A|}{2} + \frac{1}{2|A|}. \tag{3.87}$$

The central energy and pressure at this minimal radius is readily calculated to be:

$$\rho_c = \frac{24|A|}{\kappa_5(1+\mu A^2)^2}, \qquad p_c = \frac{16|A|}{\kappa_5(\mu A^2-1)(1+\mu A^2)^2}, \tag{3.88}$$

which shows that the central pressure diverges as $\mu A^2 \to 1$. However, for $|A| = 1/\sqrt{\mu}$ the trajectory just touches the event horizon of the black hole, which is the source of this divergent pressure. This is analogous to the divergence of central pressure in the four-dimensional TOV system, which is indicative of the existence of a Chandrasekhar limit for the mass of the star.

Some examples of the solutions to the brane TOV equations are given in figure

3.5. Notice that as the brane trajectory is moved away from the horizon, the pressure of the matter on the brane decreases; in fact, in the final plot, the pressure is hardly distinguishable from the axis. Also note that as μA^2 increases, the spread of the matter on the brane increases. In these spacetimes, there is no actual black hole in the bulk, since it is the bulk to the right of the brane that is retained. In fact, it is the combination of the bulk Weyl curvature and the brane bending which produces the fully coupled gravitational solution.

To sum up: the pure Schwarzschild spacetime has a rich set of brane trajectories, most of which are closed. However, there is a class of asymptotically flat branes ($B = 0$) which have a localised source satisfying (mostly) the dominant energy condition (DEC) (*i.e.* energy is greater than the pressure: $\rho \geq |P|$). Thus, the $B = 0$ trajectories have precisely the energy-pressure profile one would expect for an isolated gravitating star.

3.4 Braneworld stars: A Schwarzschild–AdS bulk

Having independently studied static branes embedded in either an Anti-de Sitter or Schwarzschild background, we can now extend the analysis one step further to explore a static brane embedded in a five-dimensional Schwarzschild–Anti de Sitter (Sch–AdS) spacetime. Since the RS model is a brane in AdS spacetime, we expect that any consistent brane trajectories in a Sch–AdS bulk will potentially correspond to either brane stars or black holes. We emphasise that these solutions will not just be brane solutions, but full brane *and bulk* solutions, since the full Israel equations for a brane embedded in a chosen bulk background have been solved.

When computing the energy and pressure for a spherically symmetric brane, we need to take into account the background brane tension. This is because the empty brane in the RS scenario contains a non-zero energy-momentum. Using (3.40), we can deduce the background brane tension

$$\rho_b = \frac{6k(a-b)}{\kappa_5\sqrt{1-4ab}}\,. \tag{3.89}$$

We can guess the geometry of the trajectories by considering the following two

limiting cases:

• For large values of r, we expect the background geometry to be dominated by the cosmological constant. Therefore, the pure AdS solutions are a good approximation to the trajectories at large enough r.

• If $\mu k^2 \ll 1$, *i.e.* if the black hole is much smaller than the AdS scale, we expect near the vicinity of the horizon the pure Schwarzschild solutions to be good approximation for the brane trajectories.

So, for small mass black holes, we might expect the Sch–AdS brane trajectories to be well approximated by some combination of the pure Schwarzschild and pure AdS branes trajectories. For convenience and easy comparison with the pure AdS limit, we set $\tilde{r} = 0$ at $r = \infty$. This means that the range of $\tilde{r}$ in Sch–AdS is finite and decreases sharply with increasing μ. This suggests that trajectories in large mass Sch–AdS black hole spacetimes are more finely tuned, and possibly more restricted than in small mass black hole spacetimes.

The metric function $U(r)$ for the Sch–AdS bulk is given by

$$U(r) = 1 + k^2 r^2 - \frac{\mu}{r^2} \tag{3.90}$$

and is not covered by the general metric ansatz studied in the previous section. Setting $U(r) = 0$ yields the following expressions

$$r_+^2 = \frac{-1 + \sqrt{1 + 4k^2\mu}}{2k^2}, \qquad r_-^2 = \frac{-1 - \sqrt{1 + 4k^2\mu}}{2k^2} \tag{3.91}$$

with r_+ corresponding to the black hole horizon. Using (3.36), we can compute an exact analytic expression for the modified radial variable

$$\tilde{r}(r) = \frac{1}{kr_+} \int dy \left(1 - \frac{r_-^2}{r_+^2} \sin^2 y\right)^{-\frac{1}{2}}, \qquad y = \sin^{-1}\left(\frac{r}{r_-}\right). \tag{3.92}$$

In fact, the last expression is an elliptic integral[1] and is usually written as

[1] We use the following Mathematica definition of an elliptic integral of the first kind $\text{EllipticF} = \int_0^\phi \frac{d\theta}{\sqrt{1+k\sin^2\theta}}$.

$$\tilde{r}(r) = \frac{1}{kr_+} \text{Elliptic F}\left[\sin^{-1}\left(\frac{r}{r_-}\right), \frac{r_-^2}{r_+^2}\right] . \tag{3.93}$$

Although this is an exact solution, the expression is of limited use because of the imaginary value of r_- and the presence of the Elliptic function. However, it can be used to give numerical solutions for the brane. Before we numerically solve for the brane equations, let us deduce some general properties of the brane trajectories.

We are clearly interested in branes which have matter that can be interpreted as a gravitating source, *i.e.* we would like to have an energy excess at the center of the brane. This surplus energy will correspond to candidate solutions for brane stars or black holes. We can see therefore that, unless we have a closed bubble, this will in general correspond to ρ being a decreasing function of r. Using (3.33) and (3.34), we compute

$$\rho' = \frac{2\mu\rho_0}{r^3}(\cos\chi)' \tag{3.94}$$

hence, ρ is a decreasing function of r (if $\cos\chi$ is also decreasing). However, from (3.40), we determine that ρ is asymptotically dominated by

$$\rho = \frac{\rho_0}{r}\sqrt{U}(ae^{\tilde{r}} - be^{-\tilde{r}}) \propto (\cos\chi)' . \tag{3.95}$$

Thus, any positive energy brane trajectory $\rho > 0$ will have $(\cos\chi)' > 0$ near infinity, and hence, ρ will be increasing near infinity (but at a very slow rate), corresponding to an energy deficit at large r. However, this underdensity will prove to be extremely marginal, and many trajectories have, as their main feature, energies significantly in excess of their background value.

Like the AdS spacetime, we can classify the Sch–AdS trajectories according to whether they asymptote the AdS boundary at $\chi \neq 0$, at $\chi = 0$ (*i.e.* are open branes), or do not reach the boundary at all (*i.e.* are closed bubbles). These respective class of brane trajectories are highlighted as:

- $a + b < 1$ corresponds to a subcritical brane.
- $a + b = 1$ corresponds to a critical brane.
- $a + b > 1$ corresponds to a supercritical brane.

3.4.1 Supercritical branes: $a + b > 1$

All closed trajectories are supercritical. The characteristic features of supercritical trajectories are qualitatively similar to the pure Schwarzschild case; the branes will either form closed loops or arcs which terminate on the horizon. If the following inequality

$$|\cos\chi| \simeq |ae^{\tilde{r}_+} + be^{-\tilde{r}_+}| \leq 1 \tag{3.96}$$

is satisfied, then these solutions will correspond to arcs terminating on the horizon (see the pink trajectory of figure 3.6). For these solutions, the energy density remains positive and increases towards the center of the brane. Analogous to the pure Schwarzschild branes, the pressure becomes singular at the horizon. On the other hand, if the inequality is not satisfied, then these trajectories will correspond to closed bubbles on the RHS of the horizon. Again, this type of behaviour has been found previously for the pure Schwarzschild background. For closed loops forming on the RHS of the horizon, the energy density decreases near the vicinity of the horizon but increases towards the most distant point of the brane (see the green and blue trajectories of figure 3.6). A uniformly increasing behaviour for the energy density is found also in the case of brane trajectories that enclose the black hole horizon (see the red trajectory of figure 3.6): ρ reaches its maximum positive value at the point of the brane located farthest away from the black hole, although care must be taken over the choice of a and b to ensure that ρ remains positive throughout the trajectory. A sample of supercritical branes for fixed background parameters $k = 1$ and $\mu = 0.03$, and various values of the parameters a and b of the general solution (3.38) is shown in figure 3.6.

3.4.2 Critical branes: $a + b = 1$

The trajectories for critical branes asymptote the AdS boundary at exactly $\chi = 0$. The trajectories are thus open, and may or may not touch the black hole horizon depending on the exact values of the parameters a and b. In order to demonstrate when this happens, we consider the constraint

$$a - b < |\tanh\tilde{r}_+/2| \tag{3.97}$$

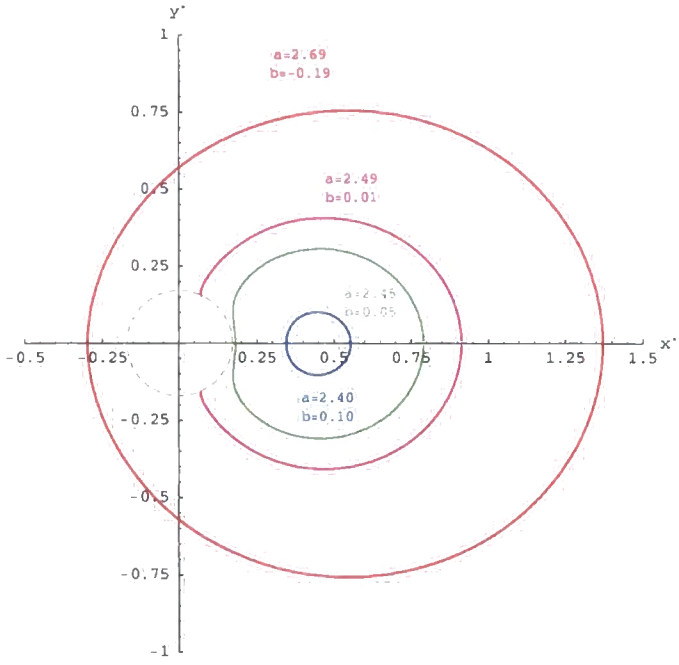

Figure 3.6: A sample of supercritical brane trajectories with $a + b > 1$ in a five-dimensional Schwarzschild–Anti de Sitter background of fixed parameters $k = 1$ and $\mu = 0.03$. The dashed line denotes again the horizon.

which corresponds to a trajectory which remains on the RHS of the horizon. When the branes reach a point of close proximity to the horizon, it bends away, avoiding the horizon and eventually escaping to infinity. Conversely, if $a - b$ equals or exceeds the above bound, then the brane will terminate on the horizon (see the pink trajectory of figure 3.7). A sample of critical trajectories in a Sch–AdS background is shown in figure 3.7(a). In figure 3.7(b) we show the energy and pressure profiles for a sequence of critical branes in a Sch–AdS background, displaced an increasing distance from the horizon. Notice that as the value of the $a - b$ parameter decreases, the brane shifts towards the right.

The behaviour of the energy density and pressure strongly depends on the location of the brane relative to the black hole. For branes that avoid the horizon the energy density is again positive, peaking at the center, and dropping rapidly to the background value, undershooting it very slightly to form an underdense region at large r. The pressure also reaches its maximum value at the center, but is uniformly decreasing with r, at a much slower rate, consistent with the pressure excess

observed for the pure AdS branes. Apart from this pressure excess, the other main difference with pure Schwarzschild trajectories, is whether branes satisfy the DEC ($\rho \geq P$) at their center. This depends crucially on the choice of $a - b$. In pure Schwarzschild, the DEC is satisfied except for branes which skirt extremely close to the horizon (see the first graph of figure 3.5), where the local Weyl curvature causes the pressure diverges. This phenomenon is also observed for the Sch–AdS branes skimming close to the horizon (graph 1 of figure 3.7(b)). However, as we decrease $a - b$ (or increase b), the central energy dominates the pressure for only a finite range of b (graph 2 of figure 3.7(b)) before once again dropping below the pressure (graph 3 of figure 3.7(b)). Thus, the DEC is not universally satisfied. This is because the further we move away from the horizon the AdS curvature becomes more dominant, and as we have already seen for pure AdS branes, the effect of the AdS curvature is to induce a non-vanishing pressure excess. Therefore, the energy density and pressure observed at the center of the branes for critical trajectories, corresponds to a distribution of a positive mass source. Furthermore, the DEC can be satisfied at the center of the matter distribution.

3.4.3 Subcritical branes: $a + b < 1$

The family of subcritical branes are largely similar to critical branes. They correspond to open trajectories that asymptote the AdS boundary, although at $\chi \neq 0$ this time. The same bound as the critical case $|\cos\chi| \simeq |ae^{\tilde{r}_+} + be^{-\tilde{r}_+}| \leq 1$ applies and determines whether the brane terminates on the event horizon or remains on the RHS of it. As the brane trajectories in this case look very similar (apart from the angle of approach from the AdS boundary) to the ones presented in figure 3.7(a), we will not present another graph here. Also, the energy density and pressure profiles turn out to be analogous to the graphs presented in 3.7(b). Therefore, for a large family of parameters a and b, we obtain solutions with a positive energy excess at the center of the brane.

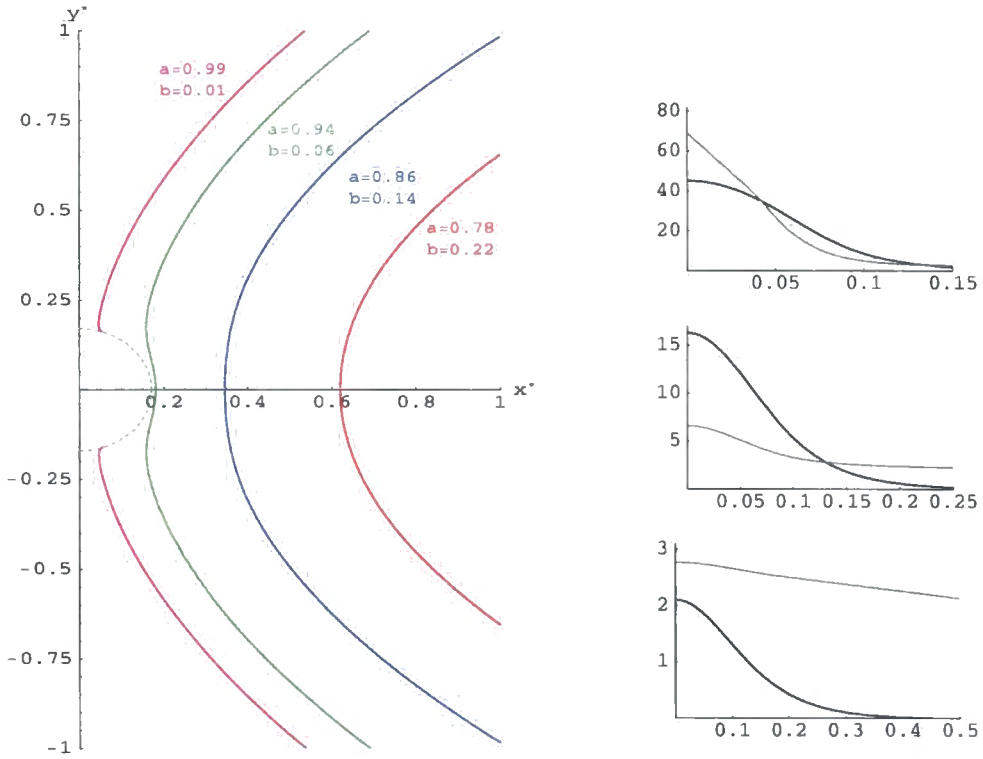

Figure 3.7: (a) A sample of critical brane trajectories with $a + b = 1$ in a five-dimensional Schwarzschild–Anti de Sitter background of fixed parameters $k = 1$ and $\mu = 0.03$. The dashed line denotes again the horizon. (b) A set of plots of the brane energy (black line) and pressure (grey line) for a sequence of critical branes moving away from the horizon.

Karch–Randall trajectory: $a + b = 0$

One special subcritical trajectory found in the pure AdS case was the Karch–Randall trajectory ($A + B = 0$). Extending this to Sch–AdS case gives

$$\cos\chi = a(e^{\tilde{r}} - e^{-\tilde{r}}) = 2a\sinh\tilde{r}\,. \tag{3.98}$$

Differentiating the last equation with respect to r shows that $(\cos\chi)' > 0$ for a positive energy trajectory $a > 0$. Having already shown that $\rho \propto (\cos\chi)'$, this implies that the energy density always increases with r. Thus, whether or not these trajectories terminate on the horizon, they will always correspond to energy deficits on the brane, and hence negative mass sources from the point of view of a brane observer.

The special Schwarzschild trajectory

Finally, one other special trajectory that emerged in the previous section was the pure Schwarzschild trajectory which was nonsingular on the horizon, intersecting it perpendicularly and extending to the origin. This corresponds to $ae^{\tilde{r}_+} = be^{-\tilde{r}_+}$ (note that in the condition $A = -B$ for the pure Schwarzschild case, we had set $\tilde{r} = 0$ at the horizon $r_+ = \sqrt{\mu}$). Extending this concept to Sch–AdS gives

$$\cos\chi = 2ae^{\tilde{r}_+}\cosh(\tilde{r} - \tilde{r}_+)\,. \tag{3.99}$$

These trajectories can be super- sub- or precisely critical, depending on the magnitude of a, however, for all of these trajectories $(\cos\chi)' > 0$, hence they correspond to energy deficits on the brane.

Summary

In this section we have shown that the Sch–AdS bulk gave rise to supercritical, critical and subcritical brane trajectories. These brane trajectories which are depicted in figures 3.6 and 3.7 have obvious similarities with the ones presented in the previous section. As expected, the brane trajectories in a bulk containing both a mass and a negative cosmological constant exhibit a combination of characteristic features that appeared either in the case of an pure AdS or a pure Schwarzschild background.

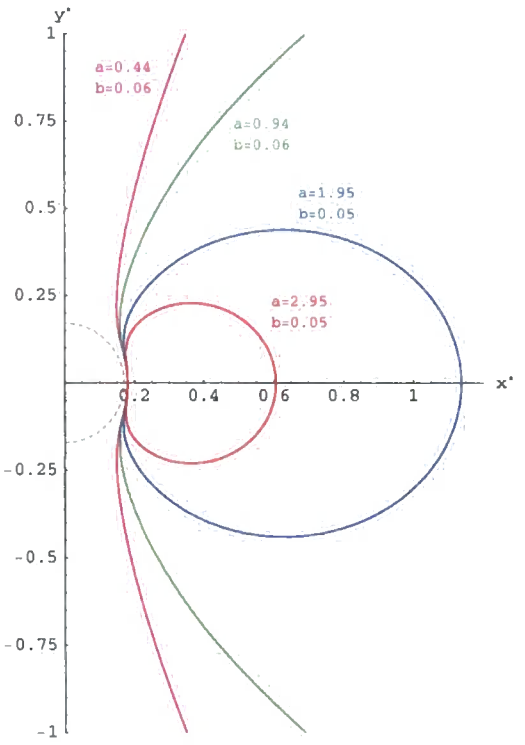

Figure 3.8: A mixture of brane trajectories in a five-dimensional Schwarzschild–Anti de Sitter background of fixed parameters $k = 1$ and $\mu = 0.03$.

In figure 3.8, we present a mixture of supercritical, critical and subcritical branes. We have chosen the parameters a and b in this particular case such that the branes remain on the RHS of the horizon. Apart from the brane bending away to avoid the horizon, these trajectories resemble similar characteristics with the ones presented in figure 3.1.

We comment that the study of Sch–AdS backgrounds with larger mass parameter μ has led to similar families of trajectories. As mentioned previously, as μ increases, the range of the $\tilde{r}$-coordinate decreases, and an increased accuracy is necessary in our numerical analysis in order to produce the corresponding trajectories. Apart from being numerically more sensitive, the study of large mass Sch–AdS backgrounds yields the same characteristics for the allowed brane trajectories.

Finally, we state that for the Sch–AdS background, some of the static solutions corresponding to the TOV equations showed characteristic features of brane stars. However, for our solutions to have a truly realistic interpretation of a brane star, we require the energy conditions to be satisfied universally. Unfortunately, our re-

sults were not 100% satisfying since the pressure component did not go to zero; it reached a constant asymptotic value at large radii from the center of the matter distribution on the brane, resulting in a surplus pressure. This unphysical asymptotic behaviour can be resolved by perturbing the trajectory or making it time-dependent; we consider the latter case next.

3.5 The time-dependent brane

Having analysed the static brane trajectories in a spherically symmetric background, finding brane black hole and stellar solutions, we now comment on the time-dependent case. Although the non-static brane trajectories are more complex to study, it may give some insight into highly time-dependent and complicated processes such as a black hole leaving the brane or the emission of thermal radiation from a four-dimensional brane black hole [79–81]. The above time-dependent processes are most likely to correspond to some perturbed version of a time-dependent brane trajectory in five-dimensional Sch–AdS spacetime. For a brane that cuts through the black hole horizon, this would appear to describe black hole formation via the transport of a bulk black hole to the brane. The subsequent departure of the brane black hole into the bulk would correspond to its decay. The first work in this area involved probe branes [80, 90–92]. It is to date, the only available study describing black holes departing the brane and has relevance for LHC (Large Hadron Collider) black holes. Although the full problem of solving the non-static brane equations is beyond the scope of this section, we will explore the various issues involved in finding a time-dependent brane black hole trajectory, such as might be appropriate to the above processes; black hole recoil and evaporation (both phenomena are discussed in detail in the following chapter).

3.5.1 The Randall–Sundrum brane trajectory

In addition to the work on probe branes, the issue of time dependence has also been considered in [75–77]. In Ref. [75, 76] it was argued that the spacetime surrounding a collapsing brane star would be time-dependent even though the exte-

rior spacetime was vacuum. Moreover, the conjecture put forward by Emparan, Fabbri and Kaloper [65] (where quantum black holes appear as holograms in AdS braneworlds) led Tanaka [77] to argue that the braneworld black hole metric must be time-dependent. In fact, the RS brane trajectory turns out to be time-dependent when written in global AdS coordinates. To see this explicitly, (*i.e.* to show that the RS brane trajectory is not a static slicing in global AdS coordinates), we consider a transformation[2] between the planar and globally spherically symmetric spacetimes. In planar coordinates, the RS metric takes the form

$$ds^2 = \frac{1}{k^2u^2}\left[-dt^2 + du^2 + d\mathbf{x}^2\right] \tag{3.100}$$

with the brane positioned at $ku = e^{kx}|_{x=0} = 1$. The transformation between the RS planar and global spherically symmetric coordinates is given by:

$$ku = \left[\sqrt{1+k^2r^2}\cos k\tau - kr\cos\chi\right]^{-1} \tag{3.101}$$

$$kt = (ku)\sqrt{1+k^2r^2}\sin k\tau \tag{3.102}$$

$$k|\underline{x}| = (ku)kr\sin\chi\,. \tag{3.103}$$

After the transformation, the planar metric changes to

$$ds^2 = -U(r)d\tau^2 + \frac{dr^2}{U(r)} + r^2(d\chi^2 + \sin^2\chi d\Omega_{II}^2) \tag{3.104}$$

which corresponds to the five-dimensional spherically symmetric spacetime. This transformation is valid for the metric function $U = 1 + k^2r^2$, corresponding to an AdS_5 spacetime. As a result of the transformation, the shape of the brane $\chi(\tau, r)$ changes. We determine the form of the trajectory $\alpha(\tau, r)$ directly and explicitly in terms of the variable $\alpha = r\cos\chi$. The pure tension brane trajectory has an exact solution

$$\alpha(\tau, r) = \frac{1}{k}\sqrt{1+k^2r^2}\cos k\tau - \frac{1}{k} \tag{3.105}$$

which is naturally time-dependent with energy density

$$\rho = \rho_{RS} = \frac{6k}{\kappa_5} \tag{3.106}$$

[2]The details of the transformation are given in Appendix A.4.

as expected. Therefore, the RS brane trajectory is *time-dependent* in global AdS coordinates. In fact, the trajectory in global coordinates is oscillatory; it starts off at the AdS boundary, moving in to the origin when it closes off the whole AdS boundary, then moving back again [78].

3.5.2 Exact branes

We review the argument that there is no time-dependent trajectory which corresponds to a pure vacuum brane embedded in a black-hole bulk background. Setting $v = -1$ in the brane equations (3.22)–(3.27) results in considerable simplifications. Once again, the energy density

$$\rho = \frac{\rho_0}{r^2}\left[U(\alpha' r - \alpha) + \alpha\right] \tag{3.107}$$

(which in principle can be a (τ, r)-dependent quantity) solves (3.26) and (3.27). In addition, (3.24) can be rewritten as

$$\begin{aligned} r\dot{\alpha}' - \frac{1}{2}\frac{U' r \dot{\alpha}}{U} &= 0 \\ \frac{\partial}{\partial\tau}\frac{\partial}{\partial r}\left(U^{-1/2}\alpha\right) &= 0 \end{aligned} \tag{3.108}$$

which is integrable. The last equation determines the form of the time-dependent brane trajectory

$$\alpha(\tau, r) = f(\tau)\sqrt{U(r)} + g(r) \tag{3.109}$$

where $f(\tau)$ and $g(r)$ are, at the moment, arbitrary functions. If we substitute the above form of $\alpha(\tau, r)$ into (3.23), we find

$$\sqrt{U}\left[\frac{1}{2}U''r^2 - U'r + U - 1\right] f(\tau) + Ur^2 g'' + (g'r - g)\left[\frac{U'r}{2} - U\right] - g = 0. \tag{3.110}$$

The only way for this equation to be satisfied, for all τ, with $f(\tau) \neq 0$, is for the factor preceding $f(\tau)$ to be equal to zero:

$$\frac{1}{2}U''r^2 - U'r + U - 1 = 0 \tag{3.111}$$

which has as a solution

$$U(r) = 1 + Cr + Dr^2 \tag{3.112}$$

for constants C and D. Thus a brane with equation of state $w = -1$ can only be embedded in a bulk with the above solution for the metric function.

General case

Clearly, if the trajectory is time-dependent, then the energy density will also be time-dependent. Since we know the general form of the brane trajectory (3.109) and the corresponding solution of the bulk metric function (3.112), we can compute the general equation for the time-dependent energy density. First, we determine the arbitrary constants $f(\tau)$ and $g(r)$. The combination of equations (3.22) and (3.23) yields a simple expression

$$\ddot{\alpha} + U^2\alpha'' = 0\,. \tag{3.113}$$

Substituting (3.109) and (3.112) into the last equation gives

$$\ddot{f}(\tau) + f(\tau)\left[\frac{UU''}{2} - \frac{(U')^2}{4U}\right] + U\sqrt{U}g''(r) = 0\,. \tag{3.114}$$

For a time-dependent solution ($f(\tau) \neq 0$), the above equation is satisfied for $g'' = 0$. Setting $-\lambda^2$ as a proportionality constant in the assumption

$$\ddot{f}(\tau) = -\lambda^2 f(\tau) \tag{3.115}$$

yields the constraint

$$\lambda^2 = \frac{UU''}{2} - \frac{(U')^2}{4U}\,. \tag{3.116}$$

Inserting equations (3.111) and $g'' = 0$ into (3.110) gives

$$(g'r - g)\left(\frac{U'r}{2} - U\right) - g = 0 \tag{3.117}$$

which can be easily solved for the general metric function given in (3.112) and for $g(r) = g_1 r + g_0$. This determines the constant

$$g_1 = \frac{g_0 C}{2} \tag{3.118}$$

and hence the solution

$$g(r) = g_0 \left(\frac{Cr}{2} + 1 \right) . \tag{3.119}$$

Next we Taylor expand the second term of equation (3.116):

$$\begin{aligned} \frac{(U')^2}{4U} &= \frac{(C+2Dr)^2}{4}(1 + Cr + Dr^2)^{-1} \\ &= \left(\frac{C^2}{4} + +CDr + D^2r^2 \right) (1 - Cr - Dr^2 \ldots) \\ &= \frac{C^2}{4} + CDr + D^2r^2 + \mathcal{O}(C^2, D^2, CD) \end{aligned} \tag{3.120}$$

where we have neglected orders of constants greater than 2. Substituting (3.120) into (3.116) gives

$$\lambda^2 = D - \frac{C^2}{4} . \tag{3.121}$$

We equate (3.25) and (3.107) to eliminate the quantity ρ:

$$\frac{U(\alpha' r - \alpha)^2 - \alpha^2}{r^2} + 1 - \frac{\dot{\alpha}^2}{U} = \frac{36}{\kappa_5^2 \rho_0^2} . \tag{3.122}$$

Inserting the expressions for $\alpha(r)$ and $g(r)$ into the first term of the last equation gives

$$\frac{U(\alpha' r - \alpha)^2 - \alpha^2}{r^2} = \lambda^2 (g_0^2 - f^2) \tag{3.123}$$

which can be substituted back into (3.122) to give

$$\frac{36}{\kappa_5^2 \rho_0^2} = 1 - \dot{f}^2 + \lambda^2 (g_0^2 - f^2) . \tag{3.124}$$

The constant ρ_0 can be determined by substituting the general solution of the differential equation (3.115):

$$f(\tau) = E_1 \cos(\lambda \tau) + E_2 \sin(\lambda \tau) \tag{3.125}$$

into (3.124), where E_1 and E_2 are integration constants. This yields

$$\rho_0 = \frac{6}{\kappa_5} \frac{1}{\sqrt{1 + \lambda^2 (g_o^2 - E_1^2 - E_2^2)}} . \tag{3.126}$$

Equations (3.109) and (3.112) enables us to compute the expression

$$U(\alpha' r - \alpha) + \alpha = -g_0 \left(\frac{Cr}{2} + Dr^2 \right) - \frac{1}{2} r \sqrt{U} f C \tag{3.127}$$

which can be substituted into (3.107) to give a formula for the time-dependent energy density (as long as $C \neq 0$)

$$\rho(\tau, r) = -\frac{3}{\kappa_5 r} \frac{1}{\sqrt{1 + \lambda^2 (g_o^2 - E_1^2 - E_2^2)}} \left(C \left[f(\tau) \sqrt{U} + g_0 \right] + 2 g_0 D r \right) . \tag{3.128}$$

Furthermore, the substitution of $f(\tau)$ and $g(r)$ into (3.109) yields the corresponding time-dependent brane trajectory

$$\alpha(\tau, r) = \left[E_1 \cos(\lambda \tau) + E_2 \sin(\lambda \tau) \right] \sqrt{U} + g_0 \left(\frac{Cr}{2} + 1 \right) . \tag{3.129}$$

We have therefore obtained general time-dependent expressions for both the energy density and brane trajectory. Next we consider the specific case where $C = 0$ and D remains an arbitrary constant.

Isotropic case

Setting $C = 0$ yields a constant energy density

$$\rho(r) = -\frac{6 g_0 D}{\kappa_5 \sqrt{1 + D(g_o^2 - E_1^2 - E_2^2)}} \tag{3.130}$$

with the corresponding brane trajectory

$$\alpha(\tau, r) = \left[E_1 \cos(\lambda \tau) + E_2 \sin(\lambda \tau) \right] \sqrt{U(r)} + g_0 \tag{3.131}$$

where we have used (3.121) to set $\lambda^2 = D$. The energy density corresponds to an isotropic background, hence a constant curvature spacetime with $D = -\Lambda/6$. Clearly, AdS spacetime satisfies this with $D = k^2$. By setting $E_1 = k^{-1}$, $E_2 = 0$, $D = k^2$ and $g_0 = -k^{-1}$ in equations (3.130) and (3.131), we obtain the Randall-Sundrum critical energy density (3.106) and the pure tension brane trajectory in global AdS coordinates (3.105).

3.5.3 Branes with matter

In this section we explore the behaviour of time-dependent brane trajectories when matter is present on the brane. The setup is different to the static branes as we now introduce a black hole in the background spacetime which is responsible for producing a spherically symmetric matter source on the brane. Moreover, the presence of the black hole effects the brane energy-momentum. Thus, the aim of this subsection is to explore how the black hole acts on the time-dependent brane. In this analysis, we are looking for brane trajectories which have physically realistic energy-momentum profiles. These solutions may have the interpretation of the two types of quantum phenomena mentioned earlier: black hole recoil or evaporation. In order to determine whether the trajectories have a sensible brane matter source, we study whether the matter obeys the weak energy condition (WEC: $\rho \geq 0$) and the dominant energy condition (DEC: $\rho \geq |P|$). We investigate two factors which may contribute to the changing profiles of the brane energy-momentum:

- Altering the distance between the brane and the black hole.
- Modifying the brane trajectory by bending it.

By varying the above factors, we can qualitatively determine whether the WEC and the DEC are both satisfied. This will then determine whether the matter localised on the brane is physically realistic. In particular, we expect the energy density to increase towards the center of the matter distribution on the brane. We will consider each of the above effects separately as it allows us to gain insight into the nature of the brane black hole. However, we note that the complete picture would contain some combination of the above effects. Unlike the static case, we will keep the matter general (*i.e.* we will not assume that the energy-momentum takes the form of perfect isotropic fluid).

Distance between the brane and black hole

Previously, for the static brane trajectories embedded in the AdS-Schwarzschild background, we saw various brane shapes at different locations in the bulk spacetime– see figure 3.7(a). The energy profiles differ depending on the location of the brane–

see figure 3.7(b). As the brane is moved closer to the black hole horizon (*i.e.* brane and black hole separation distance decreases) the brane shape changes. We would like to determine whether the time-dependent trajectory behaves in a similar way like the static case. Moreover, we would like to determine whether the energy-momentum profiles are analogous to the static case.

We make the following ansatz: we change the form of the exact trajectory of the AdS spacetime to allow for the presence of a bulk black hole. If we push the RS brane (originally located at $z = 0$ where $ku = 1$) to the AdS boundary $ku = \epsilon$, then the modified time-dependent trajectory (3.101) takes the form:

$$\sqrt{1 + k^2 r^2} \cos k\tau - kr \cos \chi = \frac{1}{ku} = \frac{1}{\epsilon}. \tag{3.132}$$

Thus, by controlling ϵ, we can control the distance of closest approach of the bulk black hole to the brane. Recall that the energy-momentum of a surface slicing the Sch–AdS spacetime is given by the Israel junction conditions (3.8). Taking the trace of (3.8) gives $T = -\frac{6K}{\kappa_5}$. Substituting this back into (3.8) and rearranging gives the following expression:

$$T_{\mu\nu} = \frac{2}{\kappa_5}(K_{\mu\nu} - K h_{\mu\nu}) = -\frac{6k}{\kappa_5} h_{\mu\nu} + \delta t_{\mu\nu} \tag{3.133}$$

where

$$T^{RS}_{\mu\nu} = -\frac{6k}{\kappa_5} h_{\mu\nu} \tag{3.134}$$

represents the critical RS brane tension and $\delta t_{\mu\nu}$ corresponds to a small perturbation in the energy-momentum (the latter term arises as there is no brane trajectory with pure brane energy-momentum). We can now compute the energy-momentum (3.133) using the Israel equations (3.14)–(3.17). Since we want to compare this energy-momentum to the pure critical RS brane, we plot the following ratio

$$e_{\mu\nu} = \frac{K_{\mu\nu} - K h_{\mu\nu}}{-h_{\mu\nu}} = -\frac{T^{RS}_{\mu\nu}}{2h_{\mu\nu}} \tag{3.135}$$

which is equivalent to

$$e_{\mu\nu} = 3 - \frac{\delta t_{\mu\nu}}{2h_{\mu\nu}} \tag{3.136}$$

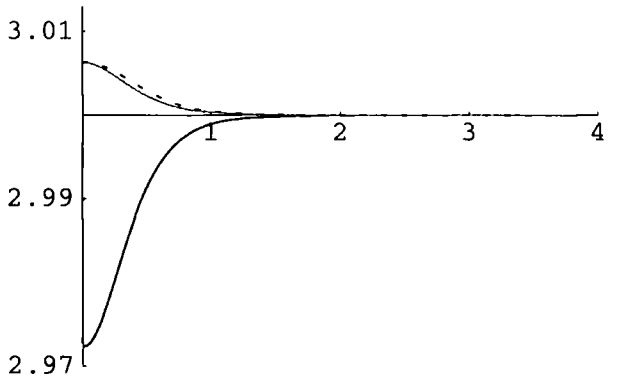

Figure 3.9: The effects of brane shift on the energy-momentum of an RS brane with a black hole in the bulk as a function of the brane radial coordinate $r \sin \chi$. The energy is given by the black line, and the pressure is given by the grey and dotted lines.

where, in the last line we have inserted (3.133) into (3.135). We have also set $k = 1$ and $\kappa_5 = 1$ for simplicity. In the last equation, the first term corresponds to the critical tension $T^{crit}_{\mu\nu} = 3$ whereas the second term corresponds to the deviation of the energy-momentum from the critical value. Since the trajectory is time-dependent, we expect the ratio $e_{\mu\nu}$ to also be time-dependent. In order to study the energy-momentum profiles, we must freeze the time. In particular, we choose the $t = 0$ braneworld slice as this slice is expected to have the greatest effect on the bulk black hole (its the point of closest proximity of the brane and black hole). Moreover, the expressions for the extrinsic curvature (3.14)–(3.17) simplify considerably since $\dot{\chi} = 0$.

Figure (3.9) shows the effect of a bulk black hole on the brane energy-momentum. We have chosen the mass of the black hole to be small $\mu = 0.1$ and the position of the RS brane to be at $ku = 0.3$. The plot shows that moving closer to the center of the matter distribution on the brane (*i.e.* moving towards the origin) decreases the brane energy (black line) from its critical value $T^{crit}_{\mu\nu} = 3$. However, the pressures (grey and dotted lines) both increase. Thus, the overall effects on the energy-momentum increases when moving closer to the center of the brane. Unfortunately, both WEC

and DEC are violated. Hence, the effect induced on the brane in presence of the black hole results in energy-momentum that is not physically sensible.

The bending of the brane

Since brane and black hole separation did not give the desired results, we will now consider the effects induced on the energy-momentum from the brane bending effect. In Ref. [50], Garriga and Tanaka showed that the brane responds to the black hole by bending. Since the analysis in [50] is restricted to the static case (and we cannot read off the corresponding time-dependent results), we will use an entirely different approach to study the effects of brane bending. We use a perturbative analysis to explore the effects induced on the brane energy-momentum from brane bending. If we consider a shift in the position of the brane $ku \rightarrow 1 + k\delta u$, then the perturbation can be given by a power law behaviour

$$k\delta u = \frac{q}{r^p} \tag{3.137}$$

where q represents the brane bending factor, p denotes the brane bending power and r is the brane radial coordinate. The modified shape of the brane for $k = 1$ is given by

$$\cos\chi(\tau, r) \sim \frac{1}{r}\left(\sqrt{1+r^2}\cos\tau - \frac{1}{1+\frac{q}{r^p}}\right) \tag{3.138}$$

We can control the brane shape by varying the constants q and p. Moreover, we can determine the energy and pressure profiles for a range of values of p and q. The value of $\frac{q}{r^p}$ determines whether the brane will bend towards or away from the black hole.

- For $q < 0$, the energy values are unrealistic; the energy falls below the pressure and therefore violates both energy conditions. This worsens the energy deficit on the brane and does not help with the DEC. All values for which $q < 0$ corresponds to the brane bending towards the black hole. No figures are shown for this case since the results do not give the desired features we are looking for.

- Figure 3.10 shows three examples of energy-momentum profiles for the case where

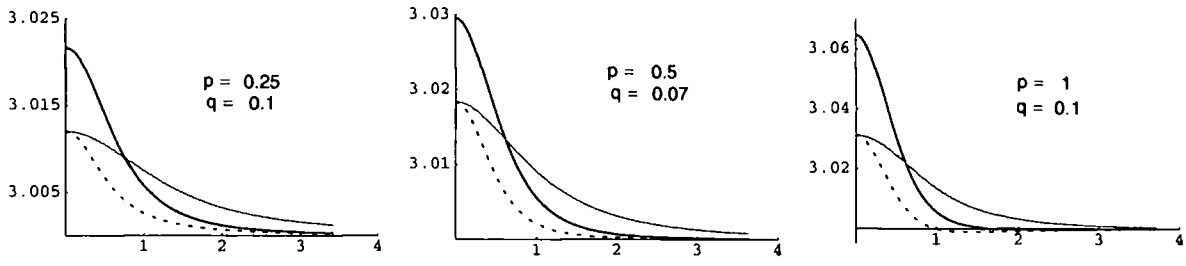

Figure 3.10: A selection of plots of brane energy-momentum with brane bending included for a range of amplitudes and powers of r.

$q > 0$ and $p < 1$. In this case the brane bends in the opposite direction, *i.e.* away from the black hole. From the origin to the intersection point, the energy deficit is removed, *i.e.* the DEC is restored at the central region of the brane (as in the static case). Moving beyond the intersection point and away from the origin leads to the violation of the DEC. Therefore, we obtain a physically realistic energy-momentum profile, but only close to the center of the brane. A physically realistic brane trajectory will therefore respond to a black hole by bending away from it. Thus, bending the brane away from the black hole gives physically sensible results than brane bending towards the black hole. (No graphs are shown for $p > 1$ since this induces an energy deficit on the brane).

As a remark, we point out that unlike the static trajectories, in these time-dependent cases, the black hole is actually in the bulk spacetime, hence these are candidate branes for black holes having recoiled into the bulk. We also state that if we increase the black hole mass, then the effects on the brane energy-momentum changes the picture surprisingly little.

To sum up: we have explored time-dependent brane trajectories in a Sch–AdS spacetime. We showed that the RS brane trajectory is time-dependent in global AdS coordinates. We also obtained expressions for the time-dependent energy density and brane equation. We then qualitatively explored the energy-momentum profiles when matter is present on the brane. We found that bending the brane away from the black hole gave better results than altering the distance between the brane and black hole.

3.6 Summary

In this chapter we have explored the permissible brane trajectories in a spherically symmetric bulk spacetime. With the aim of finding consistent brane black hole solutions, we took braneworld slices of a specific background. With the static braneworld we found solutions that were completely integrable and given in terms of an implicit function of the bulk radial variable. We found all possible complete brane and bulk solutions for a brane containing a matter distribution given in terms of a perfect isotropic fluid. These equations correspond to the brane TOV solutions which have the interpretation of braneworld stars. In fact, these solutions correspond to static slicing of a Sch–AdS bulk spacetime, with the bulk solution corresponding to the part of the Sch–AdS spacetime not containing the horizon of the black hole. Our solutions are therefore non-singular. Furthermore, we obtained solutions in which the black hole horizon appears on the brane. Unfortunately, these solutions produce a divergent pressure on the brane and are reminiscent of the singularity that appears in the TOV system when we are solving for a compact or a very large star.

Analysis of the energy density and pressure profiles revealed that all of the solutions had excess pressure at large radii which is a key feature of the pure AdS bulk slicing. This relates to the fact that the RS brane which is pure Minkowski, is not a static slicing of AdS in global coordinates; it is time-dependent. The way to resolve the problem of surplus pressure is by detuning the tension of the branes, *i.e.* to sub-critical Karch–Randall branes. Unfortunately, these branes cannot be extended to positive mass sources. Although we have been unable to find solutions with the desired features of a braneworld star, some progress in finding exact and complete solutions to the brane TOV problem has been made.

Time dependence seems to be a key feature in finding consistent solutions with the desired features of a braneworld star. Due to the complexity of the equations involved in non-static case, we only explored the qualitative effects induced on the brane energy-momentum. In this method, we froze the time and had taken the $t = 0$ slice. This particular slicing gives the smallest possible separation and it is the point at which the effect of the black hole on the brane is the greatest. This setup differs from the static case as the bulk now contains the black hole. We showed

that bending the brane away from the black hole gave better results than changing the distance between the brane and black hole. However, exact consistent solutions for time-dependent trajectories still remains to be explored.

Finally, it is important to note that in the work so far, we have made the simplifying assumption of Z_2-symmetry around the brane. However, it is important to check if any of our conclusions change significantly if we drop this restriction. In particular, for processes such as black hole recoil, we would expect the black hole to recoil on one side of the brane only, hence breaking the Z_2-symmetry. Maybe, the restrictions found in our solutions can be removed if we break the Z_2-symmetry; this is the topic of the next chapter.

Chapter 4

Asymmetric Braneworld Black Holes

In this chapter we generalise the previous work by relaxing the simplifying assumption of Z_2-reflection symmetry. We explore the possible brane trajectories that are allowed in an asymmetric (non-Z_2 symmetric) background. This setup ensures that the spacetime is distinct on each side of the brane. We consider two types of backgrounds: the Anti de Sitter–Anti de Sitter bulk and the Schwarzschild–Schwarzschild spacetime. Again, the main objective is to consistently embed a three-brane in these non-Z_2 symmetric backgrounds and determine whether the results change significantly from the previous work on the Z_2-symmetric case. Focusing on the static brane equations, we discover that the results for the brane shape, energy density and pressure are analogous to the Z_2-symmetric case. Unfortunately, the calculations for the Schwarzschild–Anti-de Sitter background are not presented as they do not give any simple analytic solutions.

4.1 Introduction

Asymmetric braneworld models are applicable in processes which occur only on one side of the brane, *e.g.* the emission of Hawking radiation and black hole recoil [79–81]. These quantum phenomena may be observed indirectly in high energy particle collisions. The sufficient energies now available (TeV-scale quantum gravity)

at the Large Hadron Collider (a ground-based particle accelerator [82–84]) or the Auger Observatory (which detects high energy cosmic rays produced in the Earth's atmosphere [85–87]) opens up the possibility for the production of mini black holes. (For a complete list of references on black hole production, involving TeV gravity, see [31, 88]). The accelerator generated black holes will decay by the emission of thermal black body radiation. As the process proceeds, the black hole will lose energy by ejecting various particles along the brane and into the bulk [79]. The visible energy released on the brane corresponds to the brane-bound particles and can be detected in the accelerators. However, the invisible energy projected into the bulk corresponds to particles that enter into the extra dimension and is detected by the missing energy signals. The decay of the black hole via the expulsion of thermal radiation is known as the Hawking effect. Eventually this process will terminate when the black hole departs the brane and enters into the realms of the higher dimensions. The latter process is known as black hole recoil and marks the end of Hawking radiation. The time scale for the black hole to escape off the brane and enter into the bulk depends on the initial mass of the generated black hole. Hence, the black hole recoil effect can occur either before or after the black hole evaporation process is completed [80].

The mechanism of black hole recoil is an important indicator for the Hawking evaporation process. The discrete Z_2-symmetry in the Randall–Sundrum scenarios rigidly fixes the small black hole on the brane, preventing it from escaping into the bulk (irrespective of whether a bulk particle is radiated by Hawking emission) [81]. Therefore, at a first glance it seems unlikely that black hole recoil can occur in the Randall–Sundrum braneworld. Also, black hole recoil seems unlikely due to a simple entropy argument [81]. The recoil of a small Randall–Sundrum brane black hole can be identified as a black hole (of mass $\mathcal{M}$ and entropy[1] $\mathcal{M}^{3/2}$) being split into two equal and symmetric smaller black holes (each with mass $\mathcal{M}/2$ and total entropy $2(\mathcal{M}/2)^{3/2} = (\mathcal{M})^{3/2}/\sqrt{2}$). However, this process is forbidden in higher dimensions as it violates the conservation of energy and the non-decreasing property of entropy.

[1] A five-dimensional black hole of mass $\mathcal{M}$ has entropy proportional to $\mathcal{M}^{3/2}$ [60].

Fortunately, this entropy argument is not precise since two crucial factors have not been taken into account: a portion of the brane is excised by the black hole when it interacts with the brane, thus increasing the black hole mass (This feature is seen in probe brane calculations of [89–91]). Moreover, the brane tends to respond to the black hole by bending away from it. This means that more than half of the black hole horizon is sticking out of the bulk. Thus, the consideration of brane capture by the black hole together with the brane bending effect lead to a more precise estimate for the mass and entropy of the black hole. The recoiled black holes now have a greater entropy than the initial brane black hole, making the recoil process entropically permissible. Since the black hole recoil mechanism does not necessarily require a Z_2-symmetric setup, we can generalise the work of the previous chapter by breaking the Z_2-symmetry to explore the subject of asymmetric braneworld black holes. (For a cosmological analysis of black holes being radiated into a non-Z_2 symmetric spacetime together with graviton emission from a braneworld into an asymmetric bulk, see Ref. [93,94]).

4.2 The general brane equations

In this section we derive the general brane equations for the asymmetric model. We need to be careful and treat each side of the brane separately. The quantities on each side of the bulk are made distinct by using the following sign convention: the variables on the left side of the brane are labeled with a '+' sign. Conversely, the variables to the right of the brane are labeled with a '−' sign.

Our starting point is the five-dimensional spherically symmetric coordinate system as before, with the line-element given by

$$ds^2 = -U(r)dt^2 + \frac{dr^2}{U(r)} + r^2(d\chi^2 + \sin^2\chi d\Omega_{II}^2) \tag{4.1}$$

where $U(r)$ denotes a general function of the global radial coordinate and $d\Omega_{II}^2$ is the line-element on a unit 2-sphere. We consider configurations within the asymmetric Randall–Sundrum II model with a single brane of positive tension.

The position of the brane in the five-dimensional spacetime is given by the following 5-vector

$$X^\mu = (t(\tau), r(\rho), \chi(\rho), \theta, \phi) \tag{4.2}$$

with $t(\tau) = \lambda\tau$ where λ denotes a general scale factor. The symbol τ represents the braneworld coordinate time with respect to a co-moving observer on the brane and t denotes the time coordinate in the bulk spacetime. This equation suggests that although the background maybe the same, the time coordinates on each side of the spacetime do not necessarily have to be the same and may therefore differ.

We can form a new basis in terms of the (unnormalised) tangent vectors and the (normalised) unit normal vector:

$$\begin{aligned} T^\mu &= (1,0,0,0,0) \\ R^\mu &= (0,r',\chi',0,0) \\ \Theta^\mu &= (0,0,0,1,0) \\ \Phi^\mu &= (0,0,0,0,1) \\ n_\mu &= \frac{1}{n}(0,-\chi',r',0,0) \end{aligned} \tag{4.3}$$

where n represents some normalisation constant. The overdot and prime respectively denote partial differentiation with respect to the proper time τ and proper distance ρ. The last equation for the unit normal is obtained by using the property that the tangent vectors are orthogonal to the unit normal: $R^\mu n_\mu = 0$ and $T^\mu n_\mu = 0$. Since R^μ and n_μ are both spacelike: $R^\mu R_\mu = 1$ and $n_\mu n^\mu = 1$, we are able to compute the following two constraints:

$$\frac{r'^2}{U} + r^2\chi'^2 = 1 \tag{4.4}$$

$$\chi'^2 U + \frac{r'^2}{r^2} = n^2 \tag{4.5}$$

which can be combined together to yield the normalisation constant

$$n = \frac{\sqrt{U}}{r}. \tag{4.6}$$

The non-Z_2 symmetric Israel junction conditions [70], triggered by the presence of the brane with a non-vanishing distributional energy-momentum tensor $T_{\mu\nu}$, take the form

$$\Delta K_{\mu\nu} = K^+_{\mu\nu} - K^-_{\mu\nu} = \frac{\kappa_5}{3}(3T_{\mu\nu} - h_{\mu\nu}T) \tag{4.7}$$

where $\kappa_5 = 8\pi G_5$ is the five-dimensional gravitational constant. As before, the tensor $h_{\mu\nu} = g_{\mu\nu} - n_\mu n_\nu$ projects vectors onto the wall, whereas its tangential components give the induced metric on the wall. We notice that by breaking the Z_2-symmetry, the jump in extrinsic curvature for the asymmetric model (4.7) is modified from the Z_2-symmetric case (3.8) by an overall factor of 2. The definition of the extrinsic curvature on each side of the brane is given explicitly by

$$K^+_{\mu\nu} = -h^\rho_\mu h^\sigma_\nu \nabla_{(\rho} n^+_{\sigma)} \tag{4.8}$$

$$K^-_{\mu\nu} = h^\rho_\mu h^\sigma_\nu \nabla_{(\rho} n^-_{\sigma)} \tag{4.9}$$

where the '+' and '−' signs distinguish the left and right sides of the bulk, respectively. In the definition of the extrinsic curvature for the left side of the brane (4.8), we have taken into account an overall relative negative sign. This ensures that the brane produced after patching together the left and right sides of the bulk spacetimes satisfies the Israel junction conditions (4.7).

Again we deviate from the simplified ansatz of Chamblin, Hawking and Reall [37] in which the brane was characterised by a constant self-energy. We assume that the matter distribution on the brane, given in terms of the energy-momentum tensor, takes the form of a perfect isotropic fluid

$$T_{\mu\nu} = [\tilde{\rho}(\rho) + P(\rho)]\, h_{\mu\sigma} h_{\nu\rho} u^\sigma u^\rho + P(\rho) h_{\mu\nu} \tag{4.10}$$

with the energy density and pressure given by $\tilde{\rho}(\rho)$ and $P(\rho)$ respectively. The 4-velocity vector u^μ is parallel to the timelike tangent vector T^μ and satisfies the normalisation condition $u^\mu u^\nu h_{\mu\nu} = -1$.

Continuity

In the asymmetric model, we demand that the induced metric must be continuous across the brane. This constrains the four-dimensional brane coordinates on either side of the spacetime, hence giving the following restrictions

$$r_+ \sin\chi_+ = r_- \sin\chi_- \tag{4.11}$$

$$U_+ = \lambda\, U_- \,. \tag{4.12}$$

Here, λ represents some general scale factor, allowing for the fact that time on each side may run at a different rate.

Time parameterisation

The time coordinate can be parameterised differently according to the following prescription

$$dt = \frac{dt}{d\tau} d\tau = \dot{t} d\tau \tag{4.13}$$

where the metric function $g_{tt} = -U$ is now modified to $g_{\tau\tau} = -U\dot{t}^2$. The previous line-element (4.1) becomes

$$ds^2 = -U(r)\, \dot{t}^2 d\tau^2 + \frac{dr^2}{U(r)} + r^2(d\chi^2 + \sin^2\chi d\Omega_{II}^2) \tag{4.14}$$

and the continuity restriction (4.12) is transformed to

$$U_+ \dot{t}_+^2 = U_- \dot{t}_-^2 \,. \tag{4.15}$$

4.2.1 The general Israel and conservation equations

Using the form of the energy-momentum tensor given in (4.10), we can compute the Israel equations for a brane containing a perfect fluid:[2]

[2]The details of the computation of the extrinsic curvatures are given in Appendix A.2.

$$\triangle K_{\tau\tau} = \left[\frac{\chi' U' U \dot{t}^2}{2nr'}\right]_-^+ = \left(\frac{2}{3}\tilde{\rho} + P\right) U\dot{t}^2 \tag{4.16}$$

$$\triangle K_{\theta\theta} = \frac{1}{n}\left[-\chi' U r \sin^2\chi + r' \sin\chi\cos\chi\right]_-^+ = \frac{\tilde{\rho}}{3} r^2 \sin^2\chi \tag{4.17}$$

$$\triangle K_{\rho\rho} = -\frac{1}{n}\left[\frac{U\chi''}{r'} + \frac{2U\chi'}{r}\right]_-^+ = \frac{\tilde{\rho}}{3} \tag{4.18}$$

where we have used the time parameterisation (4.15) in the time-component of the Israel equation (4.16) and the following non-zero components of the four-dimensional metric tensor: $h_{\tau\tau} \equiv g_{\tau\tau} = -U\dot{t}^2$, $h_{\theta\theta} = r^2 \sin^2\chi$ and $h_{\rho\rho} = 1$. For simplicity, we have set $\kappa_5 = 1$.

Differentiating (4.17) with respect to ρ gives an additional but not independent equation from conservation of energy-momentum:

$$\frac{\tilde{\rho}'}{3} = \left[\frac{\chi' r'}{nr^2}\left(U - 1 - \frac{1}{2}\frac{U' r}{r'}\right)\right]_-^+ . \tag{4.19}$$

Inserting the definition of the normalisation constant (4.6) into equations (4.16)–(4.19) and writing each side of the bulk explicitly yields the Israel and conservation equations:

$$\frac{2}{3}\tilde{\rho} + P = \frac{\chi'_+ U'_+ r_+}{2r'_+\sqrt{U_+}} + \frac{\chi'_- U'_- r_-}{2r'_-\sqrt{U_-}} \tag{4.20}$$

$$\frac{\tilde{\rho}}{3} = \frac{r'_+ \cot\chi_+}{\sqrt{U_+} r_+} - \chi'_+\sqrt{U_+} + \frac{r'_- \cot\chi_-}{\sqrt{U_-} r_-} - \chi'_-\sqrt{U_-} \tag{4.21}$$

$$-\frac{\tilde{\rho}}{3} = r_+\sqrt{U_+}\left[\frac{\chi''_+}{r'_+} + \frac{2\chi'_+}{r_+}\right] + r_-\sqrt{U_-}\left[\frac{\chi''_-}{r'_-} + \frac{2\chi'_-}{r_-}\right] \tag{4.22}$$

$$\frac{\tilde{\rho}'}{3} = \frac{\chi'_+ r'_+}{r_+\sqrt{U_+}}\left[U_+ - 1 - \frac{1}{2}\frac{U'_+ r_+}{r'_+}\right] + \frac{\chi'_- r'_-}{r_-\sqrt{U_-}}\left[U_- - 1 - \frac{1}{2}\frac{U'_- r_-}{r'_-}\right] \tag{4.23}$$

where all the primes denote partial differentiation with respect to ρ.

We can therefore successfully embed a four-dimensional brane containing a perfect fluid in a five-dimensional asymmetric background defined by a single function

$U(r)$ as long as we can obtain a consistent set of functions: $\tilde{\rho}(\rho)$, $P(\rho)$ and $\chi(\rho)$ - with the latter denoting the position of the brane in the five-dimensional spacetime - satisfying (4.20)–(4.23).

4.2.2 A general metric function

To solve the general brane equations (4.20)–(4.23) for a general metric function, we begin with the following three equations: (4.4), (4.11) and (4.12). They are given respectively as:

$$\frac{r_{\pm}'^2}{U_{\pm}} + r_{\pm}^2 \chi_{\pm}'^2 = 1 \tag{4.24}$$

$$r_+ \sin\chi_+ = r_- \sin\chi_- \tag{4.25}$$

$$U_+ = \lambda U_- \,. \tag{4.26}$$

We will assume that the negative constraint of (4.24) holds:

$$\frac{r_-'^2}{U_-} + r_-^2 \chi_-'^2 = 1 \,. \tag{4.27}$$

In order to ensure consistency in the setup, we would like to show that the positive constraint of (4.24)

$$\frac{r_+'^2}{U_+} + r_+^2 \chi_+'^2 = 1 \tag{4.28}$$

which can be rewritten as

$$\left(\frac{r_+'}{r_+}\right)^2 + U_+ \chi_+'^2 - \frac{U_+}{r_+^2} = 0 \tag{4.29}$$

also holds. In order to produce a consistent set of equations, we would like to compute the following quantities: r_+, r_+' and χ_+', expressing them entirely in terms of the negative variables r_- and χ_-. Substituting these derived quantities back into equation (4.29) will give the desired consistency relations. We can then solve the general brane equations (4.20)–(4.23).

We start the analysis by working with a general metric function corresponding to an Schwarzschild–Anti de Sitter spacetime. The bulk metric function on each side of the brane is described by

$$U_+(r) = 1 + K_+^2 r_+^2 - \frac{M_+}{r_+^2}, \qquad U_-(r) = 1 + k_-^2 r_-^2 - \frac{m_-}{r_-^2} \tag{4.30}$$

where the constants K_+ and M_+ (k_- and m_-) denote the inverse Anti-de Sitter radius and Schwarzschild mass parameter for the left (right) side of the bulk spacetime. The explicit substitution of U_+ into the continuity relation (4.26) yields the expression

$$r_+^2 = \frac{1}{2K_+^2}\left[(\lambda U_- - 1) \pm \sqrt{(1-\lambda U_-)^2 + 4K_+^2 M_+}\right] \tag{4.31}$$

with the valid solution corresponding to the positive sign. Differentiating (4.26) with respect to ρ yields a further relation

$$\frac{r_+'}{r_+} = \lambda\left[\frac{r_-'}{r_-}\right]\left[\frac{1 - U_- + 2k_-^2 r_-^2}{1 - \lambda U_- + 2K_+^2 r_+^2}\right]. \tag{4.32}$$

We have therefore computed r_+ and $\frac{r_+'}{r_+}$ explicitly in terms of minus variables (with the exception of the constant terms K_+ and M_+ since these are ρ-independent). We need to derive one further quantity: χ_+'. This term is obtained by defining

$$\cot\chi_+ = \frac{r_+\cos\chi_+}{r_+\sin\chi_+} = \frac{r_+}{r_-\sin\chi_-}\sqrt{1-\sin^2\chi_+} \tag{4.33}$$

and replacing for $\sin\chi_+$ using (4.25). This gives

$$\cot\chi_+ = \frac{\sqrt{r_+^2 - r_-^2\sin^2\chi_-}}{r_-\sin\chi_-} \tag{4.34}$$

which can be subsequently rearranged and differentiated with respect to ρ

$$\frac{\partial}{\partial\rho}(\cot\chi_+ r_-\sin\chi_-) = \frac{\partial}{\partial\rho}(r_+^2 - r_-^2\sin^2\chi_-)^{\frac{1}{2}} \tag{4.35}$$

to yield

$$\chi'_+ = [(r_+^2 - r_-^2 \sin^2\chi_-)^{-\frac{1}{2}}(r_+r'_+ - r_-r'_- \sin^2\chi_- - r_-^2 \sin\chi_- \cos\chi_-\chi'_-) \\ - \cot\chi_+ r_- \cos\chi_-\chi'_- - \cot\chi_+ r'_- \sin\chi_-] \left[\frac{-1}{r_- \sin\chi_-(1+\cot^2\chi_+)}\right] . \tag{4.36}$$

We have now obtained expressions for r_+, r'_+ and χ'_+ entirely in terms of its negative counterparts. These terms can now be substituted into the positive constraint (4.29) to yield the consistency relations.

Since the brane equations for an asymmetric Schwarzschild–Anti de Sitter spacetime are difficult to solve analytically, we study two simpler backgrounds. First, we study three possible cases which involves a distinct *Anti-de Sitter* bulk spacetime on either side of the brane:

- **Case 1:** $K_+ = k_- = 1$ and λ general.
- **Case 2:** K_+, k_- and λ all general.
- **Case 3:** K_+, k_- general and $\lambda = 1$.

We then study the case of a brane embedded between two distinct *Schwarzschild* backgrounds:

- **Case 4:** M_+, m_- general and $\lambda = 1$.

4.3 A five-dimensional Anti-de Sitter bulk

Case 1: $K_+ = k_- = 1$ and λ general

In this section we solve the brane equations of motion for a brane embedded in an asymmetric, five-dimensional Anti-de Sitter (AdS) bulk spacetime. We set the inverse AdS radii to equal unity: $K_+ = k_- = 1$ and set the mass parameters to zero: $M_+ = m_- = 0$. We leave the scale factor λ to be general. Continuity of the bulk metric function (4.26) yields the expression

$$r_+ = \sqrt{\lambda(1 + r_-^2) - 1} \tag{4.37}$$

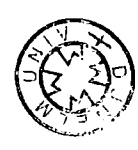

which can be differentiated with respect to ρ to give

$$r'_+ = \frac{\lambda r_- r'_-}{\sqrt{\lambda(1+r_-^2)-1}}. \tag{4.38}$$

Substituting the above expressions for r_+ and r'_+ into (4.34) and (4.36) enables us to compute the terms $\cot\chi_+$ and hence χ'_+ in terms of r_- and χ_-. This then allows us to write the positive constraint (4.29) entirely in terms of negative variables:

$$\frac{-2(\lambda-1)\left[r'^2\cos 2\chi + \sin^2\chi\,[1+r^4-r^2(-2+r'^2)] - r'\sin 2\chi(1+r^2)\sqrt{1-\frac{r'^2}{1+r^2}}\,\right]}{(1+r^2)(-1+\lambda+\lambda r^2)\,[2(\lambda-1)+(-1+2\lambda+\cos 2\chi)r^2]} = 0. \tag{4.39}$$

For convenience, we have dropped the minus subscripts in the latter equation since all quantities are negative. The consistency relations are determined by writing the expression in the large square brackets in the numerator of (4.39) as a perfect square. Equation (4.39) then simplifies to

$$\frac{-(\lambda-1)\left[r'\cos\chi - \sin\chi(1+r^2)^{\frac{1}{2}}(1+r^2-r'^2)^{\frac{1}{2}}\right]^2}{(1+r^2)(-1+\lambda+\lambda r^2)\,[(\lambda-1)(1+r^2)+r^2\cos^2\chi]} = 0 \tag{4.40}$$

and can be solved by setting the numerator to zero. For the case $\lambda \neq 1$, the consistency relations are:

$$r'_- = \frac{(1+r_-^2)\sin\chi_-}{\sqrt{1+r_-^2\sin^2\chi_-}} \tag{4.41}$$

$$\chi'_- = \frac{\cos\chi_-}{r_-\sqrt{1+r_-^2\sin^2\chi_-}} \tag{4.42}$$

where the last line has been obtained by resubstituting r'_- back into the negative constraint (4.27). Inserting the derived quantities: $r_+, r'_+, \cot\chi_+, \chi'_+, r_-$ and χ_- into the general brane equations (4.20)–(4.23) yields the Israel and conservation equations:

$$P+\frac{2}{3}\tilde{\rho} = \frac{\sqrt{\lambda}r_-\cos\chi_- + \sqrt{\lambda(1+r_-^2)-(1+r_-^2\sin^2\chi_-)}}{\sqrt{\lambda(1+r_-^2)}\sqrt{1+r_-^2\sin^2\chi_-}} \tag{4.43}$$

$$\frac{\tilde{\rho}}{3} = 0 \tag{4.44}$$

$$\frac{\tilde{\rho}'}{3} = 0 \tag{4.45}$$

where equations (4.21) and (4.22) are identical and are given by (4.44). The above results clearly imply zero energy density on the brane. This suggests that a brane trajectory does not exist. We therefore do not derive any further equations here and instead, study a more general case.

Case 2: K_+, k_- and λ all general

We generalise the above results by studying the case where K_+, k_- and λ are all general. After a lengthy calculation we arrive at the following expression obtained from the positive constraint (4.29):

$$\begin{aligned}-2K_+^2(\lambda-1)\left[r'\cos\chi-\sin\chi(1+k^2r^2)^{\frac{1}{2}}(1+k^2r^2-r'^2)^{\frac{1}{2}}\right]^2 \\ +2r^2(K_+^2-k^2)\left[K_+^2\sin^2\chi(1+k^2r^2)+\lambda\,k^2r'^2\right]=0\,.\end{aligned} \tag{4.46}$$

Again, we have dropped the minus subscripts on all negative quantities, with the exception of the ρ-independent term K_+. Now, it is not trivial to solve for r'_- since we would obtain a quadratic equation in r'^2_-, giving us quite complicated consistency relations, hence rather lengthy expressions for the brane equations. This makes the system of equations more complicated to solve. Instead, we study a solvable class of solutions for the AdS background. In this case, we set the general scale factor to unity ($\lambda = 1$) and keep the inverse of the AdS radii (K_+ and k_-) general.

4.3.1 A solvable class of solutions

We compute the brane equations for an asymmetric model involving an AdS bulk on either side of the brane. We assume that the background on each side of the four-

dimensional hypersurface is distinct and is characterised by a differing cosmological constant. We find complete analytic solutions for the shape of the brane, the energy density and pressure. We show that these results are analogous to the Z_2-symmetric AdS case.

Case 3: K_+, k_- general and $\lambda = 1$

The bulk metric functions for each side of the brane are given by

$$U_+ = 1 + K_+^2 r_+^2, \qquad U_- = 1 + k_-^2 r_-^2 \tag{4.47}$$

where K_+ and k_- correspond to the inverse AdS radii on the left and right sides of the wall, respectively. Assuming that the scale factor in (4.26) is equal to unity $\lambda = 1$, then continuity of the bulk metric function yields

$$r_+^2 = \frac{U_- - 1}{K_+^2} = \frac{k_-^2 r_-^2}{K_+^2} \tag{4.48}$$

which can be differentiated with respect to ρ to give

$$\frac{r_+'}{r_+} = \frac{r_-'}{r_-}. \tag{4.49}$$

The substitution of (4.48) into (4.34) forms the relevant expression for $\cot\chi_+$ in the background geometry of AdS spacetime:

$$\cot\chi_+ = \frac{\sqrt{k_-^2 - K_+^2 \sin^2\chi_-}}{K_+ \sin\chi_-}. \tag{4.50}$$

Furthermore, equations (4.48) and (4.49) can be inserted into the positive constraint (4.29) to give

$$\chi_+' = \frac{K_+}{k_- r_-} \cos\chi_-. \tag{4.51}$$

Once again, if we assume that the negative constraint (4.27) holds, then the consistency relations required for the positive constraint (4.29) to also be valid are given by two first order, coupled differential equations:

$$r'_- = \frac{K_+}{k_-}\sqrt{1+k_-^2 r_-^2}\sin\chi_- \tag{4.52}$$

$$\chi'_- = \frac{1}{r_-}\sqrt{1-\frac{K_+^2}{k_-^2}\sin^2\chi_-}\,. \tag{4.53}$$

Equations (4.48)–(4.53) are then used to substitute the derived functions: r_+, r'_+, χ'_+ (and hence χ''_+), $\cot\chi_+$, r'_- and χ'_- into the general brane equations of motion (4.20)–(4.23). This yields the following set of Israel and conservation equations for the AdS background:

$$\frac{2}{3}\tilde{\rho}+P = \frac{k_- r_-}{\sqrt{1+k_-^2 r_-^2}}g(\chi_-) \tag{4.54}$$

$$\frac{\tilde{\rho}}{3} = \frac{1}{k_- r_-}\left[1-\sqrt{1+k_-^2 r_-^2}\right]g(\chi_-) \tag{4.55}$$

$$\frac{\tilde{\rho}'}{3} = 0 \tag{4.56}$$

where the common term is given by the function

$$g(\chi_-) = \left[K_+\cos\chi_- + \sqrt{k_-^2 - K_+^2\sin^2\chi_-}\right]. \tag{4.57}$$

We note that equations (4.21) and (4.22) are identical and are given by equation (4.55). Equations (4.54)–(4.56) can be solved straightforwardly to give complete analytic expressions for the brane shape, energy density and pressure. The integration of (4.56) shows that the energy density is constant throughout the brane $\tilde{\rho} = \rho_0$, where ρ_0 represents an integration constant.

The equation that governs the shape of the brane is derived by rewriting (4.55) in terms of the bulk metric function[3]

$$\left[\frac{\rho_0}{3}\frac{\sqrt{U-1}}{(1-\sqrt{U})} - K_+\cos\chi_-\right]^2 = k_-^2 - K_+^2\sin^2\chi_- \tag{4.58}$$

[3]For convenience, we have dropped the subscript notation on the bulk metric function U since $U_+ = U_-$.

where $U = 1 + k_- r_-^2$. Expanding and simplifying the last equation yields the shape of the brane

$$r_- \cos \chi_- = A(\sqrt{U} - 1) + B(\sqrt{U} + 1) \tag{4.59}$$

with the constants A and B given by:

$$A = \frac{3(k_-^2 - K_+^2)}{2K_+ k_- \rho_0} \tag{4.60}$$

$$B = -\frac{\rho_0}{6K_+ k_-}. \tag{4.61}$$

We notice that the brane equation (4.59) is identical to the Z_2-symmetric AdS case (3.55) even though we have differing constants: (4.60) and (4.61). This implies that the brane trajectories for the asymmetric AdS background are exactly the same as the Z_2-symmetric AdS background and are given in the previous chapter in figure 3.1.

Next we compute an expression for the energy density on the brane. Equations (4.60) and (4.61) can be rearranged as

$$\tilde{\rho} = \rho_0 = -6K_+ k_- B = \frac{3}{2}\frac{(k_-^2 - K_+^2)}{K_+ k_- A}. \tag{4.62}$$

In order to eliminate the positive constant K_+ in the above expression, we write

$$K_+ = \frac{k_-}{\sqrt{1 - 4ABk_-^2}} \tag{4.63}$$

and re-substitute it back into (4.62). This gives a formula for the energy density

$$\tilde{\rho} = \frac{6k_- \; k_-(-B)}{\sqrt{1 - 4ABk_-^2}} \tag{4.64}$$

which is constant throughout the brane. Furthermore, the energy density remains positive for $B < 0$. Expression (4.64) is very similar to the Z_2-symmetric AdS case (3.57), except now the energy density only depends on a single constant B. (In the Z_2-symmetric case, the energy density depended on both constants A and B).

Finally, the equation of state can be obtained by rewriting (4.54) as

$$P = -\frac{2}{3}\rho_0 + \frac{k_- r_-}{\sqrt{1+k_-^2 r_-^2}}\left[\frac{\rho_0}{3}\frac{k_- r_-}{\left(1-\sqrt{1+k_-^2 r_-^2}\right)}\right]. \tag{4.65}$$

Re-expressing the last equation in terms of the bulk metric function and using (4.55) determines the pressure on the brane

$$P = -\rho_0\left[1+\frac{1}{3\sqrt{U}}\right] \tag{4.66}$$

which is always negative. The expression for the pressure is also similar to the Z_2-symmetric AdS case (3.59).

To sum up, we have computed expressions for the brane shape, energy density and pressure for a three-brane embedded in an asymmetric AdS background (for K_+, k_- general and $\lambda = 1$). We have found that all three expressions are analogous to the results obtained in the Z_2-symmetric AdS case.

4.4 A five-dimensional Schwarzschild bulk

We follow the same procedure used for the non-Z_2 symmetric AdS background to compute the brane equations corresponding to an asymmetric Schwarzschild bulk spacetime. We assume that the spacetime on either side of the four-dimensional hypersurface is now characterised by a differing mass term. We find complete analytic solutions for the shape of the brane, the energy density and pressure. We determine that these results are analogous to the Z_2-symmetric case.

Case 4: M_+, m_- general and $\lambda = 1$.

We write the bulk metric functions on either side of the brane as

$$U_+ = 1 - \frac{M_+}{r_+^2}, \qquad U_- = 1 - \frac{m_-}{r_-^2} \tag{4.67}$$

where the constants M_+ and m_- are mass parameters which are responsible for creating a Schwarzschild background on the left and right sides of the brane, respectively. The mass parameters on each side of the hypersurface are related to the

actual mass of the bulk black hole μ by the relations $\mu_- = \frac{3\pi m_-}{8G_5}$ or $\mu_+ = \frac{3\pi M_+}{8G_5}$, where G_5 denotes the five-dimensional Newton constant. Continuity of the bulk metric function (4.26) for the case $\lambda = 1$, implies

$$r_+^2 = \frac{M_+}{1-U_-} = \frac{M_+ r_-^2}{m_-} \tag{4.68}$$

which can be differentiated with respect to ρ to give

$$\frac{r'_+}{r_-} = \frac{r'_-}{r_-}. \tag{4.69}$$

Inserting equation (4.68) into (4.34) yields the relevant expressions for $\cot\chi_+$ corresponding to the Schwarzschild bulk geometry:

$$\cot\chi_+ = \frac{\sqrt{M_+}\sqrt{\frac{1}{m_-} - \frac{1}{M_+}\sin^2\chi_-}}{\sin\chi_-}. \tag{4.70}$$

Moreover, the expressions for r_+ and r'_+ can be substituted into the positive constraint (4.29) to give

$$\chi'_+ = \sqrt{\frac{m_-}{M_+}}\frac{1}{r_-}\cos\chi_-. \tag{4.71}$$

Again, if we suppose that the negative constraint (4.27) holds, we can construct consistency relations in order for the positive constraint (4.29) to also hold:

$$r'_- = \sqrt{\frac{m_-}{M_+}}\sqrt{1-\frac{m_-}{r_-^2}}\sin\chi_- \tag{4.72}$$

$$\chi'_- = \frac{1}{r_-}\sqrt{1-\frac{m_-}{M_+}\sin^2\chi_-}. \tag{4.73}$$

This gives us two first order coupled differential equations which are functions of r_- and χ_-. Equations (4.68)–(4.73) are then used to replace the derived quantities: r_+, r'_+, χ'_+ (and hence χ''_+), $\cot\chi_+$, r'_- and χ'_- into the original brane equations (4.20)–(4.23). This enables us to express the Israel and conservation equations for the Schwarzschild background as:

$$\frac{2}{3}\tilde{\rho} + P = \frac{m_-}{r_-^3\sqrt{1-\frac{m_-}{r_-^2}}} f(\chi_-) \tag{4.74}$$

$$\frac{\tilde{\rho}}{3} = \frac{1}{r_-}\left[1-\sqrt{1-\frac{m_-}{r_-^2}}\right] f(\chi_-) \tag{4.75}$$

$$\frac{\tilde{\rho}'}{3} = -\frac{2m_-}{r_-^4}\sqrt{\frac{m_-}{M_+}}\sin\chi_- f(\chi_-) \tag{4.76}$$

where the common term appearing in the above system of equations is given explicitly by

$$f(\chi_-) = \left[\sqrt{\frac{m_-}{M_+}}\cos\chi_- + \sqrt{1-\frac{m_-}{M_+}\sin^2\chi_-}\ \right]. \tag{4.77}$$

Note that equations (4.21) and (4.22) are equivalent and equal to equation (4.75). Next, we solve equations (4.74)–(4.76) for the brane shape, energy density and pressure. The presence of the common factor (4.77) in the Israel and conservation equations allows for considerable simplification.

First, we compute the expression for the energy density on the brane. Dividing (4.76) by (4.75) gives

$$\frac{\tilde{\rho}'}{\tilde{\rho}} = \frac{-2m_-\sqrt{\frac{m_-}{M_+}}\sin\chi_-}{r_-^2\left[r_- - \sqrt{r_-^2-m_-}\right]}. \tag{4.78}$$

Inserting equation (4.72) into the last equation eliminates the ρ-dependence, giving

$$\frac{d\tilde{\rho}}{\tilde{\rho}} = \frac{-2m_-dr_-}{r_-\left[r_- - \sqrt{r_-^2-m_-}\right]\sqrt{r_-^2-m_-}}. \tag{4.79}$$

A simple substitution

$$\sin v = \frac{\sqrt{m_-}}{r_-} \tag{4.80}$$

enables us to rewrite (4.79) as

$$\int\frac{d\tilde{\rho}}{\tilde{\rho}} = 2\int\frac{\sin v}{1-\cos v}dv. \tag{4.81}$$

The last equation can be easily integrated to give an expression for the energy density

$$\tilde{\rho} = \rho_0(1 - \sqrt{U})^2 \tag{4.82}$$

where ρ_0 represents an integration constant. In order to determine ρ_0 explicitly, we rewrite (4.75) in terms of the bulk metric function[4]

$$\left[\frac{\rho_0}{3} r_-(1 - \sqrt{U}) - \sqrt{\frac{m_-}{M_+}} \cos\chi_-\right]^2 = 1 - \frac{m_-}{M_+} \sin^2\chi_- \tag{4.83}$$

where $U = 1 - \frac{m_-}{r_-^2}$. Expanding and simplifying the last equation yields the following formula for the shape of the brane

$$r_- \cos\chi_- = r_-^2 \left[A(\sqrt{U} - 1) + B(\sqrt{U} + 1)\right] \tag{4.84}$$

where the constants A and B are defined by:

$$A = -\frac{\rho_0}{6}\sqrt{\frac{M_+}{m_-}} \tag{4.85}$$

$$B = \frac{3}{2}\frac{1}{\rho_0 m_-}\sqrt{\frac{M_+}{m_-}}\left[\frac{m_-}{M_+} - 1\right]. \tag{4.86}$$

Again, the brane equation (4.84) is exactly the same as the Z_2-symmetric Schwarzschild background (3.67) with the exception of the differing constants A and B. The brane trajectories for the asymmetric Schwarzschild background are therefore equivalent to the ones presented in the previous chapter in figures 3.2–3.4.

The energy density is formulated by rearranging the above constants: (4.85) and (4.86). This gives

$$\rho_0 = -6A\sqrt{\frac{m_-}{M_+}} = \frac{3}{2Bm_-}\sqrt{\frac{M_+}{m_-}}\left[\frac{m_-}{M_+} - 1\right]. \tag{4.87}$$

[4]As in the AdS case, we have dropped the subscript notation on the bulk metric function since $U_+ = U_-$.

In order to eliminate the square root terms in the above expression, we write

$$\sqrt{\frac{m_-}{M_+}} = \frac{1}{\sqrt{4ABm_- + 1}} \tag{4.88}$$

and re-substitute it back into (4.87) to give

$$\rho_0 = \frac{-6A}{\sqrt{1 + 4ABm_-}} . \tag{4.89}$$

Inserting (4.89) into (4.82) gives a formula for the brane energy density

$$\tilde{\rho} = \frac{-6A}{\sqrt{1 + 4ABm_-}}(1 - \sqrt{U})^2 \tag{4.90}$$

which is positive for $A < 0$. Notice that $\tilde{\rho}$ is not constant for these branes (unlike the AdS case). Again, we find that the relation for the energy density depends only on a single constant A (unlike the Z_2-symmetric case (3.68) which involved both constants A and B).

Finally, the equation of state can be obtained by rewriting (4.74) as

$$P = -\frac{2}{3}\tilde{\rho} + \frac{m_-}{r_-^3\sqrt{U}}\left[\frac{\tilde{\rho} r_-}{3(1 - \sqrt{U})}\right] . \tag{4.91}$$

Re-expressing the last equation entirely in terms of the bulk metric function yields the following expression for the pressure induced on the brane

$$P = -\tilde{\rho} + \frac{\rho_0}{3\sqrt{U}}\left(1 - \sqrt{U}\right)^2\left(1 + 2\sqrt{U}\right) . \tag{4.92}$$

Again, the pressure is similar to the Z_2-symmetric Schwarzschild case (3.69).

To sum up: we have computed expressions for the brane shape, energy density and pressure for a three-brane embedded in an asymmetric Schwarzschild background (for M_+, m_- general and $\lambda = 1$). We have found that all three expressions are similar to the results obtained in the Z_2-symmetric Schwarzschild case.

4.5 Summary

In this chapter, we have found consistent brane embeddings for the asymmetric AdS–AdS background (K_+, k_- general) and Schwarzschild–Schwarzschild background (M_+, m_- general) for the particular case where $\lambda = 1$. In the analysis, we have obtained expressions for the brane shape, the energy density and pressure, all of which are analogous to the Z_2-symmetric case. The complete details regarding the brane trajectories have been covered previously in chapter 3. Unfortunately, the calculations for brane trajectories in an asymmetric Schwarzschild–AdS background has proven to be difficult; the complexity of the equations makes it hard to find simple analytic solutions. These problems may be overcome if we use numerical methods; this is work for future research.

Chapter 5

Black String Instability in Heterotic M-theory

In this chapter we compute scalar and gravitational fluctuations around a flat background in low energy heterotic M-theory. A general coordinate transformation shows that the interbrane distance (*i.e.* the radion) is coupled to the bulk scalar field. In order to determine the gravitational interaction on the brane, we use the formalism presented in chapter 2 to find complete solutions describing the massive gravitons. This enables us to compute the corrections to the Newtonian potential together with the brane graviton propagator. We show that the power law corrections to the Newtonian potential and the form of the four-dimensional propagator are modified from the Randall–Sundrum scenario. Our analysis also determines the instability of a black string. As an application to the work presented in the previous chapters, we comment on work which is currently in progress; the exploration of possible brane black hole solutions in low energy heterotic M-theory.

5.1 Introduction

In general relativity, four-dimensional black holes are known to be classically stable. However, their higher dimensional analogues (*i.e.* black strings) are unstable. Black strings instabilities (or Gregory–Laflamme instabilities) were initially discovered in vacuum [59, 60]. These instabilities can be understood in different ways. If we

assume that the five-dimensional (un)charged black string has a cylindrical event horizon, then the black string instability comes into play when its length reaches a critical value. At this critical length, the black string becomes unstable to classical linear perturbations and fragments. This phenomena can be understood in a simple example provided by the soap bubble analogy. Once a soap bubble reaches a certain length, it too becomes unstable and 'pops.' Entropy arguments can also be used to provide an explanation to the black string instability phenomena. In this case, one can associate an entropy to the event horizon (proportional to its area) of the black string. Calculations show that for a cylindrical event horizon, there exists a critical length of the black string (say $\mathcal{L}$) above which the entropy of a five-dimensional compact black hole [95] (of radius r) is greater than the entropy of the black string (of equivalent mass). At this point, the critical length of the black string exceeds the black hole radius *i.e.* $\mathcal{L} > r$ and the solution ceases to be stable. It is now entropically favorable for the mass to localise into spherical black holes [95].

The corresponding metric of the vacuum black string is given explicitly by adding an extra flat y direction (which is parallel to the string) to the four-dimensional Schwarzschild line element:

$$ds^2 = -\left(1-\frac{2M}{r}\right)dt^2 + \left(1-\frac{2M}{r}\right)^{-1}dr^2 + r^2 d\Omega_{II}^2 + dy^2 . \tag{5.1}$$

This metric is referred to as the Kaluza–Klein black string metric. Since the background space is vacuum, the TTF gauge for h_{ab} (*i.e.* $h^a_a = h^a_{b;a} = 0$) can be used to solve the perturbation equations. Studying the evolution of small perturbations $h_{ab} = \delta g_{ab}$ around a black string determines that the metric perturbation satisfies the Lichnerowicz equation[1]

$$\triangle_L h_{ab} = \delta_a{}^c \delta_b{}^d \Box h_{cd} + 2R_a{}^c{}_b{}^d h_{cd} = 0 . \tag{5.2}$$

The last equation can be decomposed into scalar, vector and tensor components. For any unstable mode, the vector and scalar modes were shown to be zero, reducing

[1]Using the Lichnerowicz operator given previously in chapter 2 of equation (2.21).

the system of linearised equations to a single tensor perturbation

$$(\triangle_L^{(4)} + m^2)h_{\mu\nu} = 0\,. \tag{5.3}$$

This expression corresponds to the effective four-dimensional massive Lichnerowicz equation. The mass term arises from the y-dependence on the perturbation and $\triangle_L^{(4)}$ represents the four-dimensional Lichnerowicz operator. The solution to (5.3) was shown to exhibit an instability in the s-wave mode. Pictorially, the effect of the instability is to cause the event horizon of the black string to collapse in some regions of the extra dimension and expand in others. In other words, the instability causes the horizon to ripple. Ultimately, the cylindrical event horizon of the black string fragments quantum mechanically into a periodic array of higher dimensional black holes.

The black string instability was then extended to non-vacuum spacetimes, in particular, the Anti-de Sitter (AdS) background [58]. In a previous chapter we had discussed the Chamblin, Hawking and Reall black string [37] in which the authors obtained the black string metric by adding an additional warp factor in front of the four-dimensional line-element of the vacuum metric (5.1). If we now account for Z_2-symmetry in the background AdS spacetime, we obtain

$$ds^2 = e^{\pm 2k|y|}\left[-\left(1-\frac{2M}{r}\right)dt^2 + \left(1-\frac{2M}{r}\right)^{-1}dr^2 + r^2 d\Omega_{II}^2\right] + dy^2\,. \tag{5.4}$$

This metric is known as the Randall–Sundrum (RS) black string metric. Since this line-element contains a bulk cosmological constant (present in the warp factor $a(y) = e^{\pm k|y|}$), we expect the instability argument for the RS black string to be different from the Kaluza–Klein black string. Thus, by studying the evolution of perturbations around the RS black string, we determine that the linearised field equations reduces to

$$\Box^{(4)}h_{\mu\nu} + 2R^{(4)}_{\mu\lambda\nu\rho}h^{\lambda\rho} - \left[a^4\left(a^{-2}h_{\mu\nu}\right)'\right]' = 0 \tag{5.5}$$

where $R^{(4)}_{\mu\lambda\nu\rho}$ and $\Box^{(4)}$ denote the four-dimensional Schwarzschild Riemann tensor and the wave operator, respectively. If we set

$$h_{\mu\nu} = \chi_{\mu\nu} u_m(y) \tag{5.6}$$

where the y-dependent function is given by

$$u_m(y) = \left[\mathcal{A} J_2\left(\frac{m}{k} e^{ky}\right) - \mathcal{B} N_2\left(\frac{m}{k} e^{ky}\right)\right] \tag{5.7}$$

then the arbitrary constants $\mathcal{A}$ and $\mathcal{B}$ can be chosen so that the perturbation satisfies the boundary conditions. Thus, for the RS black string, the tensor perturbation becomes

$$\left[a^4 \left(a^{-2} h_{\mu\nu}\right)'\right]' = m^2 h_{\mu\nu} \tag{5.8}$$

and $\chi_{\mu\nu}$ satisfies the following equation of motion

$$(\triangle_L^{(4)} + m^2)\chi_{\mu\nu} = 0\,. \tag{5.9}$$

Therefore, the form of the four-dimensional instability for the RS black string is the same as the Kaluza–Klein black string (as equations (5.3) and (5.9) are similar). However, for the RS black string, we obtain an additional y-dependent part (5.7) relevant for the RS background. Hence, the evolution of black string is different to the Kaluza–Klein black string; we now get an accumulation of "mini" black holes with the frequency of ripples increasing as the AdS horizon is approached: $y \to \pm\infty$.

So far, we have discussed black string instabilities in vacuum and AdS spacetimes. In this chapter we extend the analysis further to explore the instability of a black string in the background of low energy heterotic M-theory.

5.2 Perturbation equations

In this section we describe the static LOSW model and give the background solution using a modified metric ansatz from the one presented in section 2.2. By considering bulk perturbations, we are able to derive the five-dimensional, linearised scalar and gravitational field equations.

5.2.1 Heterotic M-theory

We consider the dimensionally reduced five-dimensional effective action derived by Lukas *et al* [32]. The action consists of terms which describe gravity, the bulk scalar field and two boundary branes, respectively,

$$\begin{aligned} S^{(5)} = \frac{1}{2\kappa_5}\int d^5x\sqrt{-g}\left[R - \frac{1}{2}(\partial\phi)^2 - \frac{1}{3}\alpha^2 e^{-2\phi}\right] \\ + \frac{\sqrt{2}\alpha}{\kappa_5}\left[\int_{y=-y_0} d^4x\sqrt{-g^-}e^{-\phi} - \int_{y=+y_0} d^4x\sqrt{-g^+}e^{-\phi}\right] \end{aligned} \tag{5.10}$$

where R is the five-dimensional Ricci scalar, $g^{\pm}_{\mu\nu}$ is the induced metric on each brane, $\kappa_5 = 8\pi G_5$ is the five-dimensional gravitational constant[2] and α is an arbitrary coupling constant which parameterises the number of units of 4-form flux which threads the Calabi-Yau [105]. The symbol ϕ represents the bulk scalar field[3] supporting each of the boundary branes. The branes have equal and opposite tensions and are positioned parallel to each other at $y = \pm y_0$ (where y is the transverse direction to the brane). We will impose a Z_2-symmetry at the position of each of the branes (*i.e.* we identify the points $y \leftrightarrow -y$). This setup therefore corresponds to five-dimensional gravity with a bulk scalar field, coupled to each brane.

The resulting five-dimensional equations of motion following from the action (5.10) are

$$\begin{aligned} G^{(5)}_{ab} =& \frac{1}{2}\phi_{,a}\,\phi_{,b} - \frac{1}{4}g_{ab}\phi_{,}{}^{c}\,\phi_{,c} - \frac{1}{6}g_{ab}\alpha^2 e^{-2\phi} \\ &+ \sqrt{2}\alpha[\delta(y+y_0) - \delta(y-y_0)]g_{\mu\nu}\delta^{\mu}_{a}\delta^{\nu}_{b}\frac{e^{-\phi}}{\sqrt{g_{yy}}} \end{aligned} \tag{5.11}$$

$$\Box^{(5)}\phi = -\frac{2}{3}\alpha^2 e^{-2\phi} + 2\sqrt{2}\alpha[\delta(y+y_0) - \delta(y-y_0)]\frac{e^{-\phi}}{\sqrt{g_{yy}}} \tag{5.12}$$

where $G^{(5)}_{ab}$ and $\Box^{(5)} = \eta^{\mu\nu}\partial_\mu\partial_\nu + \partial_y{}^2$ represent the five-dimensional Einstein tensor and curved space d'Alembertian operator, respectively. We note that the Greek

[2]For simplicity, we will set the five-dimensional gravitational constant to unity κ_5=1.

[3]In Ref. [32] and chapter 2, the scalar field ϕ is related to the field V by the relation $V = e^{\phi}$.

indices run over the four dimensions $\mu, \nu = 0, 1, 2, 3$ whereas the Latin indices run over all five dimensions $a, b = 0, 1, 2, 3, 4$.

In order to find a three-brane solution in the background of heterotic M-theory, we start with the metric ansatz[4]

$$ds^2 = a^2(y)\eta_{\mu\nu}dx^\mu dx^\nu + dy^2 \tag{5.13}$$

where the brane scale factor $a(y)$ is a function of the fifth dimension. The general solution for this ansatz which satisfies the equations of motion is given by

$$a(y) = H^{1/6} \tag{5.14}$$

$$\phi(y) = \ln H \tag{5.15}$$

$$H(y) = \sqrt{2}\alpha|y| + c_0\,, \qquad -y_0 \leq y \leq y_0 \tag{5.16}$$

where c_0 is an arbitrary constant and H represents the harmonic linear function which is fixed by the boundary source terms. The metric (5.13) therefore solves the background equations of heterotic M-theory (5.11)–(5.12) with the solutions given by (5.14)–(5.16).

5.2.2 Scalar and gravitational perturbations

We now derive the five-dimensional scalar and gravitational perturbations with respect to the background metric. In order to deal with the Z_2-symmetry as well as the junction conditions at the branes, we make the following gauge choice that preserves the Gaussian Normal coordinate system: $g_{yy} = 1$, $g_{\mu y} = 0$. This specific gauge choice allows us to perturb the brane system such that the brane stays at the coordinate origin $y = 0$.

Consider the following linearised metric and scalar field perturbations around a background solution

$$g_{ab} \rightarrow g_{ab} + h_{ab} \tag{5.17}$$

$$\phi \rightarrow \phi + \delta\phi \tag{5.18}$$

[4]The metric ansatz of chapter 2, equation (2.105) is modified by setting $b(y) = 1$.

where h_{ab} and $\delta\phi$ are small variations of the metric tensor and scalar field, respectively. We seek solutions of the form $\phi = \phi(y)$ and $\delta\phi = \delta\phi(x^\mu, y)$ where the perturbation of the scalar field is now a function of both x^μ and y.

Rewriting the Einstein equation (5.11) entirely in terms of the Ricci tensor

$$R_{ab} = \frac{1}{2}\phi_{,a}\,\phi_{,b} + \frac{1}{9}\alpha^2 g_{ab} e^{-2\phi} - \frac{4\sqrt{2}}{3}\alpha[\mathcal{D}]e^{-\phi}g_{ab} + \sqrt{2}\alpha[\mathcal{D}]e^{-\phi}g_{\mu\nu}\delta^\mu_a\delta^\nu_b \tag{5.19}$$

and using the definition of the Lichnerowicz operator[5] previously stated in equation (2.21), enables us to compute the linearised Einstein field equation

$$\begin{aligned}\Delta_L h_{ab} = &-2\phi_{,(a}\,(\delta\phi)_{,b)} - \frac{2}{9}\alpha^2 e^{-2\phi}(h_{ab} - 2g_{ab}\delta\phi) \\ &+ \frac{8\sqrt{2}}{3}\alpha[\mathcal{D}]e^{-\phi}(h_{ab} - g_{ab}\delta\phi) - 2\sqrt{2}\alpha[\mathcal{D}]e^{-\phi}(h_{\mu\nu} - g_{\mu\nu}\delta\phi)\delta^\mu_a\delta^\nu_b\,.\end{aligned} \tag{5.20}$$

The linearised scalar field equation is

$$-h^{cd}\nabla_c\nabla_d\phi + \Box^{(5)}\delta\phi - \nabla_c\phi\nabla_d\bar{h}^{cd} = \frac{4}{3}\alpha^2 e^{-2\phi}\delta\phi - 2\sqrt{2}\alpha[\mathcal{D}]e^{-\phi}\delta\phi \tag{5.21}$$

where we have set $[\mathcal{D}] = [\delta(y + y_0) - \delta(y - y_0)]$ to represent the boundary of space-time.

The bulk gravitational equations (5.20) can be decomposed into scalar, vector and tensor components. These three equations together with the dilaton equation (5.21) are given respectively:

$$\frac{1}{a^2}\left[a^2\left(\frac{h}{a^2}\right)'\right]' = -12\frac{a'}{a}(\delta\phi)' + 8\left(\frac{a'}{a}\right)^2\delta\phi - 16\frac{a'}{a}[\mathcal{D}]\delta\phi \tag{5.22}$$

$$\left[\frac{h_{\mu\lambda}{}^{,\lambda} - h_{,\mu}}{a^2}\right]' = 6\frac{a'}{a}(\delta\phi)_{,\mu} \tag{5.23}$$

$$\begin{aligned}\frac{\Box h_{\mu\nu} + h_{,\mu\nu} - 2h_{\lambda(\mu,\nu)}{}^{,\lambda}}{a^2} + \frac{1}{a^2}\left[a^4\left(\frac{h_{\mu\nu}}{a^2}\right)'\right]' + aa'\left[\frac{h}{a^2}\right]'\eta_{\mu\nu} \\ = 8(a')^2\eta_{\mu\nu}\delta\phi - 4[\mathcal{D}]aa'\eta_{\mu\nu}\delta\phi\end{aligned} \tag{5.24}$$

[5]In Appendix B.2, we have given the components of the Lichnerowicz operator explicitly in terms of the five-dimensional gauge quantities.

$$3\frac{a'}{a}\left[\frac{h}{a^2}\right]' = -\frac{\Box\delta\phi}{a^2} - (\delta\phi)'' - 4\frac{a'}{a}(\delta\phi)' + 24\left(\frac{a'}{a}\right)^2\delta\phi - 12\frac{a'}{a}[\mathcal{D}]\delta\phi \qquad (5.25)$$

where we have used $\alpha^2 e^{-2\phi} = 18\left(\frac{a'}{a}\right)^2$ and $\phi' = 6\frac{a'}{a}$ for the background values of the coupling constant α and the dilaton ϕ. In the above, the primes denote differentiation with respect to y. The terms $\Box h_{\mu\nu} = h_{\mu\nu,\lambda}{}^{\lambda}$ and $\Box\delta\phi = \delta\phi_{,\lambda}{}^{\lambda}$ represent the four-dimensional flat space d'Alembertian operator acting on the metric and scalar field perturbations respectively. We note that the linearised Einstein equations (5.22)–(5.24) in the transverse-traceless gauge (in which $\delta\phi = 0$) are equivalent to the Randall–Sundrum II case in the absence of brane matter sources.

5.2.3 Lorentz decomposition of the metric perturbation

To solve the vector and tensor perturbation equations (5.23) and (5.24), we take the general metric perturbation $h_{\mu\nu}$ and decompose it in terms of irreducible representations of the diffeomorphism group (*i.e.* irreducible components of the four-dimensional Lorentz group), previously discussed in Ref. [96]

$$h_{\mu\nu} = h^{tt}_{\mu\nu} + 2A_{(\mu,\nu)} + \psi_{,\mu\nu} + \frac{1}{4}\eta_{\mu\nu}\left(h - \Box\psi\right) . \qquad (5.26)$$

The transverse trace-free mode $h^{tt}_{\mu\nu}$ satisfies $h^{tt}_{\mu\nu,}{}^{\nu} = h^{tt}{}_{\mu}{}^{\mu} = 0$ and the Lorentz-gauge vector A_μ is divergence-free $A_{\mu,}{}^{\mu} = 0$. The two scalar fields are represented by ψ and $h = h_{\mu}{}^{\mu}$. We will ignore A_μ in the work as it is irrelevant for the instability analysis.

After applying the above decomposition, (5.23) and (5.24) become

$$\frac{3}{4}\left[\frac{(\Box\psi - h)_{,\mu}}{a^2}\right]' = 6\frac{a'}{a}(\delta\phi)_{,\mu} \qquad (5.27)$$

$$\begin{aligned}\frac{\Box h^{tt}_{\mu\nu}}{a^2} - \frac{(\Box\psi - h)_{,\mu\nu}}{2a^2} + \frac{1}{a^2}\left[a^4\left(\frac{h^{tt}_{\mu\nu} + \psi_{,\mu\nu}}{a^2}\right)'\right]' \\ + \eta_{\mu\nu}\left\{-\frac{\Box(\Box\psi - h)}{4a^2} - \frac{1}{4a^2}\left[a^4\left(\frac{\Box\psi - h}{a^2}\right)'\right]' + aa'\left(\frac{h}{a^2}\right)'\right\} \\ = 8(a')^2\eta_{\mu\nu}\delta\phi - 4aa'[\mathcal{D}]\eta_{\mu\nu}\delta\phi\end{aligned} \qquad (5.28)$$

where the quantities $h^{tt}_{\mu\nu}$ and ψ satisfy the four-dimensional Klein-Gordon equation $\Box h^{tt}_{\mu\nu} = m^2 h^{tt}_{\mu\nu}$ and $\Box\psi = m^2\psi$, respectively.

5.3 Solutions to the perturbation equations

In this section we solve the bulk perturbation equations for the massless and massive modes. First, we impose the transverse-tracefree (TTF) gauge to obtain the TTF component of the metric perturbation. This yields two eigenvalue solutions which correspond to the massless graviton zero mode and the massive Kaluza–Klein tower. The former solution is used in a later section to identify the graviton wavefunction. We then discard our assumption of the TTF gauge and solve the perturbation equations in general, using the Lorentz decomposition introduced in the previous section. We determine that there exists only one eigenstate for the scalar mode corresponding to the massless scalar mode.

5.3.1 Transverse-tracefree perturbations

The massive TTF eigenfunction

The TTF components of the metric perturbation: $h^{tt}_{\mu\lambda,}{}^{\lambda} = 0$ and $h^{tt} = h^{tt}{}_{\lambda}{}^{\lambda} = 0$ describes the graviton modes [39]. In order for the linearised equations (5.22)–(5.25) to be consistent we need to set $\delta\phi = 0$. The system of perturbation equations reduces to one single tensor equation

$$\left[a^4\left(\frac{h^{tt}_{\mu\nu}}{a^2}\right)'\right]' + m^2 h^{tt}_{\mu\nu} = 0 \tag{5.29}$$

and is equivalent to equation (2.25) obtained in the RSII scenario[6]. In order to solve this equation, it is convenient to make the following change of variables

$$dz = \frac{dy}{a}\,. \tag{5.30}$$

Setting $k = \frac{5\sqrt{2}\alpha}{6}$ allows us to rewrite (5.14) as

[6]We note that the warp factors are different in the LOSW and RSII models.

$$a(z) = (kz)^{1/5}\,. \tag{5.31}$$

A short calculation yields the expression

$$\ddot{h}^{tt}_{\mu\nu} - \frac{1}{5z}\dot{h}^{tt}_{\mu\nu} + \left[\frac{8}{25z^2} + m^2\right] h^{tt}_{\mu\nu} = 0 \tag{5.32}$$

where the overdot denotes differentiation with respect to the new variable z. Equation (5.32) can now be solved analytically. The massive solutions are given by the eigenfunction

$$h^{tt}_{\mu\nu} = z^{3/5}\left[\mathcal{P}_{\mu\nu}J_{1/5}(mz) + \mathcal{Q}_{\mu\nu}N_{1/5}(mz)\right] \tag{5.33}$$

where $J_n(mz)$ and $N_n(mz)$ correspondingly represent (order n) Bessel functions of the first and second kind. Here, m denotes the mass of the excitation. The symbols $\mathcal{P}_{\mu\nu}$ and $\mathcal{Q}_{\mu\nu}$ are functions of the four-dimensional coordinates x^μ (independent of z). The ratio of the constant $\mathcal{P}_{\mu\nu}/\mathcal{Q}_{\mu\nu}$ is determined by the boundary condition at the position of the visible brane $z = z_+$. At this position, we normalise $a(z)$ such that it equals unity $a(z_+) = 1$. This will eliminate one of the constants in (5.33). The remaining constant is determined by normalisation.

Let us now turn our attention to the boundary condition applied at the discontinuity of the orbifold fixed planes

$$\left(\partial_z h^{tt}_{\mu\nu} - \frac{2}{5z}h^{tt}_{\mu\nu}\right)\Big|_{z_+} = 0\,. \tag{5.34}$$

Inserting equation (5.33) into (5.34) enables us to evaluate the boundary condition at the position of the visible brane where $z_+ = \frac{1}{k}$. Using the identity for Bessel functions given previously in equation (2.40) enables us to obtain the expression

$$h^{tt}_{\mu\nu} = z^{3/5}\mathcal{Q}_{\mu\nu}\left[-\frac{N_{-4/5}(\frac{m}{k})}{J_{-4/5}(\frac{m}{k})}J_{1/5}(mz) + N_{1/5}(mz)\right] \tag{5.35}$$

where $\mathcal{Q}_{\mu\nu}$ is a normalisation constant. We can determine $\mathcal{Q}_{\mu\nu}$ by rewriting the TTF Bessel equation (5.29) in Sturm-Liouville form[7] [43]

[7]See Appendix B.5 for the definition of the Sturm-Liouville equation and its corresponding orthonormality relation.

$$\frac{d}{dz}\left[a^3\frac{d}{dz}\left(\frac{h^{tt}_{\mu\nu}}{a^2}\right)\right] = -m^2a^3\left(\frac{h^{tt}_{\mu\nu}}{a^2}\right) \tag{5.36}$$

where we identify the eigenvalue to be m^2, the eigenfunction $a^{-2}h^{tt}_{\mu\nu}$ and the weight function a^3. The orthonormality condition is therefore given by

$$\int \frac{dz\; h^{tt\;(m)}_{\mu\nu}(z)h^{tt\;(n)}_{\mu\nu}(z)}{a(z)} = \delta(m-n)\,. \tag{5.37}$$

Substituting (5.35) into the above integral and using the continuum integral relation for Bessel functions quoted previously in equation (2.43), yields the properly normalised mass eigenvalue

$$h^{tt}_{\mu\nu} = z^{3/5}\sqrt{mk^{1/5}}\frac{\left[N_{-4/5}(\frac{m}{k})J_{1/5}(mz) - J_{-4/5}(\frac{m}{k})N_{1/5}(mz)\right]}{\sqrt{J^2_{-4/5}(\frac{m}{k}) + N^2_{-4/5}(\frac{m}{k})}}\,. \tag{5.38}$$

The massless TTF eigenfunction

We now take a look at the massless case of the graviton mode. If we set $m = 0$ in (5.32), we obtain Euler's equidimensional differential equation of second order

$$\ddot{h}^{tt}_{\mu\nu} - \frac{1}{5z}\dot{h}^{tt}_{\mu\nu} + \frac{8}{25z^2}h^{tt}_{\mu\nu} = 0 \tag{5.39}$$

which has the solution

$$h^{tt}_{\mu\nu_0} = \left[\chi_{\mu\nu}z^{2/5} + \zeta_{\mu\nu}z^{4/5}\right] \tag{5.40}$$

where $\chi_{\mu\nu}$ and $\zeta_{\mu\nu}$ are functions depending on the four-dimensional coordinates x^μ. Substituting equation (5.40) into the boundary condition (5.34) implies $\zeta_{\mu\nu} = 0$ and our (unnormalised) zero mode TTF solution is simply

$$h^{tt}_{\mu\nu_0} = \chi_{\mu\nu}z^{2/5}\,. \tag{5.41}$$

This solution corresponds to the graviton zero mode which describes standard four-dimensional gravity.

In this subsection we have obtained two distinct eigenvalues corresponding to the massless and massive TTF modes. These solutions respectively describe the graviton zero mode and the Kaluza–Klein tower. Next we solve the linearised equations by discarding the TTF gauge choice.

5.3.2 The massless scalar perturbations

The massless scalar modes have been previously discussed in [97, 98]. In Ref. [97], the authors studied the setup of a five-dimensional two brane system of Randall and Sundrum. It was discovered that the motion of the branes corresponds to a massless four-dimensional scalar field called the radion. We note that this result was then generalised in Ref. [98] to include a scalar field in the bulk (the dilaton). It was shown that once the BPS conditions[8] (derived from supergravity) are imposed on the system, then the dilaton can be written in terms of the brane fluctuation parameter (the radion); the dilaton did not give rise to an additional degree of freedom. (See Ref. [99] for a further analysis on the massless modes involving BPS branes. This setup also includes two BPS branes embedded in an AdS_5 bulk containing a bulk scalar field).

In this subsection we investigate the relative motion of the heterotic branes in the LOSW model using similar techniques as [97, 98]. By considering gauge transformations for the massless scalar modes, we determine that the radion and the dilaton are both coupled together in our system, thus giving only one independent scalar degree of freedom. Moreover, we are able to identify the graviton and radion zero modes.

We use the scalar equations (5.22) and (5.25) to obtain a third order differential equation

$$\delta\phi^{(3)} + \frac{9}{5z}\delta\phi^{(2)} + \left[m^2 - \frac{57}{25z^2}\right](\dot{\delta\phi}) + \left[\frac{6m^2}{5z} + \frac{24}{25z^3}\right]\delta\phi = 0 \tag{5.42}$$

where the overdot denotes differentiation with respect to z. In the last equation we have used the fact that the scalar perturbation satisfies the four-dimensional Klein-Gordon equation: $\Box\delta\phi = m^2\delta\phi$.

Since we are interested in the zero mode solution, we set $m = 0$ in equation (5.42). This gives us Euler's equidimensional differential equation of third order

$$\delta\phi^{(3)} + \frac{9}{5z}\delta\phi^{(2)} - \frac{57}{25z^2}(\dot{\delta\phi}) + \frac{24}{25z^3}\delta\phi = 0 \tag{5.43}$$

[8]BPS condition: The superpotential that generates the bulk scalar potential is equivalent to the brane potential.

with consistent[9] analytic solutions given by

$$\delta\phi = \frac{c_1}{z^{6/5}} \tag{5.44}$$

$$h = \frac{4}{3}k^{2/5}\frac{c_1}{z^{4/5}}\,. \tag{5.45}$$

The expression for h in the last line has been obtained by substituting $\delta\phi$ of equation (5.44) into either of the scalar equations: (5.22) or (5.25). Inserting $\delta\phi$ and h (given in (5.44)–(5.45)) into the non-$\eta_{\mu\nu}$ part of equation (5.28) yields the following transverse-traceless component of the metric perturbation

$$h^{tt}_{\mu\nu} + \psi_{,\mu\nu} = k^{2/5}\left[-\frac{25}{12}c_{1,\mu\nu}z^{6/5} + \frac{5}{2}\frac{\pi_{\mu\nu}}{k^{3/5}}z^{4/5} + \chi_{\mu\nu}z^{2/5}\right] \tag{5.46}$$

where $\pi_{\mu\nu}$ and $\chi_{\mu\nu}$ are functions of the four-dimensional coordinates x^μ, and correspond to the radion and graviton respectively.[10] We note that the graviton zero mode solution was obtained previously for the massless mode in TTF gauge (5.41). We also note that in the massless sector the TTF terms: $h^{tt}_{\mu\nu} + \psi_{,\mu\nu}$ are coupled together (however, this is not the case for the massive modes).

Now that we have all the components of the decomposition, we can return to equation (5.26) to write our full metric perturbation for the zero mode in the bulk gauge

$$h_{\mu\nu} = k^{2/5}\left[-\frac{25}{12}c_{1,\mu\nu}z^{6/5} + \frac{5}{2}\frac{\pi_{\mu\nu}}{k^{3/5}}z^{4/5} + \chi_{\mu\nu}z^{2/5} + \frac{1}{3}\eta_{\mu\nu}\frac{c_1}{z^{4/5}}\right]. \tag{5.47}$$

In order to obtain the metric perturbation on the brane, we need to change coordinates. The metric and scalar field perturbations (5.17) and (5.18) allows the brane to flutter from the coordinate origin $y = 0$ to the position $y = F(x^\mu)$. By performing a gauge transformation[11] as shown in Ref. [96], we can allow the brane to return back to its original position *i.e.* the origin. The solutions for the perturbed metric and scalar field in the brane-based coordinate system are given by

[9]The consistent solutions were found by using the decomposed vector and tensor equations given in (5.27) and (5.28) respectively.

[10]The graviton [10, 11, 51] has the behaviour $\sim a^2$ whereas the radion [97] has the behaviour $\sim a^2\int a^{-4}$.

[11]The gauge transformations are given in Appendix B.6.

$$\tilde{h}_{\mu\nu} = k^{2/5}\left[-\frac{25}{12}c_{1,\mu\nu}z^{6/5} + \frac{5}{2}\frac{\pi_{\mu\nu}}{k^{3/5}}z^{4/5} + \chi_{\mu\nu}z^{2/5} + \frac{1}{3}\eta_{\mu\nu}\frac{c_1}{z^{4/5}}\right] + k^{1/5}\left[\frac{5}{2}F_{,\mu\nu}z^{6/5} - \frac{2}{5}\frac{F}{z^{4/5}}\eta_{\mu\nu}\right] \tag{5.48}$$

and

$$\tilde{\delta\phi} = \frac{c_1}{z^{6/5}} - \frac{6}{5k^{1/5}}\frac{F}{z^{6/5}} \tag{5.49}$$

respectively. Inserting the brane-based expressions for $\tilde{h}_{\mu\nu}$ and $\tilde{\delta\phi}$ into the boundary condition of the tensor perturbation

$$\left(\partial_z\tilde{h}_{\mu\nu} - \frac{2}{5z}\tilde{h}_{\mu\nu}\right)\Big|_{z_+} = -\frac{2k^{2/5}}{5z^{3/5}}\eta_{\mu\nu}\tilde{\delta\phi}\Big|_{z_+} \tag{5.50}$$

yields the following constraint

$$F_{,\mu\nu} = k^{1/5}\left[\frac{5}{6}c_{1,\mu\nu} - \frac{1}{2}\frac{\pi_{\mu\nu}}{k^{3/5}z^{2/5}}\right]. \tag{5.51}$$

The first term in the above constraint implies that c_1 is proportional to F and can therefore be gauged away on the brane. Furthermore, equation (5.49) immediately tells us that the perturbed bulk scalar field $\tilde{\delta\phi}$ can be written as a function of the brane fluctuation parameter F. This coupling suggests that the bulk scalar field and the radion correspond to only one independent scalar degree of freedom. We note that this result agrees with [98]. Equations (5.48), (5.49) and (5.51) reduce to

$$\tilde{h}_{\mu\nu} = k^{2/5}\left[\frac{5}{2}\frac{\pi_{\mu\nu}}{k^{3/5}}z^{4/5} + \chi_{\mu\nu}z^{2/5}\right] + k^{1/5}\left[\frac{5}{2}F_{,\mu\nu}z^{6/5} - \frac{2}{5}\eta_{\mu\nu}\frac{F}{z^{4/5}}\right] \tag{5.52}$$

$$\tilde{\delta\phi} = -\frac{6}{5}\frac{F}{k^{1/5}z^{6/5}} \tag{5.53}$$

$$F_{,\mu\nu} = -\frac{1}{2}\frac{\pi_{\mu\nu}}{k^{2/5}z^{2/5}}. \tag{5.54}$$

Contracting the last equation with $\eta^{\mu\nu}$ confirms that the radion is massless $\Box F = 0$. Inserting the expression for $\tilde{h}$ and $\tilde{\delta\phi}$ into the boundary condition for the scalar perturbation

$$\left(\partial_z\tilde{h} - \frac{2}{5z}\tilde{h}\right)\Big|_{z_+} = -\frac{8}{5}\frac{k^{2/5}}{z^{3/5}}\tilde{\delta\phi}\Big|_{z_+} \tag{5.55}$$

provides a second verification that the radion is indeed a massless scalar field. Finally, the substitution of $\tilde{h}$ and $\delta\tilde{\phi}$ into the dilaton boundary condition

$$\partial_z \delta\tilde{\phi}\Big|_{z_+} = -\frac{6}{5z}\delta\tilde{\phi}\Big|_{z_+} \tag{5.56}$$

shows that the dilaton boundary condition is also consistent. Consistency of all three boundary conditions (*i.e.* tensor, scalar, dilaton) implies that we have a complete set of consistent solutions for the metric and scalar perturbations.

5.3.3 Including the second brane

In this section we follow the methods of [98] to compute the full metric perturbation including both the background and the perturbation. So far, our analysis has been restricted to the existence of a single brane. We therefore introduce the second brane into the setup to complete our analysis. Each brane has its own metric tensor. We define $h^+_{\mu\nu}$ as the metric tensor in the region of the positive tension brane positioned at $z = z_+$. Conversely, $h^-_{\mu\nu}$ corresponds to the metric tensor in the region of the negative tension brane located at $z = z_-$. Although the metric tensor is single-valued for each brane in each patch, we would like to construct a metric tensor that is single-valued throughout the bulk. We therefore need to consider two coordinate patches. The first coordinate patch includes the brane located at $y = +y_0$ and the second includes the brane located at $y = -y_0$. Each coordinate patch is Gaussian Normal with respect to the brane it includes (but it does not have to be Gaussian Normal with respect to the other brane).

Our solutions in each patch will depend on the appropriate value of the brane fluctuation parameter F. Normalising the value of the scale factor $a(z)$ so that it equals unity $a(z_+) = 1$ on the positive tension brane gives

$$y_+ = +y_0 = \frac{1 - c_0}{\sqrt{2}\alpha} \qquad \text{or} \qquad z_+ = \frac{1}{k} \tag{5.57}$$

$$y_- = -y_0 = \frac{c_0 - 1}{\sqrt{2}\alpha} \qquad \text{or} \qquad z_- = \frac{1}{k}(2c_0 - 1)^{5/6} \,. \tag{5.58}$$

Substituting these values of z into (5.54) gives the following values of the brane

fluctuation parameter of each brane

$$F^{+}_{,\mu\nu} = -\frac{\pi_{\mu\nu}}{2} \tag{5.59}$$

$$F^{-}_{,\mu\nu} = -\frac{\pi_{\mu\nu}}{2\left(2c_0 - 1\right)^{1/3}} \,. \tag{5.60}$$

The metric tensor (5.52) which is a solution of the gravitational equations can be rewritten in terms of the brane scale factor

$$\tilde{h}_{\mu\nu} = a^2\chi_{\mu\nu} + \pi_{\mu\nu}\left(a^2\int\frac{dy}{a^4}\right) + 2F_{,\mu\nu}\left(a^2\int\frac{dy}{a^2}\right) - 2F\eta_{\mu\nu}a^2\left(\frac{a'}{a}\right) \tag{5.61}$$

where we have previously identified the graviton zero mode with the $\chi_{\mu\nu}$ term and the radion zero mode with the $\pi_{\mu\nu}$ term. Equation (5.54) enables us to rewrite the expression for $\pi_{\mu\nu}$ in terms of the scale factor

$$\pi_{\mu\nu} = -2F_{,\mu\nu}a_0^2 \tag{5.62}$$

where a_0 comes from evaluating at the boundary of the brane concerned. Inserting (5.62) into (5.61) yields the following expression

$$\tilde{h}_{\mu\nu} = a^2\chi_{\mu\nu} - 2a_0^2F_{,\mu\nu}\left(a^2\int\frac{dy}{a^4}\right) + 2\,F_{,\mu\nu}\left(a^2\int\frac{dy}{a^2}\right) - 2\,F\eta_{\mu\nu}a^2\left(\frac{a'}{a}\right) \tag{5.63}$$

which is exactly the same as [98] where $F \equiv -f \equiv -\xi_y$.

In order to construct a metric tensor that is single-valued throughout the bulk, we require the brane fluctuation to be single-valued. This is accomplished by using the second term of the latter expression and requiring

$$a_+^2F^{+} \equiv a_-^2F^{-} \equiv F \tag{5.64}$$

where $a_\pm$ denotes the value of the scale factor at each brane and F is the four-dimensional massless field which relates the fluctuations of one brane to the fluctuations of the second brane. The metric tensor in the patch surrounding the positive tension brane at $y_+ = +y_0$ reads

$$\tilde{h}^{+}_{\mu\nu} = a^2\chi_{\mu\nu} - 2F_{,\mu\nu}\left(a^2\int\frac{dy}{a^4}\right) + 2\,F_{,\mu\nu}\left(\frac{a^2}{a_+^2}\int\frac{dy}{a^2}\right) - 2\,\eta_{\mu\nu}\frac{a^2}{a_+^2}\left(\frac{a'}{a}\right)F \tag{5.65}$$

and for the second patch in the vicinity of the negative tension brane at $y_- = -y_0$, the metric tensor reads

$$\tilde{h}^-_{\mu\nu} = a^2\chi_{\mu\nu} - 2\,F_{,\mu\nu}\left(a^2\int\frac{dy}{a^4}\right) + 2\,F_{,\mu\nu}\left(\frac{a^2}{a_-^2}\int\frac{dy}{a^2}\right) - 2\,\eta_{\mu\nu}\frac{a^2}{a_-^2}\left(\frac{a'}{a}\right)F\,. \quad (5.66)$$

Since the two patches are different, the metric tensor cannot be patched up. To resolve this problem, we perform the following gauge transformation that preserves the Gaussian Normal coordinate system and which translates the second brane:

$$y \to y + \left(\frac{1}{a_-^2} - \frac{1}{a_+^2}\right)F\,. \quad (5.67)$$

This transforms the induced metric on the second brane $h^-_{\mu\nu}$ into the induced metric on the first brane $h^+_{\mu\nu}$, giving a single coordinate chart which includes both branes. Moreover, the coordinate transformation (5.67) alters the location of the negative tension brane to position

$$T(x) = y_- + \left(\frac{1}{a_-^2} - \frac{1}{a_+^2}\right)F\,. \quad (5.68)$$

This expression shows that the position of the second brane depends on the brane fluctuation parameter. In fact, $T(x)$ represents the physical distance between the branes (*i.e.* measures the size of the extra dimension) and is referred to as the radion. In fact, the radion measures the brane bending of the negative tension brane.

To complete this analysis, we would like to find a metric tensor in a form such that the size of the interval does not fluctuate *i.e.* the walls remain in a fixed coordinate position. We therefore perform an additional transformation defined by

$$y \to y - \left(\frac{1}{a^2} - \frac{1}{a_+^2}\right)F \quad (5.69)$$

which subsequently rescales the size of the bulk. This ensures that both walls are fixed and flat in the coordinates with the second brane rigidly fixed at $y = y_-$.

If we impose that there is no vector component in the metric tensor, then one can transform according to the infinitesimal transformation

$$x^\mu \to x^\mu + \xi^\mu \quad (5.70)$$

where

$$\xi_\mu = \frac{a^2}{a_+^2}\int dy \left(\frac{a_+^2}{a^4} - \frac{1}{a^2}\right) F_{,\mu}\,. \tag{5.71}$$

The metric tensor then becomes

$$\tilde{h}_{\mu\nu} = a^2\chi_{\mu\nu} - 2\frac{a'}{a}\frac{a^2}{a_+^2}\eta_{\mu\nu}F\,. \tag{5.72}$$

This enables us to write an expression for the complete metric including both the background and the perturbation:

$$\begin{aligned} ds^2 = a^2 &\left[y - \left(\frac{1}{a^2} - \frac{1}{a_+^2}\right)F\right]\eta_{\mu\nu}dx^\mu dx^\nu \\ &+ \left[1 - \partial_y\left(\frac{1}{a^2} - \frac{1}{a_+^2}\right)F\right]^2 dy^2 \\ &+ \left[a^2\chi_{\mu\nu} - 2\frac{a'}{a}\frac{a^2}{a_+^2}\eta_{\mu\nu}F\right]dx^\mu dx^\nu\,. \end{aligned} \tag{5.73}$$

If we set

$$\mathcal{S}(x,y) = y - \frac{F}{a^2}\,, \qquad g_{\mu\nu} = \eta_{\mu\nu} + \chi_{\mu\nu}\,, \tag{5.74}$$

then the above metric (5.73) simplifies (to linear order) considerably to

$$ds^2 = a^2\left[\mathcal{S}(x,y)\right]g_{\mu\nu}dx^\mu dx^\nu + (\partial_y\mathcal{S})^2 dy^2 \tag{5.75}$$

which is a generalisation of the metric derived in [97].

Finally, we apply the same analysis to construct a single-valued scalar field perturbation throughout the bulk. Rewriting (5.53) in terms of the brane scale factor using the quantities defined in (5.14)–(5.16) gives

$$\delta\tilde{\phi} = \phi' F \tag{5.76}$$

where $\phi' = 6a'a^{-1}$. The scalar perturbation in the vicinity of the positive and negative tension patches are given respectively as

$$\delta\tilde{\phi}^+ = \frac{\phi'}{a_+^2}F\,, \qquad \delta\tilde{\phi}^- = \frac{\phi'}{a_-^2}F\,. \tag{5.77}$$

Using the change of coordinates (5.67) in the second patch allows $\delta\phi^-$ to transform into $\delta\phi^+$ throughout the bulk, leading to a single-valued coordinate chart for the scalar field fluctuation

$$\delta\tilde{\phi} = \frac{\phi'}{a^2}F\,. \tag{5.78}$$

Thus, the inclusion of the second brane into the configuration has enabled us to construct a metric tensor and a scalar field perturbation which are single-valued throughout the bulk. Out results are analogous to [98]. This is expected since the perturbation equations in the latter paper are exactly the same as the ones presented in this chapter, even though both setups are in fact distinct (their setup involves eleven-dimensional supergravity with BPS conditions imposed on the system).

Finally, we make a remark that there is only one scalar eigenvalue corresponding to the massless scalar mode. In other words, there is no massive tower in the scalar sector.

5.4 Branes with matter

In this section we introduce an additional matter source on the brane which leads to a modification of the original perturbation equations (5.22)–(5.25). The extra matter present on the brane causes the brane to respond by bending. By changing to a coordinate system in which the branes are once again Gaussian Normal, we show that the brane fluctuation parameter and the perturbation of the trace of the energy-momentum are coupled together. We then employ the same methods as presented in chapter 2 to derive the Newtonian potential on the brane and the tensor structure of the massless four-dimensional graviton propagator. We show that the corrections to the Newtonian potential and the form of the brane graviton propagator in the LOSW model are modified from the RSII scenario.

5.4.1 The modified linearised field equations

Previously, we had solved the perturbation equations in vacuum $\Delta_L h_{ab} = -2\delta R_{ab} = 0$. We now solve the non-vacuum linearised equations *i.e.* with the presence of matter

on the branes. The bulk equations of motion now obey the following relation

$$\Delta_L h_{ab} = -2\delta R_{ab} \neq 0\,. \tag{5.79}$$

The Ricci tensor (5.19) and the linearised Einstein field equation (5.20) are both modified to

$$R_{ab} \;\rightarrow\; R_{ab} + \kappa_5[\mathcal{D}]\left[T_{\mu\nu}\delta^\mu_a\delta^\nu_b - \frac{1}{3a^2}T g_{ab}\right] \tag{5.80}$$

$$\Delta_L h_{ab} \;\rightarrow\; \Delta_L h_{ab} - 2\kappa_5[\mathcal{D}]\left[\delta T_{\mu\nu}\delta^\mu_a\delta^\nu_b - \frac{1}{3a^2}\delta T g_{ab}\right] \tag{5.81}$$

where we have allowed for a general matter perturbation on the brane. The symbol $T = T^\mu_\mu$ denotes the trace of the energy-momentum tensor $T_{\mu\nu}$. Equation (5.81) enables us to compute the modified scalar (5.22) and tensor (5.24) perturbations equations respectively:

$$\frac{1}{a^2}\left[a^2\left(\frac{h}{a^2}\right)'\right]' = -12\frac{a'}{a}(\delta\phi)' + 8\left(\frac{a'}{a}\right)^2\delta\phi - 16\frac{a'}{a}[\mathcal{D}]\delta\phi + \frac{2\kappa_5}{3a^2}[\mathcal{D}]\delta T \tag{5.82}$$

$$\begin{aligned}&\frac{\Box h_{\mu\nu} + h_{,\mu\nu} - 2h_{\lambda(\mu,\nu)}{}^\lambda}{a^2} + \frac{1}{a^2}\left[a^4\left(\frac{h_{\mu\nu}}{a^2}\right)'\right]' + aa'\left[\frac{h}{a^2}\right]'\eta_{\mu\nu}\\ &= 8(a')^2\eta_{\mu\nu}\delta\phi - 4[\mathcal{D}]aa'\eta_{\mu\nu}\delta\phi - 2\kappa_5[\mathcal{D}]\left[\delta T_{\mu\nu} - \frac{1}{3}\delta T\eta_{\mu\nu}\right]\end{aligned} \tag{5.83}$$

The vector equation (5.23) and dilaton equation (5.25) remain unchanged. The corresponding tensor and scalar boundary conditions (5.50) and (5.55) evaluated at $z = z_+$ will change accordingly:

$$\partial_z\tilde{h}_{\mu\nu} - \frac{2}{5z}\tilde{h}_{\mu\nu} \;=\; -\frac{2k^{2/5}}{5z^{3/5}}\eta_{\mu\nu}\tilde{\delta\phi} - \kappa_5(kz)^{1/5}\left[\delta T_{\mu\nu} - \frac{1}{3}\delta T\eta_{\mu\nu}\right] \tag{5.84}$$

$$\partial_z\tilde{h} - \frac{2}{5z}\tilde{h} \;=\; -\frac{8}{5}\frac{k^{2/5}}{z^{3/5}}\tilde{\delta\phi} + \frac{\kappa_5}{3}\delta T(kz)^{1/5}\,. \tag{5.85}$$

The latter two boundary conditions yields the following constraint

$$F_{,\mu\nu} = k^{1/5}\left[\frac{5}{6}c_{1,\mu\nu} - \frac{1}{2}\frac{\pi_{\mu\nu}}{k^{3/5}z^{2/5}}\right] - \frac{\kappa_5}{2}\left[\delta T_{\mu\nu} - \frac{1}{3}\delta T\eta_{\mu\nu}\right]\,. \tag{5.86}$$

As before, c_1 is proportional to F and can therefore be gauged away on the brane. Equation (5.54) is now modified to

$$F_{,\mu\nu} = -\frac{1}{2}\frac{\pi_{\mu\nu}}{k^{2/5}z^{2/5}} - \frac{\kappa_5}{2}\left[\delta T_{\mu\nu} - \frac{1}{3}\delta T\eta_{\mu\nu}\right] . \tag{5.87}$$

Contracting the latter constraint with $\eta^{\mu\nu}$ yields an expression for the coupling between the brane fluctuation and the trace of the energy-momentum perturbation on the brane:

$$\Box F = \frac{\kappa_5}{6}\delta T^{\mu}_{\mu} . \tag{5.88}$$

This expression will be used shortly in the computation of the brane graviton propagator.

5.4.2 The Newtonian potential on the brane

First we compute the Newtonian potential on the brane to study the localisation of gravity. Our starting point is the definition of the Bessel function

$$J_p(x) = \sum_{n=0}^{\infty} \frac{(-1)^n}{n!\,\Gamma(p+n+1)}\left(\frac{x}{2}\right)^{2n+p} \tag{5.89}$$

which is valid for all values of p. The following approximation $J_{-p}(x) \sim N_p(x)$ for Bessel functions of fractional order (*i.e.* non-integer values of p) enables us to rewrite the massive wavefunction (5.38) as

$$\psi_m(z) = \frac{z^{3/5}\sqrt{mk^{1/5}}\left[J_{4/5}(\frac{m}{k})J_{1/5}(mz) - J_{-4/5}(\frac{m}{k})J_{-1/5}(mz)\right]}{\sqrt{J^2_{-4/5}(\frac{m}{k}) + J^2_{4/5}(\frac{m}{k})}} \tag{5.90}$$

where we have set $h^{tt}_{\mu\nu} \equiv \psi_m$. The first term of (5.89) which corresponds to $n = 0$ is given by

$$J_p(x) \sim \frac{1}{\Gamma(p+1)}\left(\frac{x}{2}\right)^p \tag{5.91}$$

and is valid for small values of x (*i.e.* as $x \to 0$). Setting $p = \pm 1/5$ determines the following expressions

$$J_{1/5}(mz) = \frac{1}{\Gamma(\frac{6}{5})}\left(\frac{mz}{2}\right)^{1/5} , \qquad J_{-1/5}(mz) = \frac{1}{\Gamma(\frac{4}{5})}\left(\frac{mz}{2}\right)^{-1/5} . \tag{5.92}$$

The last two terms will be used to calculate the static gravitational potential between two unit masses which are a distant r apart on the positive tension brane. As in chapter 2, the interaction of the two particles on the brane corresponds to a Yukawa-type interaction. We therefore use the expression for the potential defined previously in equation (2.54). Inserting (5.92) into (5.90) and evaluating for $m \ll k$ enables us to deduce the dominant term of the eigenfunction

$$\psi_m^2(z) \sim \frac{J^2_{-4/5}\left(\frac{m}{k}\right)}{\left(J^2_{-4/5}\left(\frac{m}{k}\right) + J^2_{4/5}\left(\frac{m}{k}\right)\right)} \frac{ma_-^6}{k\,\Gamma^2(\frac{4}{5})} \left(\frac{mz}{2}\right)^{-2/5} \tag{5.93}$$

where $a_- = (kz_-)^{1/5}$. Substituting this back into the Yukawa potential (2.54) (where $y = 0$ is equivalent to $z = 1/k$) and integrating using the standard integral defined previously in (2.55), yields an expression for the corrections to the Newtonian potential

$$V_{KK}(r) = -\frac{G_5}{r^{13/5}} \frac{\beta}{k^{3/5}} \tag{5.94}$$

where we have set

$$\beta = \frac{\Gamma(\frac{8}{5})\, 2^{2/5} a_-^6}{\Gamma^2(\frac{4}{5})}. \tag{5.95}$$

If we set $G_4 = G_5 k$, then the total potential is given by

$$V_{LOSW}(r) \sim -\frac{G_4}{r}\left(1 + \frac{\beta}{r^{8/5}k^{8/5}}\right) \tag{5.96}$$

where the first term corresponds to the massless graviton zero mode and the second term denotes the contribution arising from the massive gravitons. Clearly, the corrections are a slight modification to the RSII scenario (2.57). At large distances away from the brane $r \gg k^{-1}$, standard four-dimensional gravity is reproduced in the LOSW model. Therefore, the LOSW model has succeeded in exhibiting brane-localised gravity.

5.4.3 The brane graviton propagator

Next we compute the tensor structure of the four-dimensional massless graviton propagator. Our starting point is the definition of the Green's function in the

LOSW model

$$G_R(x,z;\tilde{x},\tilde{z}) = \frac{4\alpha}{a_+^8}\, a^2(z)a^2(\tilde{z})D_0(x-\tilde{x}) + \int_0^\infty dm\ \psi_m(z)\psi_m(\tilde{z})D_m(x-\tilde{x}) \quad (5.97)$$

where $\alpha = k/5$, $D_0(x-\tilde{x})$ and $D_m(x-\tilde{x})$ represent the massless and massive Green's functions in four dimensions (defined explicitly in equations (2.82)–(2.83)). The eigenfunction $\psi_m(z)$ has been defined previously in (5.38). The above expression is different from the RSII model by a normalisation constant. (Also, the definition of the warp factors in the RS and LOSW models are distinct). Restricting the perturbation exclusively to the brane: $y = \tilde{y} = 0$ (or $z = \tilde{z} = k^{-1}$) reduces the Green's function to a simple expression

$$G_R(x,0;\tilde{x},0) = 4\alpha\ D_0(x-\tilde{x}) + \int_0^\infty dm\ |\psi_m(0)|^2 D_m(x-\tilde{x})\,. \quad (5.98)$$

The metric perturbation relating the Randall–Sundrum and Gaussian Normal coordinate systems[12] is given by

$$h_{\mu\nu}(x,y) = \bar{h}_{\mu\nu} + 2a^2(y)F_{,\mu\nu}\int\frac{dy}{a^2} - 2a(y)a'(y)\eta_{\mu\nu}F \quad (5.99)$$

$$h_{\mu\nu}(x,z) = \bar{h}_{\mu\nu} + \frac{a^6(z)}{2\alpha}F_{,\mu\nu} - 2\eta_{\mu\nu}F\frac{\alpha}{a^4(z)}\,. \quad (5.100)$$

On the brane, (5.100) becomes

$$\bar{h}_{\mu\nu} = h^{(m)}_{\mu\nu} + h^{(f)}_{\mu\nu} - \frac{F_{,\mu\nu}}{2\alpha} + 2\eta_{\mu\nu}F\alpha\,. \quad (5.101)$$

Some of the terms in the latter expression can be gauged away appropriately, giving a simple expression

$$\bar{h}_{\mu\nu}(x,0) = h^{(m)}_{\mu\nu} + 2\alpha F\eta_{\mu\nu} \quad (5.102)$$

where

$$h^{(m)}_{\mu\nu}(x,0) = -16\pi G_5\int d^4\tilde{x}\ G_R(x,0;\tilde{x},0)(T_{\mu\nu} - \frac{1}{3}T\eta_{\mu\nu})(\tilde{x}) \quad (5.103)$$

$$F(x) = 8\pi G_5\int d^4\tilde{x}\ D_0(x-\tilde{x})\frac{T(\tilde{x})}{6}\,. \quad (5.104)$$

[12]See Appendix B.6 for the transformation between the bulk gauge and the brane-based gauge.

Zero mode approximation

The first term of the Green's function (5.98):

$$G_R^{zm}(x,0;\tilde{x},0) = 4\alpha D_0(x-\tilde{x}) \tag{5.105}$$

corresponds to the massless graviton mode. The corresponding metric perturbation is found by inserting (5.105) into (5.103) and using (5.104). The zero mode contribution to equation (5.102) is then given by

$$\begin{aligned}\bar{h}_{\mu\nu}^{zm} &= -16\pi G_5 \int d^4\tilde{x}\ (4\alpha)\ D_0(x-\tilde{x})(T_{\mu\nu} - \frac{1}{3}T\eta_{\mu\nu}) + 16\pi G_5 \alpha \eta_{\mu\nu} \int d^4\tilde{x}\ D_0(x-\tilde{x})\frac{T}{6} \\ &= -16\pi G_5 \int d^4\tilde{x}\ D_0(x-\tilde{x})(4\alpha)(T_{\mu\nu} - \frac{3}{8}T\eta_{\mu\nu})\,. \end{aligned} \tag{5.106}$$

Clearly, the tensor structure of the induced metric does not correspond to four-dimensional Einstein gravity.

The corrections to Einstein gravity

The second term of the Green's function (5.98):

$$G_R^{ctm}(x,0;\tilde{x},0) = \int_0^\infty dm\ |\psi_m(0)|^2 D_m(x-\tilde{x}) \tag{5.107}$$

arises from the massive graviton modes. The corresponding metric perturbation is found by substituting (5.107) into (5.103). Equation (5.102) for the massive modes becomes

$$\bar{h}_{\mu\nu}^{ctm} = -16\pi G_5 \int d^4\tilde{x}\ D_m(x-\tilde{x}) \int_0^\infty dm\ \frac{m^{3/5}}{k^{3/5}} \frac{2^{2/5} a_-^6}{\Gamma^2\left(\frac{4}{5}\right)} (T_{\mu\nu} - \frac{1}{3}T\eta_{\mu\nu})\,. \tag{5.108}$$

The total metric perturbation is then obtained by adding equations (5.106) and (5.108): $\bar{h}_{\mu\nu} = \bar{h}_{\mu\nu}^{zm} + \bar{h}_{\mu\nu}^{ctm}$. This gives the following expression

$$\begin{aligned}\bar{h}_{\mu\nu} = &-16\pi G_5 \int d^4\tilde{x}\ D_0(x-\tilde{x})(4\alpha)(T_{\mu\nu} - \frac{3}{8}T\eta_{\mu\nu}) \\ &- 16\pi G_5 \int d^4\tilde{x}\ D_m(x-\tilde{x}) \int_0^\infty dm\ \frac{m^{3/5}}{k^{3/5}} \frac{2^{2/5} a_-^6}{\Gamma^2\left(\frac{4}{5}\right)} (T_{\mu\nu} - \frac{1}{3}T\eta_{\mu\nu})\,. \end{aligned} \tag{5.109}$$

If we use the Green's function for the Laplacian operator (2.93) for the LOSW model, then the last equation reduces to

$$\bar{h}_{\mu\nu} = \frac{4G_4}{r}\int d^3\tilde{x}\left[\frac{4}{5}\left(T_{\mu\nu}-\frac{3}{8}T\eta_{\mu\nu}\right)+\int_0^\infty dm\, m^{3/5}e^{-mr}\,\frac{1}{k^{8/5}}\,\frac{2^{2/5}a_-^6}{\Gamma^2\left(\frac{4}{5}\right)}\left(T_{\mu\nu}-\frac{1}{3}T\eta_{\mu\nu}\right)\right]. \tag{5.110}$$

The standard integral (2.55) is used in the last line to determine the metric perturbation outside a spherically symmetric source

$$\bar{h}_{\mu\nu}(x,0) = \frac{4G_4}{r}\int d^3\tilde{x}\left[\frac{4}{5}\left(T_{\mu\nu}-\frac{3}{8}T\eta_{\mu\nu}\right)+\frac{\beta}{r^{8/5}k^{8/5}}\left(T_{\mu\nu}-\frac{1}{3}T\eta_{\mu\nu}\right)\right] \tag{5.111}$$

where β has been defined previously in (5.95). In order to determine the corrections explicitly, we substitute into the last equation, the expression for a point mass source on the brane, previously quoted in equation (2.99). The desired expression for the induced metric on the brane is

$$\bar{h}_{\mu\nu}(x,0) = \frac{2G_4m}{r}\left[\mathrm{diag}\left(\frac{1}{5}(5,3,3,3)\right)+\frac{2\beta}{3k^{8/5}r^{8/5}}\mathrm{diag}(2,1,1,1)\right] \tag{5.112}$$

with the corresponding linearised metric components

$$\bar{h}_{tt} = \frac{2G_4m}{r}\left(1+\frac{4\beta}{3k^{8/5}r^{8/5}}\right), \qquad \bar{h}_{ij} = \frac{2G_4m}{r}\left(\frac{3}{5}+\frac{2\beta}{3k^{8/5}r^{8/5}}\right)\delta_{ij}. \tag{5.113}$$

The time-component of the induced metric then determines the Newtonian potential, describing the attraction between two particles which are separated a distant r apart on the heterotic brane:

$$\phi(r) = \frac{1}{2}\bar{h}_{tt} = \frac{G_4m}{r}\left(1+\frac{4\beta}{3k^{8/5}r^{8/5}}\right). \tag{5.114}$$

Thus, the corrections are negligible for large distances from the brane $r \gg k^{-1}$ and we reproduce the results of standard four-dimensional gravity. We note that the corrections to the Newtonian potential are enhanced by a factor of 4/3 from the potential derived previously using the Yukawa-type of interaction (5.96). This is because matter sources were not taken into account when computing the Yukawa

potential. The difference in the numerical coefficient is therefore a net result of the brane-bending effect[13]. The same ambiguity in the numerical coefficient has been observed in chapter 2 when computing the Newtonian potential for the RSII case.

So far, our analysis of gravity localisation has been limited exclusively to the existence of a single brane. A final step would require the presence of the second brane. This will enable us to obtain the relative strengths of the radion couplings to the matter source present on each of the branes and hence determine whether our results are in agreement with the analysis of Garriga and Tanaka [50]. In other words, we would like to determine whether the LOSW model recovers linearised Brans-Dicke gravity on both heterotic branes. This is work currently in progress and will be presented in the upcoming paper [2].

5.5 Discussion

In this chapter we have studied scalar and gravitational perturbations in the static LOSW model. By explicitly changing to a brane-based coordinate system, we have been able to identify the graviton and radion zero modes. The general gauge transformations have also shown that the dilaton can be written as a function of the radion, therefore giving only one independent scalar degree of freedom. Moreover, we found complete solutions describing the massive gravitons. The wavefunction of the gravitons enabled us to determine the form of the Newtonian potential on the brane and the tensor structure of the brane graviton propagator. Our results show that the corrections to the Newtonian potential in the LOSW model are slightly modified in contrast to the corrections computed in the RSII scenario.

It is natural to ask what happens in the case of a black string [37]. In this situation, we use equation (5.13) to modify the flat metric on the brane to the Schwarzschild spacetime $\eta_{\mu\nu} \to g^{\text{Sch}}_{\mu\nu}$. This metric also solves the background equations of heterotic M-theory with the solutions given by equations (5.14)–(5.16). For the Schwarzschild background, we obtain extra Christoffel symbols ${\Gamma^{\mu}_{\nu\kappa}}^{(5)} = {\Gamma^{\mu}_{\nu\kappa}}^{(4)}$ which were previously zero for the flat case. This gives additional terms in the lin-

[13]The correct result for the Newtonian potential is (5.114), not (5.96).

earised perturbation equations. To be more specific, the extra terms are contained in the d'Alembertian operator only. This does not affect the transverse-tracefree eigenvalues, implying that the set of perturbation equations for the black string case are essentially the same as for the flat background. Our previous analysis then proves the instability of a black string.

It is important to note that we have only looked at the static LOSW model. Since we live in an expanding universe, a more realistic model would involve incorporating some time dependence into the theory [100]. We would therefore like to solve the perturbations around a black string consisting of two separating or colliding heterotic branes [101]- [106]. As we slowly stretch or squash the black string in this expanding cosmological background, we would expect the onset of the Gregory-Laflamme instability [59]. Our methods can also be generalised to the case of a magnetically charged black string [60]. In this case, we would like to determine whether the instability is generic *i.e.* does it still exist in the presence of a charged black string or brane. We can also follow the work of [107] to obtain cosmological solutions of the LOSW model. Further extensions could include inflationary braneworld models where matter is localised on the two branes [108] or the more challenging case of a rotating black string [109].

Finally, as an application to the work presented in chapters 3 and 4, we are currently exploring black holes in the background of heterotic M-theory. As before, we study the permissible braneworld trajectories in this background by considering a perfect isotropic fluid source on the heterotic brane. These solutions will be equivalent to the brane Tolman–Oppenheimer–Volkoff equations. Any physically realistic energy and pressure profiles will determine that these solutions have the interpretation of braneworld stars. This is work currently in progress.

Chapter 6

Conclusions

In this thesis we have explored the behaviour of strong and weak gravity in two distinct higher-dimensional models (*i.e.* the Randall–Sundrum II model and the LOSW model). First, we reviewed preliminary results based on the Randall–Sundrum II scenario featuring a single, positive tension three-brane embedded in an AdS_5 spacetime. In particular, we calculated the gravitational fluctuations in this background to determine the nature of gravity. After computing the full mass spectrum of the graviton modes, we determined that the power law corrections to the Newtonian potential are suppressed far away from the four-dimensional hypersurface implying that gravity is effectively localised on the brane. A further confirmation of gravity localisation was provided through the computation of the four-dimensional graviton propagator. Results revealed that the tensor structure of the brane graviton propagator corresponds to four-dimensional Einstein gravity. Thus, a braneworld observer experiences standard, four-dimensional, non-brane gravity in the TeV range; a regime which current accelerators can probe.

Next, we introduced the eleven-dimensional Hořava–Witten construction. For the theory to be realistic, six of the extra spatial dimensions are wrapped up on a compact manifold giving rise to an effective five-dimensional theory known as the LOSW model. As a result of the compactification, a scalar field is generated in the bulk making the model distinct to its descendant (*i.e.* Randall–Sundrum I). Unfortunately, the extra dimensions in the LOSW model are virtually impossible to probe as exceedingly high energy scales are required.

After establishing the Randall–Sundrum II and LOSW braneworlds, we explored the impact of strong gravitating objects within these two higher-dimensional models. First, we investigated the possibility of obtaining a solution relating to a black hole on the Randall–Sundrum brane. We then explored the possibility of describing a black string in the background of low energy heterotic M-theory. In each model, we employed two different approaches to study the behaviour of gravity. We applied a non-perturbative method in the Randall–Sundrum II model to study the effects of strong gravity. Conversely, a perturbative analysis was used in the LOSW to explore the effects of weak gravity.

While failing to solve the longstanding problem of finding a metric which corresponds to a black hole on the Randall–Sundrum brane, we instead made progress in obtaining solutions relating to braneworld stars. However, our solutions exhibited an asymptotic pressure excess at increasing radii from the braneworld. For a truly localised source, we expect the matter distribution to be peaked at the central region of the brane and suppressed far from it. One way to overcome the obstruction of surplus pressure is though the introduction of time dependence. Unfortunately, complexity arises when time dependence is permitted into the system of brane equations. Moreover, generalisation of this work to asymmetric spacetimes in the hope of finding a wider class of solutions has also proven to be quite difficult. Since our analysis has been limited exclusively to analytical solutions, future directions may involve numerical simulations. This may overcome the above problems and hence produce a more extensive range of solutions with the desired qualities of a braneworld star.

Despite not being able to experimentally test the LOSW model, theoretical progress however has been made through the study of scalar and gravitational fluctuations. Our results show that the radion and dilaton are both connected, giving one solitary degree of freedom. Our analysis also extends to prove the instability of a black string. We then studied the nature of gravity in this model by computing the full mass spectrum of the massive gravitons. Our results determine that the power law corrections to the Newtonian potential and the form of the brane propagator in the LOSW model are modified from the Randall–Sundrum II scenario. More-

over, the corrections to the potential at large distances away from the brane become damped implying that the LOSW model also reproduces the results of standard four-dimensional gravity. We note that the analysis of gravity localisation has been limited exclusively to the existence of a single brane. The introduction of a second brane will enable us to obtain the relative strengths of the radion couplings to the matter source present on each brane and hence determine whether the model recovers linearised Brans-Dicke gravity on both heterotic branes. This field of research is currently underway. Finally, another active field of research involves the exploration of possible black hole solutions in the background of low energy heterotic M-theory. This work is also currently in progress. The final results will be presented in the upcoming paper [2].

We conclude this thesis by saying that the five-dimensional Randall–Sundrum braneworld can certainly be put to the test in the forthcoming Large Hadron Collider. The possibility of probing the extra dimension in this braneworld is highly exciting. The most robust probes of higher-dimensional physics will correspond to the Kaluza–Klein gravitons which may determine whether the tested braneworld is a true representation of nature. We therefore wait for any possible experimental signatures which may provide vital information regarding our hypothesised extra-dimensional world.

Appendix A

Detailed calculations–Braneworld stars

A.1 The five-dimensional Christoffel symbols

If we take the bulk metric to have signature $(-,+,+,+,+)$, then the five-dimensional spherically symmetric metric takes the following form:

$$ds^2 = -U(t,r)\,d\tau^2 + \frac{dr^2}{U(t,r)} + r^2(d\chi^2 + \sin^2\chi\, d\Omega_{II}^2)\,.$$

where $U(t,r)$ denotes a general time-dependent bulk metric function. We state the following definition of the Christoffel symbol

$$\Gamma^a_{bc} = \frac{1}{2}g^{ae}\left(g_{be,c} + g_{ce,b} - g_{bc,e}\right)$$

and g_{ab} denotes the metric tensor with its corresponding inverse given by g^{ab}. The non-zero Christoffel symbols are then given by:

$$\Gamma^t_{tt} = \frac{\dot{U}}{2U}\,, \qquad \Gamma^t_{rr} = -\frac{\dot{U}}{2U^3}\,, \qquad \Gamma^r_{tr} = -\frac{\dot{U}}{2U}\,,$$

$$\Gamma^t_{tr} = \frac{U'}{2U}\,, \qquad \Gamma^r_{tt} = \frac{UU'}{2}\,, \qquad \Gamma^r_{\chi\chi} = -Ur\,, \qquad \Gamma^r_{rr} = -\frac{U'}{2U}\,,$$

$$\Gamma^r_{\theta\theta} = -Ur\sin^2\chi\,, \qquad \Gamma^\chi_{\chi r} = \frac{1}{r}\,, \qquad \Gamma^\chi_{\theta\theta} = -\sin\chi\cos\chi\,,$$

$$\Gamma^r_{\phi\phi} = -Ur\sin^2\chi\sin^2\theta\,, \qquad \Gamma^\chi_{\phi\phi} = -\sin\chi\cos\chi\sin^2\theta.$$

where the prime and overdot denote partial differentiation with respect to r and t, respectively.

A.2 Extrinsic curvature

We use a geodesic equation approach to determine the components of the extrinsic curvatures. Let us consider the time-component of the extrinsic curvature:

$$\begin{aligned} K_{TT} &= T^\mu T^\nu K_{\mu\nu} = T^\mu T^\nu \nabla_\mu n_\nu = -(T^\mu \nabla_\mu T^\nu) n_\nu \\ &= -(\nabla_T T^\nu) n_\nu \end{aligned}$$

In the last line we have used the orthogonality property between the tangent and normal vectors: $T^\mu n_\mu = 0$. We set $T^\mu = dX^\mu/d\tau$ to represent the tangent vector to the curve $X^\mu(\tau)$ where τ is an affine parameter. Then,

$$\begin{aligned} T^\mu(\nabla_\mu T^\nu) &= T^\mu \left[\partial_\mu T^\nu + \Gamma^\nu_{\mu\sigma} T^\sigma\right] \\ &= \frac{\partial^2 X^\nu}{\partial \tau^2} + \Gamma^\nu_{\mu\sigma} \frac{\partial X^\mu}{\partial \tau} \frac{\partial X^\sigma}{\partial \tau} \end{aligned}$$

and the time-component of the extrinsic curvature is given by

$$K_{TT} = -n_\nu \left[\frac{\partial^2 X^\nu}{\partial \tau^2} + \Gamma^\nu_{\mu\sigma} \frac{\partial X^\mu}{\partial \tau} \frac{\partial X^\sigma}{\partial \tau}\right].$$

The remaining components of the extrinsic curvature are obtained in an analogous way.

A.3 Consistency check for a time-dependent metric function

Having included time-dependence in the bulk metric function $U = U(t, r)$, we now check for consistency using the Israel equations. We find that the set of equations are only valid when the metric function is static: $U = U(r)$.

The position of the brane in the bulk is given by the 5-vector $X^\mu = (\tau, r, \chi(\tau, r), \theta, \phi)$. This determines the form of the tangent vectors and the unit normal:

$$T^\mu = (1, 0, \dot{\chi}, 0, 0)\,, \quad R^\mu = (0, 1, \chi', 0, 0)\,, \quad n_\mu = n(\dot{\chi}, \chi', -1, 0, 0)\,.$$

The normalisation constant is given by

$$-\frac{1}{n^2} = \left(-\frac{\dot{\chi}^2}{U} + U\chi'^2 + \frac{1}{r^2}\right).$$

For simplicity, we set $\lambda = \frac{\kappa_5}{6}\rho$ and consider a cosmological constant brane with $v = -1$. Then, the Israel equations are explicitly given by:

$$\begin{aligned}
K_{TT} &= n\left[\ddot{\chi} + Ur\chi'\dot{\chi}^2 - \frac{1}{2}UU'\chi' - \frac{\dot{U}\dot{\chi}}{2U}\right] = \lambda\left(U - r^2\dot{\chi}^2\right) \\
K_{RR} &= n\left[\chi'' + \frac{2\chi'}{r} + \frac{U'\chi'}{2U} + Ur\chi'^3 + \frac{\dot{U}\dot{\chi}}{2U^3}\right] = -\lambda\left(\frac{1}{U} + r^2\chi'^2\right) \\
K_{TR} &= n\left[\dot{\chi}' + \frac{\dot{\chi}}{r} + Ur\chi'^2\dot{\chi} - \frac{U'\dot{\chi}}{2U} + \frac{\dot{U}\chi'}{2U}\right] = -\lambda r^2\dot{\chi}\chi' \\
K_{\Theta\Theta} &= n\left[Ur\chi'\sin^2\chi - \sin\chi\cos\chi\right] = -\lambda r^2\sin^2\chi\,.
\end{aligned}$$

In order to check the Israel equations for consistency, we respectively take the τ and r derivatives of the inverse of the normalisation constant n:

$$\begin{aligned}
\frac{\partial}{\partial\tau}(n^{-1}) &= n\left[U\dot{\chi}'\chi' - \frac{\dot{\chi}\ddot{\chi}}{U}\right] \\
\frac{\partial}{\partial r}(n^{-1}) &= n\left[-\frac{\dot{\chi}\dot{\chi}'}{U} + \frac{1}{2}\frac{\dot{\chi}^2U'}{U^2} + \frac{1}{2}U'\chi'^2 + U\chi'\chi'' - \frac{1}{r^3}\right].
\end{aligned}$$

We can eliminate the double derivatives by using the expressions for K_{TT}, K_{RR} and K_{TR}. For further simplification, we make use of the $K_{\Theta\Theta}$ equation, re-expressed as

$$n\left(\chi' Ur - \cot\chi\right) = -\lambda r^2\,.$$

This determines the consistency equations

$$\chi'\left[\frac{U'}{2}-\frac{U}{r}+\frac{1}{r}\right]-\frac{\dot{U}\dot{\chi}}{2U^3} = 0$$

$$\dot{\chi}\left[\frac{U'}{2}-\frac{U}{r}+\frac{1}{r}\right]-\frac{\dot{U}\chi'}{2} = 0$$

which can be solved simultaneously to give

$$\frac{1}{2}\dot{U}\left[\chi'^2+\frac{\dot{\chi}^2}{U^2}\right]=0\,.$$

Since $\chi'^2+\frac{\dot{\chi}^2}{U^2}>0$, then $\dot{U}=0$ and hence $U=U(r)$. Thus, the bulk metric function is time-independent $U\neq U(t,r)$.

For a static bulk metric function $U(r)$, the consistency equations are given by

$$\chi'\left[\frac{U'}{2}-\frac{U}{r}+\frac{1}{r}\right]=0\,,\qquad \dot{\chi}\left[\frac{U'}{2}-\frac{U}{r}+\frac{1}{r}\right]=0\,.$$

The only trivial solution satisfying both of the equations above corresponds to the Anti-de Sitter (AdS) bulk $U(r)=1+k^2r^2$.

A.4 Transformation between brane and spherical polar coordinates

Consider a setup involving a positive tension four-dimensional hypersurface embedded in a five-dimensional background with negative cosmological constant. The solution to the five-dimensional Einstein equations is then given by the conformally flat background metric

$$ds^2=e^{-2kz}\left[-dt^2+du^2+d\mathbf{x}^2\right]=\frac{1}{k^2u^2}\left[-dt^2+du^2+d\mathbf{x}^2\right]$$

which is precisely the RS metric

$$ds^2=e^{-2k|z|}\left[-dt^2+d\mathbf{x}^2\right]+dz^2$$

with the new coordinate u satisfying

$$u=\frac{1}{k}e^{kz}\,.$$

At $z = 0$, the position of the wall is simply $u = 1/k$.

The following re-parameterisation

$$\begin{aligned} t^* &= \frac{t}{ku} \\ \mathbf{x}^* &= \frac{\mathbf{x}}{ku} \\ w^* - u^* &= \frac{1}{k^2 u} \\ w^* + u^* &= \frac{\mathbf{x}^2 - t^2}{u} + u \end{aligned}$$

converts the RS metric to a five-dimensional hyperboloid

$$ds^2 = -dt^{*2} - dw^{*2} + du^{*2} + d\mathbf{x}^{*2}$$

with the constraint

$$-t^{*2} - w^{*2} + u^{*2} + \mathbf{x}^{*2} = \frac{1}{k^2}\,.$$

Next we transform to spherical polar coordinates using

$$\begin{aligned} \mathbf{x}^* &= r \sin\chi.\ \mathbf{n} \\ u^* &= r\cos\chi \\ t^* &= \frac{1}{k}\sqrt{1+k^2r^2}\sin k\tau \\ w^* &= \frac{1}{k}\sqrt{1+k^2r^2}\cos k\tau \end{aligned}$$

where $\mathbf{n}$ is a unit normal vector in the spherical polar coordinate system. This yields the AdS_5 metric in spherical polars

$$ds^2 = -(1+k^2r^2)d\tau^2 + \frac{dr^2}{(1+k^2r^2)} + r^2(d\chi^2 + \sin^2\chi d\Omega_{II}^2)\,.$$

Thus, the overall transformation between the planar $\rightarrow$ spherical coordinates [78] is given by:

$$\begin{aligned} kr &= \frac{1}{2ku}\left[\left(k^2\zeta^2 - 1\right)^2 + 4k^2\mathbf{x}^2\right]^{1/2} \\ \tan k\tau &= \frac{2kt}{k^2\zeta^2 + 1} \\ \tan\chi &= \frac{2k|\mathbf{x}|}{k^2\zeta^2 - 1} \end{aligned}$$

where $\zeta^2 = u^2 + \mathbf{x}^2 - t^2$.

The transformation can also be obtained in the opposite direction. The transformation from globally spherically symmetric $\rightarrow$ planar is given by

$$\begin{aligned} ku &= \left[\sqrt{1+k^2r^2}\cos k\tau - kr\cos\chi\right]^{-1} \\ kt &= ku.\sin k\tau\sqrt{1+k^2r^2} \\ k|\mathbf{x}| &= ku.kr\sin\chi\,. \end{aligned}$$

Since we now have the transformation rules between the planar and global spherical coordinates, we can analyse the images of the brane trajectories at different positions in the brane gauge. The image of the wall at $r = 0$ in the RS planar gauge implies $\mathbf{x}^* = u^* = 0$ and hence

$$\frac{\mathbf{x}}{ku} = \frac{1}{2}\left[u + \frac{\mathbf{x}^2 - t^2}{u} - \frac{1}{k^2u}\right] = 0\,.$$

At $\mathbf{x} = 0$, the equation simplifies to

$$u^2 - t^2 = \frac{1}{k^2}$$

which is a hyperbola in planar spacetime. At $t = 0$, the hyperbola touches the wall at $u = 1/k$. The image of the wall at $u = 1/k$ yields the AdS wall trajectory

$$\frac{1}{k}\sqrt{1+k^2r^2}\cos k\tau - r\cos\chi = \frac{1}{k}\,.$$

Furthermore, if we set $\tau = 0$, the wall corresponds to a paraboloid

$$r\left(kr\sin^2\chi - 2\cos\chi\right) = 0\,.$$

Thus, the branes are actually evolving in the non-planar spacetime. The walls start off planar (*i.e.* flat), then become parabolic, then planar again. They continue to oscillate in this manner indefinitely [78]. In accordance with the work in chapter 3, we replace $\alpha = r\cos\chi$ in the above equation to obtain the brane trajectory

$$\alpha(\tau, r) = \frac{1}{k}\sqrt{1+k^2r^2}\cos k\tau - \frac{1}{k}\,.$$

The transformation shows that the Randall–Sundrum brane trajectory is **time-dependent** in global AdS coordinates.

Appendix B

Detailed calculations–Braneworld black string

B.1 Definitions and notations

We take the five-dimensional metric to have signature $(-,+,+,+,+)$. The Riemann curvature tensor is defined in terms of the Christoffel symbols

$$R^{a}{}_{bcd} = \Gamma^{a}_{bd,c} - \Gamma^{a}_{bc,d} + \Gamma^{a}_{ec}\Gamma^{e}_{bd} - \Gamma^{a}_{ed}\Gamma^{e}_{bc}$$

where

$$\Gamma^{a}_{bc} = \frac{1}{2}g^{ae}\left(g_{be,c} + g_{ce,b} - g_{bc,e}\right)$$

and g_{ab} denotes the induced metric, with its inverse given by g^{ab}. The Ricci tensor and Ricci scalar are given by the following contractions

$$R_{bd} = g^{ac}R_{abcd}\,, \qquad R = g^{bc}R_{bc}\,.$$

The Einstein tensor is written in terms of the Ricci tensor and Ricci scalar

$$G_{ab} = R_{ab} - \frac{1}{2}g_{ab}R\,.$$

We will define the form of the perturbation as

$$h^{ab} = g^{ac}g^{bd}\delta g_{cd}$$

and the variation of the Christoffel symbol as

$$\delta\Gamma^{c}_{ab} = \frac{1}{2}\left(h^{c}_{b;a} + h^{c}_{a;b} - h_{ab;}{}^{c}\right)\,.$$

B.2 The flat background

Consider the flat metric:

$$ds^2 = a^2(y)\eta_{\mu\nu}dx^\mu dx^\nu + dy^2 .$$

Using prime to denote differentiation with respect to y, we compute the following quantities:

The non-zero Christoffel symbols:

$$\Gamma^y_{\nu\kappa} = -aa'\eta_{\nu\kappa} , \qquad \Gamma^\mu_{y\kappa} = \frac{a'}{a}\delta^\mu_\kappa .$$

The elements of the Riemann curvature tensors:

$$R^\lambda{}_{\mu\lambda\nu} = -a'^2\eta_{\mu\nu} , \qquad R^y{}_{\mu y\nu} = -aa''\eta_{\mu\nu} , \qquad R^\mu{}_{y\nu y} = -\frac{a''}{a}\delta^\mu_\nu .$$

The Ricci tensors:

$$R_{\mu\nu} = -(3a'^2 + aa'')\eta_{\mu\nu} , \qquad R_{yy} = -4\frac{a''}{a} .$$

The Ricci scalar:

$$R = -12\frac{a'^2}{a^2} - 8\frac{a''}{a} .$$

The Einstein tensors:

$$G_{\mu\nu} = 3(a'^2 + aa'')\eta_{\mu\nu} , \qquad G_{yy} = 6\frac{a'^2}{a^2} .$$

The components of the Lichnerowicz operator:

$$\Delta_L h_{yy} = \frac{h''}{a^2} - 2\frac{a'h'}{a^3} + 2\left(\frac{a'^2}{a^4} - \frac{a''}{a^3}\right)h$$

$$\Delta_L h_{\mu y} = \left(\frac{h_{,\mu} - h_{\mu\rho}{}^{,\rho}}{a^2}\right)'$$

$$\Delta_L h_{\mu\nu} = \frac{1}{a^2}\left(\Box^{(4)}h_{\mu\nu} + h_{,\mu\nu} - h_{\nu\rho,\mu}{}^{\rho} - h_{\mu\rho,\nu}{}^{\rho}\right) + h''_{\mu\nu} - 2\left(\frac{a''}{a} + \frac{a'^2}{a^2}\right)h_{\mu\nu}$$
$$+ \eta_{\mu\nu}\left(\frac{a'}{a}h' - 2\frac{a'^2}{a^2}h\right) - \frac{2}{9}\alpha^2 e^{-2\phi}h_{\mu\nu} + \frac{2\sqrt{2}}{3}h_{\mu\nu}\alpha[\mathcal{D}]e^{-\phi} .$$

The five-dimensional d'Alembertian operator and the trace-reversed metric perturbation are defined by

$$\Box = \nabla_a \nabla^a = g^{ab} \nabla_a \nabla_b$$
$$\bar{h}_{ab} = h_{ab} - \frac{1}{2} h^{(5)e}{}_{e} g_{ab}.$$

The trace of the four and five dimensional quantities are related by

$$h^{(5)e}{}_{e} = \frac{h^{(4)\lambda}{}_{\lambda}}{a^2}.$$

B.3 Changing to a conformal variable

We use the following definition $a(y) = H^{1/6}(y) = (c_0 - by)^{1/6}$ to compute the derivatives of the warp factor:

$$a' = -\frac{b}{6a^5}, \qquad a'' = -\frac{5b^2}{36a^{11}}, \qquad a^{(3)} = -\frac{55b^3}{216a^{17}}.$$

The change of variables $dy = adz$ enables us to compute

$$\begin{aligned}
\frac{d}{dy} &= \frac{1}{a}\frac{d}{dz} \\
\frac{d^2}{dy^2} &= \frac{1}{a^2}\frac{d^2}{dz^2} - \frac{a'}{a^2}\frac{d}{dz} \\
\frac{d^3}{dy^3} &= \frac{1}{a^3}\frac{d^3}{dz^3} - 3\frac{a'}{a^3}\frac{d^2}{dz^2} + \left[2\frac{(a')^2}{a^3} - \frac{a''}{a^2}\right]\frac{d}{dz}
\end{aligned}$$

which can be simplified further to

$$\begin{aligned}
\frac{d}{dy} &= \frac{1}{a}\frac{d}{dz} \\
\frac{d^2}{dy^2} &= \frac{1}{a^2}\frac{d^2}{dz^2} + \frac{b}{6a^7}\frac{d}{dz} \\
\frac{d^3}{dy^3} &= \frac{1}{a^3}\frac{d^3}{dz^3} + \frac{b}{2a^8}\frac{d^2}{dz^2} + \frac{7b^2}{36a^{13}}\frac{d}{dz}.
\end{aligned}$$

The warp factor in the z-variable is given by $a(z) = (kz)^{1/5}$ with $k = -\frac{5b}{6}$ and $b = \sqrt{2}\alpha$.

B.4 Perturbation equations in the z-variable

The perturbation equations (5.22)–(5.25) can rewritten in the z-variable as:

$$\begin{aligned}
\ddot{h} - \frac{3}{5z}\dot{h} + \frac{12}{25z^2}h &= k^{2/5}z^{2/5}\left[-\frac{12}{5z}(\dot{\delta\phi}) + \frac{8}{25z^2}\delta\phi\right] \\
\frac{3}{5z}\dot{h} - \frac{6}{25z^2}h &= k^{2/5}z^{2/5}\left[-\frac{3}{5z}(\dot{\delta\phi}) + \left(\frac{24}{25z^2} - m^2\right)\delta\phi - (\ddot{\delta\phi})\right] \\
h^{(3)} + \frac{1}{5z}\ddot{h} - \frac{21}{25z^2}\dot{h} &= k^{2/5}z^{2/5}\left[\frac{32}{25z^2}(\dot{\delta\phi}) + \left(\frac{-64}{25z^3} + \frac{12m^2}{5z}\right)\delta\phi\right]
\end{aligned}$$

where the overdot denotes differentiation with respect to the conformal variable z. The first two equations denote the scalar and dilaton equations respectively. The last equation is a combination of the tensor and vector equations $[\mathrm{tr}(\mu\nu) + (\mu y)^{,\mu}]$. (Note that $\mathrm{tr}(\mu\nu)$ corresponds to the trace of the tensor equation).

B.5 Sturm-Liouville form

The Sturm-Liouville equation has the form:

$$\frac{d}{dz}\left[v(z)\frac{d}{dz}\phi(z)\right] = -\lambda w(z)\phi(z)$$

where λ is the eigenvalue, $\phi(z)$ is the eigenfunction and $w(z)$ is the weight function. The normalised eigenfunctions form an orthonormal basis

$$\int \phi_m(z)\phi_n(z)w(z)dz = \delta(m-n)\,.$$

B.6 Gauge transformations

Having solved the perturbation equations in the bulk, we would now like to find the perturbation on the brane. To do this, we need to change from a coordinate system where the brane is located at $y = F$, into a new coordinate system where the brane lies at the coordinate origin $y = 0$. The gauge transformations required to do this

must preserve the Gaussian normal coordinate system of equation (2.19). Let us consider the transformation properties under the following diffeomorphisms

$$y \to \tilde{y} = y + \xi^y(x^\mu, y)$$
$$x^\mu \to \tilde{x}^\mu = x^\mu + \xi^\mu(x^\mu, y)$$

where ξ^μ denotes a general vector field. Using the explicit infinitesimal transformation rules given by the gauge invariance property

$$h_{ab} \to h_{ab} + \nabla_a \xi_b + \nabla_b \xi_a$$
$$\delta\phi \to \delta\phi + \xi^a \nabla_a \phi,$$

we are able to compute the components of the metric perturbation together with the scalar field perturbation. The metric perturbation transforms according to

$$\tilde{h}_{\mu\nu} = h_{\mu\nu} + \partial_\mu \xi_\nu + \partial_\nu \xi_\mu + 2aa'\eta_{\mu\nu}\xi_y$$
$$\tilde{h}_{\mu y} = h_{\mu y} + \partial_\mu \xi_y + \partial_y \xi_\mu - 2\frac{a'}{a}\xi_\mu$$
$$\tilde{h}_{yy} = h_{yy} + 2\partial_y \xi_y$$
$$\tilde{F} = F + \xi_{y(y=0)}$$

with the brane located at $y = F(x^\mu)$. The perturbation of the scalar field transforms as

$$\tilde{\delta\phi} = \delta\phi + \xi^y \partial_y \phi\,.$$

If we now apply the Gaussian normal gauge (in which any orthogonal component of the metric perturbation vanishes), we find that the vector field ξ^a satisfies

$$\xi^y = f(x^\mu)$$
$$\xi^\mu = -\eta^{\mu\nu} f_{,\nu} \left(\int \frac{dy}{a^2} \right) + \eta^{\mu\nu} \epsilon_\nu(x^\mu)$$

where we can set $\epsilon_\nu = 0$ in the last line. We are then left with the following set of transformations

$$\tilde{h}_{\mu\nu} = h_{\mu\nu} - 2a^2 f_{,\mu\nu} \left(\int \frac{dy}{a^2} \right) + 2aa'\eta_{\mu\nu} f$$
$$\tilde{F} = F + f$$
$$\tilde{\delta\phi} = \delta\phi + f\phi'\,.$$

By setting $f = -F$, we can bring the brane back to the origin of the coordinate system. This is reflected in our gauge transformation, which is now simply

$$\tilde{h}_{\mu\nu} = h_{\mu\nu} + 2a^2 F_{,\mu\nu}\left(\int \frac{dy}{a^2}\right) - 2aa'\eta_{\mu\nu}F$$

$$\tilde{F} = 0$$

$$\tilde{\delta\phi} = \delta\phi - 6\frac{a'}{a}F$$

where $\delta\phi$ corresponds to the scalar field fluctuation as measured when the brane resides at $y = \xi_y$. We have therefore explicitly chosen coordinates which are brane-based and the bulk metric perturbation equation now contains explicit residual F-term pieces describing the brane fluctuation. Therefore, in the brane-based coordinate system, the metric decomposition (5.26) is modified to

$$\tilde{h}_{\mu\nu} = h^{tt}_{\mu\nu} + \psi_{,\mu\nu} + \frac{1}{4}(h - \Box\psi)\eta_{\mu\nu} + 2a^2 F_{,\mu\nu}\left(\int \frac{dy}{a^2}\right) - 2aa'\eta_{\mu\nu}F$$

which can be expressed in the z-variable as

$$\tilde{h}_{\mu\nu} = h^{tt}_{\mu\nu} + \psi_{,\mu\nu} + \frac{1}{4}(h - \Box\psi)\eta_{\mu\nu} + k^{1/5}\left[\frac{5}{2}F_{,\mu\nu}z^{6/5} - \frac{2}{5}\eta_{\mu\nu}\frac{F}{z^{4/5}}\right].$$

The scalar field perturbation in the brane-based approach reads

$$\tilde{\delta\phi} = \delta\phi - \frac{6}{5k^{1/5}}\frac{F}{z^{6/5}}.$$

The F terms in the latter two equations, *i.e.* the residual terms, ensure that the brane is Gaussian normal at the origin of the coordinate system.

Bibliography

[1] S. Creek, R. Gregory, P. Kanti and B. Mistry, "Braneworld stars and black holes," Class. Quant. Grav. **23**, 6633 (2006) [arXiv:hep-th/0606006].

[2] R. Gregory, A. Leksono, B. Mistry, "On black holes in heterotic braneworlds," To appear [hep-th].

[3] G. Nordstrom, "On the possibility of unifying the electromagnetic and the gravitational fields," Phys. Z. **15**, 504 (1914) [arXiv:physics/0702221].

[4] T. Kaluza, "On The Problem Of Unity In Physics," Sitzungsber. Preuss. Akad. Wiss. Berlin (Math. Phys.) **1921** (1921) 966.

[5] O. Klein, "Quantum theory and five-dimensional theory of relativity," Z. Phys. **37** (1926) 895 [Surveys High Energ. Phys. **5** (1986) 241].

[6] P. C. W. Davis and J. Brown, "Superstrings: A Theory of Everything," Cambridge University Press (1998).

[7] V. A. Rubakov, "Large and infinite extra dimensions: An introduction," Phys. Usp. **44**, 871 (2001) [Usp. Fiz. Nauk **171**, 913 (2001)] [arXiv:hep-ph/0104152].

[8] P. Halpern, "The Great Beyond: Higher Dimension, Parallel Universes, and the Extraordinary Search for a Theory of Everything," John Wiley and Sons. Inc (2004).

[9] L. Randall, "Warped Passages: Unravelling the Universe's Hidden Dimensions," Penguin Books (2005).

[10] L. Randall and R. Sundrum, "A large mass hierarchy from a small extra dimension," Phys. Rev. Lett. **83**, 3370 (1999) [arXiv:hep-ph/9905221].

[11] L. Randall and R. Sundrum, "An alternative to compactification," Phys. Rev. Lett. **83**, 4690 (1999) [arXiv:hep-th/9906064].

[12] V. A. Rubakov and M. E. Shaposhnikov, "Extra Space-Time Dimensions: Towards A Solution To The Cosmological Constant Problem," Phys. Lett. B **125**, 139 (1983).

[13] V. A. Rubakov and M. E. Shaposhnikov, "Do We Live Inside A Domain Wall?," Phys. Lett. B **125**, 136 (1983).

[14] K. Akama, "An Early Proposal Of 'Brane World'," Lect. Notes Phys. **176**, 267 (1982). [arXiv:hep-th/0001113].

[15] N. Arkani-Hamed, S. Dimopoulos and G. Dvali, "The hierarchy problem and new dimensions at a millimeter," Phys. Lett. **B429**, 263 (1998) [hep-ph/9803315].

[16] N. Arkani-Hamed, S. Dimopoulos and G. Dvali, "Phenomenology, astrophysics and cosmology of theories with sub-millimeter dimensions and TeV scale quantum gravity," Phys. Rev. D **59**, 086004 (1999) [hep-ph/9807344].

[17] I. Antoniadis, N. Arkani-Hamed, S. Dimopoulos and G. Dvali, "New dimensions at a millimeter to a Fermi and superstrings at a TeV," Phys. Lett. B **436**, 257 (1998) [hep-ph/9804398].

[18] G. H. A. Cole, "Wandering Stars: About Planets and Eco-Planets, An Introductory Notebook," Imperial College Press, (2006).

[19] W. J. Kaufmann, "Black holes and warped spacetime", W. H. Freeman and Company (1967).

[20] S. M. Carroll, "Spacetime and geometry: An introduction to general relativity," San Francisco, USA: Addison-Wesley (2004).

[21] K. Schwarzschild, "On The Gravitational Field Of A Mass Point According To Einstein's Theory," Sitzungsber. Preuss. Akad. Wiss. Berlin (Math. Phys.) **1916**, 189 (1916) [arXiv:physics/9905030].

[22] K. Ferguson, "Prisons of Light: Black Holes," Cambridge University Press (1996).

[23] N. I. Shakura and R. A. Sunyaev, "Black holes in binary systems. Observational appearance," Astron. Astrophys. **24**, 337 (1973).

[24] D. Lynden-Bell, "Galactic nuclei as collapsed old quasars," Nature **223**, 690 (1969).

[25] J. Kormendy and D. Richstone, "Inward bound: The Search for supermassive black holes in galactic nuclei," Ann. Rev. Astron. Astrophys. **33**, 581 (1995).

[26] R. Schodel *et al.*, "A Star in a 15.2 year orbit around the supermassive black hole at the center of the Milky Way," Nature **419**, 694 (2002).

[27] M. Rees "Before the Beginning: Our Universe and Others," Addison-Wesley (1997).

[28] S. W. Hawking, "Particle Creation By Black Holes," Commun. Math. Phys. **43**, 199 (1975) [Erratum-ibid. **46**, 206 (1976)].

[29] A. Celotti, J. C. Miller and D. W. Sciama, "Astrophysical evidence for the existence of black holes," Class. Quant. Grav. **16**, A3 (1999) [arXiv:astro-ph/9912186].

[30] J. L. Lehners, P. Smyth and K. S. Stelle, "Stability of Horava-Witten spacetimes," Class. Quant. Grav. **22**, 2589 (2005) [arXiv:hep-th/0501212].

[31] P. Kanti, "Black holes in theories with large extra dimensions: A review," Int. J. Mod. Phys. A **19**, 4899 (2004) [arXiv:hep-ph/0402168].

[32] A. Lukas, B. A. Ovrut, K. S. Stelle and D. Waldram, "The universe as a domain wall," Phys. Rev. D **59**, 086001 (1999) [arXiv:hep-th/9803235].

[33] P. Horava and E. Witten, "Heterotic and type I string dynamics from eleven dimensions," Nucl. Phys. B **460**, 506 (1996) [arXiv:hep-th/9510209].

[34] P. Horava and E. Witten, "Eleven-Dimensional Supergravity on a Manifold with Boundary," Nucl. Phys. B **475** (1996) 94 [arXiv:hep-th/9603142].

[35] E. Witten, "Strong Coupling Expansion Of Calabi-Yau Compactification," Nucl. Phys. B **471**, 135 (1996) [arXiv:hep-th/9602070].

[36] T. Banks and M. Dine, "Couplings and Scales in Strongly Coupled Heterotic String Theory," Nucl. Phys. B **479**, 173 (1996) [arXiv:hep-th/9605136].

[37] A. Chamblin, S. W. Hawking and H. S. Reall, "Brane-world black holes," Phys. Rev. D **61**, 065007 (2000) [arXiv:hep-th/9909205].

[38] D. A. Easson, "The interface of cosmology with string and M(illennium) theory," Int. J. Mod. Phys. A **16**, 4803 (2001) [arXiv:hep-th/0003086].

[39] P. Callin and F. Ravndal, "Higher order corrections to the Newtonian potential in the Randall-Sundrum model," Phys. Rev. D **70**, 104009 (2004) [arXiv:hep-ph/0403302].

[40] D. Langlois, "Is our universe brany?," Prog. Theor. Phys. Suppl. **163**, 258 (2006) [arXiv:hep-th/0509231].

[41] M. Abramowitz and I. A. Stegun, "Handbook of mathematical functions," Dover (1972).

[42] N. Deruelle, T. Dolezel and J. Katz, "Perturbations of brane worlds," Phys. Rev. D **63**, 083513 (2001) [arXiv:hep-th/0010215].

[43] G. F. Simmons, "Differential equations with applications and historical notes," McGraw Hill, Inc (1991).

[44] P. Callin, "Corrections to the Newtonian potential in the two-brane Randall-Sundrum model," arXiv:hep-ph/0407054.

[45] H. Kudoh and T. Tanaka, "Second order perturbations in the Randall-Sundrum infinite brane-world model," Phys. Rev. D **64**, 084022 (2001) [arXiv:hep-th/0104049].

[46] G. R. Dvali, G. Gabadadze and M. Porrati, "Metastable gravitons and infinite volume extra dimensions," Phys. Lett. B **484**, 112 (2000) [arXiv:hep-th/0002190].

[47] C. Csaki, J. Erlich and T. J. Hollowood, "Graviton propagators, brane bending and bending of light in theories with quasi-localized gravity," Phys. Lett. B **481**, 107 (2000) [arXiv:hep-th/0003020].

[48] G. R. Dvali, G. Gabadadze and M. Porrati, "A comment on brane bending and ghosts in theories with infinite extra dimensions," Phys. Lett. B **484**, 129 (2000) [arXiv:hep-th/0003054].

[49] R. Maartens, "The universe as a brane," J. Phys. Conf. Ser. **33**, 131 (2006).

[50] J. Garriga and T. Tanaka, "Gravity in the brane-world," Phys. Rev. Lett. **84**, 2778 (2000) [arXiv:hep-th/9911055].

[51] S. B. Giddings, E. Katz and L. Randall, "Linearized gravity in brane backgrounds," JHEP **0003**, 023 (2000) [arXiv:hep-th/0002091].

[52] A. Padilla, "Brane world cosmology and holography," arXiv:hep-th/0210217.

[53] M. Parry and S. Pichler, "New bulk scalar field. solutions in brane worlds," JCAP **0411**, 005 (2004) [arXiv:hep-ph/0410025].

[54] R. Gregory, "Braneworld black holes," arXiv:0804.2595 [hep-th].

[55] T. Shiromizu and M. Shibata, "Black holes in the brane world: Time symmetric initial data," Phys. Rev. D **62**, 127502 (2000) [arXiv:hep-th/0007203].

[56] A. Chamblin, H. S. Reall, H. a. Shinkai and T. Shiromizu, "Charged brane-world black holes," Phys. Rev. D **63**, 064015 (2001) [arXiv:hep-th/0008177].

[57] T. Wiseman, "Relativistic stars in Randall-Sundrum gravity," Phys. Rev. D **65**, 124007 (2002) [arXiv:hep-th/0111057].

[58] R. Gregory, "Black string instabilities in anti-de Sitter space," Class. Quant. Grav. **17**, L125 (2000) [arXiv:hep-th/0004101].

[59] R. Gregory and R. Laflamme, "Black strings and p-branes are unstable," Phys. Rev. Lett. **70**, 2837 (1993) [arXiv:hep-th/9301052].

[60] R. Gregory and R. Laflamme, "The Instability of charged black strings and p-branes," Nucl. Phys. B **428** (1994) 399 [arXiv:hep-th/9404071].

[61] M. Anber and L. Sorbo, "New exact solutions on the Randall-Sundrum 2-brane: lumps of dark radiation and accelerated black holes," JHEP **0807**, 098 (2008) [arXiv:0803.2242 [hep-th]].

[62] W. Kinnersley and M. Walker, "Uniformly Accelerating Charged Mass In General Relativity," Phys. Rev. D **2**, 1359 (1970).

[63] R. Emparan, G. T. Horowitz and R. C. Myers, "Exact description of black holes on branes," JHEP **0001**, 007 (2000) [arXiv:hep-th/9911043].

[64] R. Emparan, G. T. Horowitz and R. C. Myers, "Exact description of black holes on branes. II: Comparison with BTZ black holes and black strings," JHEP **0001**, 021 (2000) [arXiv:hep-th/9912135].

[65] R. Emparan, A. Fabbri and N. Kaloper, "Quantum black holes as holograms in AdS braneworlds," JHEP **0208**, 043 (2002) [arXiv:hep-th/0206155].

[66] J. M. Maldacena, "The large N limit of superconformal field theories and supergravity," Adv. Theor. Math. Phys. **2**, 231 (1998) [Int. J. Theor. Phys. **38**, 1113 (1999)] [arXiv:hep-th/9711200].

[67] T. Shiromizu, K. i. Maeda and M. Sasaki, "The Einstein equations on the 3-brane world," Phys. Rev. D **62**, 024012 (2000) [arXiv:gr-qc/9910076].

[68] S. S. Seahra, "Naked shell singularities on the brane," Phys. Rev. D **71**, 084020 (2005) [arXiv:gr-qc/0501018].

[69] C. Galfard, C. Germani and A. Ishibashi, "Asymptotically AdS brane black holes," Phys. Rev. D **73**, 064014 (2006) [arXiv:hep-th/0512001].

[70] W. Israel, "Singular hypersurfaces and thin shells in general relativity," Nuovo Cimento Soc. Ital. Phys. B **44**, 4349 (1966).

[71] D. Garfinkle and R. Gregory, "Corrections to the Thin Wall Approximation in General Relativity," Phys. Rev. D **41**, 1889 (1990).

[72] B. Carter and R. Gregory, "Curvature corrections to dynamics of domain walls," Phys. Rev. D **51**, 5839 (1995) [arXiv:hep-th/9410095].

[73] B. Carter, "Essentials of classical brane dynamics," Int. J. Theor. Phys. **40**, 2099 (2001) [arXiv:gr-qc/0012036].

[74] A. Karch and L. Randall, "Locally localized gravity," JHEP **0105**, 008 (2001) [arXiv:hep-th/0011156].

[75] C. Germani and R. Maartens, "Stars in the braneworld," Phys. Rev. D **64**, 124010 (2001) [arXiv:hep-th/0107011].

[76] M. Bruni, C. Germani and R. Maartens, "Gravitational collapse on the brane," Phys. Rev. Lett. **87**, 231302 (2001) [arXiv:gr-qc/0108013].

[77] T. Tanaka, "Classical black hole evaporation in Randall-Sundrum infinite braneworld," Prog. Theor. Phys. Suppl. **148**, 307 (2003) [arXiv:gr-qc/0203082].

[78] R. Gregory, V. A. Rubakov and S. M. Sibiryakov, "Brane worlds: The gravity of escaping matter," Class. Quant. Grav. **17**, 4437 (2000) [arXiv:hep-th/0003109].

[79] V. P. Frolov and D. Stojkovic, "Black hole as a point radiator and recoil effect on the brane world," Phys. Rev. Lett. **89**, 151302 (2002) [arXiv:hep-th/0208102].

[80] A. Flachi and T. Tanaka, "Escape of black holes from the brane," Phys. Rev. Lett. **95**, 161302 (2005) [arXiv:hep-th/0506145].

[81] D. Stojkovic, "Distinguishing between the small ADD and RS black holes in accelerators," Phys. Rev. Lett. **94**, 011603 (2005) [arXiv:hep-ph/0409124].

[82] S. Dimopoulos and G. L. Landsberg, "Black holes at the LHC," Phys. Rev. Lett. **87**, 161602 (2001) [arXiv:hep-ph/0106295].

[83] S. B. Giddings and S. D. Thomas, "High energy colliders as black hole factories: The end of short distance physics," Phys. Rev. D **65**, 056010 (2002) [arXiv:hep-ph/0106219].

[84] S. Dimopoulos and R. Emparan, "String balls at the LHC and beyond," Phys. Lett. B **526**, 393 (2002) [arXiv:hep-ph/0108060].

[85] J. L. Feng and A. D. Shapere, "Black hole production by cosmic rays," Phys. Rev. Lett. **88**, 021303 (2002) [arXiv:hep-ph/0109106].

[86] L. Anchordoqui and H. Goldberg, "Experimental signature for black hole production in neutrino air showers," Phys. Rev. D **65**, 047502 (2002) [arXiv:hep-ph/0109242].

[87] R. Emparan, M. Masip and R. Rattazzi, "Cosmic rays as probes of large extra dimensions and TeV gravity," Phys. Rev. D **65**, 064023 (2002) [arXiv:hep-ph/0109287].

[88] M. Cavaglia, "Black hole and brane production in TeV gravity: A review," Int. J. Mod. Phys. A **18**, 1843 (2003) [arXiv:hep-ph/0210296].

[89] V. P. Frolov, A. L. Larsen and M. Christensen, "Domain wall interacting with a black hole: A new example of critical phenomena," Phys. Rev. D **59**, 125008 (1999) [arXiv:hep-th/9811148].

[90] V. P. Frolov, M. Snajdr and D. Stojkovic, "Interaction of a brane with a moving bulk black hole," Phys. Rev. D **68**, 044002 (2003) [arXiv:gr-qc/0304083].

[91] D. Stojkovic, "Energy flux through the horizon in the black hole - domain wall systems," JHEP **0409**, 061 (2004) [arXiv:gr-qc/0409038].

[92] A. Flachi, O. Pujolas, M. Sasaki and T. Tanaka, "Dynamics of domain walls intersecting black holes," arXiv:hep-th/0601174.

[93] D. Jennings, I. R. Vernon, A. C. Davis and C. van de Bruck, "Bulk black holes radiating in non-Z(2) brane-world spacetimes," JCAP **0504**, 013 (2005) [arXiv:hep-th/0412281].

[94] I. R. Vernon and D. Jennings, "Graviton emission into non-Z(2) symmetric brane world spacetimes," JCAP **0507**, 011 (2005) [arXiv:hep-th/0412083].

[95] T. Hirayama and G. Kang, "Stable black strings in anti-de Sitter space," Phys. Rev. D **64**, 064010 (2001) [arXiv:hep-th/0104213].

[96] C. Charmousis, R. Gregory, N. Kaloper and A. Padilla, "DGP specteroscopy," JHEP **0610** (2006) 066 [arXiv:hep-th/0604086].

[97] C. Charmousis, R. Gregory and V. A. Rubakov, "Wave function of the radion in a brane world," Phys. Rev. D **62**, 067505 (2000) [arXiv:hep-th/9912160].

[98] P. Brax, C. van de Bruck, A. C. Davis and C. S. Rhodes, "Wave function of the radion with a bulk scalar field," Phys. Lett. B **531** (2002) 135 [arXiv:hep-th/0201191].

[99] G. Cynolter, "Wave function of the radion with BPS branes," Mod. Phys. Lett. A **20** (2005) 519 [arXiv:hep-th/0209152].

[100] W. Chen, Z. W. Chong, G. W. Gibbons, H. Lu and C. N. Pope, "Horava-Witten stability: Eppur si muove," Nucl. Phys. B **732**, 118 (2006) [arXiv:hep-th/0502077].

[101] P. J. Steinhardt and N. Turok, "Cosmic evolution in a cyclic universe," Phys. Rev. D **65**, 126003 (2002) [arXiv:hep-th/0111098].

[102] J. Khoury, B. A. Ovrut, P. J. Steinhardt and N. Turok, "The ekpyrotic universe: Colliding branes and the origin of the hot big bang," Phys. Rev. D **64**, 123522 (2001) [arXiv:hep-th/0103239].

[103] J. Khoury, B. A. Ovrut, N. Seiberg, P. J. Steinhardt and N. Turok, "From big crunch to big bang," Phys. Rev. D **65**, 086007 (2002) [arXiv:hep-th/0108187].

[104] J. L. Lehners, P. McFadden and N. Turok, "Colliding Branes in Heterotic M-theory," Phys. Rev. D **75**, 103510 (2007) [arXiv:hep-th/0611259].

[105] P. McFadden, PhD Thesis (2006), "A signature of higher dimensions at the cosmic singularity," arXiv:hep-th/0612008v2.

[106] B. Cuadros-Melgar and C. E. Pellicer, "Instability of the Time Dependent Horava-Witten Model," arXiv:0712.2155 [hep-th].

[107] H. A. Chamblin and H. S. Reall, "Dynamic dilatonic domain walls," Nucl. Phys. B **562**, 133 (1999) [arXiv:hep-th/9903225].

[108] R. Arnowitt, J. Dent and B. Dutta, "Five dimensional cosmology in Horava-Witten M-theory," Phys. Rev. D **70**, 126001 (2004) [arXiv:hep-th/0405050].

[109] M. S. Modgil, S. Panda and G. Sengupta, "Rotating brane world black holes," Mod. Phys. Lett. A **17**, 1479 (2002) [arXiv:hep-th/0104122].